

Alma Mater Studiorum – Università di Bologna

DOTTORATO DI RICERCA IN
Scienze Biomediche e Neuromotorie

Ciclo XXXII

Settore Concorsuale: 05/D1

Settore Scientifico Disciplinare: BIO/09

***New insight into CDKL5 deficiency disorder pathomechanism:
phosphoproteomic profiling identifies SMAD3 as a novel
downstream target of CDKL5***

Presentata da: Giorgio Medici

Coordinatore Dottorato

Prof. Pietro Cortelli



Supervisore

Prof.ssa Elisabetta Ciani



Co-Supervisore

Stefania Trazzi

Esame finale anno 2019

Summary

SUMMARY	3
AIM OF THE STUDY	5
ABSTRACT	7
INTRODUCTION	9
PROTEIN KINASES	9
CLASSIFICATION AND FUNCTION	9
STRUCTURE AND REGULATION	11
PATHOLOGICAL IMPLICATION OF KINASE MISFUNCTION	13
CDKL5 DEFICIENCY DISORDER: AN OVERVIEW	17
CDD CLINICAL FEATURES AND PHENOTYPE-GENOTYPE CORRELATION	18
CYCLIN-DEPENDENT KINASE-LIKE 5 (CDKL5)	20
CDKL5 GENE AND PROTEIN ISOFORMS	20
PATHOLOGICAL CDKL5 MUTATIONS	21
MOUSE CDKL5 ISOFORMS AND MOUSE MODELS OF CDD	23
CDKL5 PROTEIN STRUCTURE	27
CDKL5 EXPRESSION PROFILE: STAGE-, TISSUE- AND CELL TYPE-SPECIFICITY	28
CDKL5 SUBSTRATES AND FUNCTIONS	31
➤ Neuronal proliferation, differentiation and cell cycle control	31
➤ Neuronal maturation and morphology: actin and microtubule associated functions	32
➤ Neuronal function: dendritic spine structure and synapse activity	34
➤ Nuclear activity: transcriptional regulators and epigenetic and splicing factors	37
CDKL5 CONSENSUS MOTIF AND PHOSPHO-PROTEOMIC ANALYSIS	39
MATERIALS AND METHODS	42
COLONY	42
ANTIBODY MICROARRAY	42
PLASMIDS	43
QUANTITATIVE REAL TIME PCR AND STANDARD REVERSE TRANSCRIPTION-PCR	43
CO-IMMUNOPRECIPITATION ASSAYS	44
IN VITRO PHOSPHORYLATION ASSAY	44
PRIMARY HIPPOCAMPAL CULTURES	45
IMMUNOCYTOCHEMISTRY	46
LUCIFERASE ASSAY	47

WESTERN BLOT ANALYSIS	48
IN VIVO EXPERIMENTS	49
IMMUNOHISTOCHEMICAL AND HISTOLOGICAL PROCEDURES	50
STATISTICAL ANALYSIS	50
RESULTS	51
<hr/>	
PROTEIN EXPRESSION AND PHOSPHORYLATION PROFILING IN THE BRAIN OF CDKL5 KO MICE	51
REDUCED SMAD3 PROTEIN LEVELS IN THE BRAINS OF CDKL5 KO MICE	53
SMAD3 PHYSICALLY INTERACTS WITH CDKL5	57
SMAD3 IS A PHOSPHORYLATION TARGET OF CDKL5	59
CDKL5-MEDIATED PHOSPHORYLATION OF SMAD3 IS REQUIRED FOR SMAD3 PROTEIN STABILITY	60
REDUCED SMAD3 PROTEIN LEVELS IN HIPPOCAMPAL NEURONS FROM CDKL5 KO MICE	63
RESTORATION OF TGF- β /SMAD3 SIGNALING IN PRIMARY HIPPOCAMPAL NEURONS FROM <i>CDKL5</i> KO MICE RECOVERS NEURONAL SURVIVAL AND MATURATION	65
INCREASED SUSCEPTIBILITY TO NEUROTOXIC STRESS IN PRIMARY HIPPOCAMPAL NEURONS FROM CDKL5 KO MICE IS RESCUED BY TREATMENT WITH TGF- β 1.	70
TREATMENT WITH TGF- β 1 PROTECTS CA1 PYRAMIDAL NEURONS FROM <i>CDKL5</i> KO MICE AGAINST NMDA-INDUCED CELL DEATH	72
DISCUSSION	77
<hr/>	
INVOLVEMENT OF CDKL5 IN SEVERAL CELLULAR PATHWAYS	77
REDUCED SMAD3 LEVELS DUE TO CDKL5 LOSS OF FUNCTION IMPAIR NEURON SURVIVAL AND MATURATION	78
INCREASED VULNERABILITY OF <i>CDKL5</i> KO HIPPOCAMPAL NEURONS TO NEUROTOXIC STRESS IS RESCUED BY TREATMENT WITH TGF- β 1	79
CONCLUSION	82
<hr/>	
CITATIONS	83
<hr/>	

Aim of the study

Cyclin-dependent kinase-like 5 (CDKL5) is a serine/threonine protein kinase that is predominantly expressed in the brain (Williamson et al., 2012). Mutations in the X-linked *CDKL5* gene were originally identified in individuals diagnosed with the early-onset seizure variant of Rett syndrome (RTT), now known as CDKL5 deficiency disorder (Kalscheuer et al., 2003, Tao et al., 2004, Weaving et al., 2004). CDKL5 deficiency disorder (CDD) is a very severe, chronically debilitating disorder that mostly affects girls. Most children affected by this disorder suffer from seizures that begin in the first few months of life. Most cannot walk, talk, or feed themselves, and many are confined to using a wheelchair. Currently, there is no cure or effective treatment for CDD, and the mainstay of care is support for the families. Therefore, identification of treatments will represent an important social challenge.

A single protein kinase is generally expected to have multiple substrates/phosphorylation sites and thereby regulates a wide variety of cellular functions. Screening for targets of a specific kinase is mandatory in order to understand the signaling networks in which the protein kinase participates and, more importantly, to identify potential substrates for drug therapy approaches. In fact, modern drug discovery is primarily based on the search for, and subsequent testing of, drug candidates that act on preselected therapeutic targets.

To date, the phosphorylation targets/interactors of CDKL5 are largely unknown. **Therefore, knowledge of the molecular targets of CDKL5 is mandatory in order to identify potential pharmacological interventions.**

The overall objective of the proposed study was to identify new CDKL5 targets that may be key actors in the neurodevelopmental alterations that characterize CDKL5 disorder, in order to expedite the discovery of new therapies for CDD.

In particular the specific aims of the project were:

- 1- Screening of candidate phosphorylation targets/interactors of CDKL5 using phosphoproteomic arrays.

- 2- Identification of direct CDKL5 phosphorylation targets/interactors through co-immunoprecipitation and kinase assays.
- 2- Validation of CDKL5 targets identified in vitro in a model of CDD, the Cdkl5 KO mouse.
- 3- Identification of the relevance of CDKL5 targets in neuronal maturation/survival both in vitro, in primary neuronal cultures, and in vivo, in Cdkl5 KO mice

The results of this study represent a solid starting point for future studies that we plan to carry out in order to fulfill the general goal of “Identifying pharmacological interventions for CDKL5 disorder”.

Abstract

CDKL5 Deficiency Disorder (CDD) is an early-onset epileptic encephalopathy that shares common features with Rett syndrome (RTT), such as neurodevelopmental delay, stereotypic hand movements, hypotonia and impaired psychomotor development, and unique features like intractable epilepsy that is resistant to multiple antiepileptic drugs. CDD is a very severe pathology that strongly impairs the quality of life of patients and their families, and for which there are no available therapies at the moment. This disorder is caused by mutations in the cyclin-dependent kinase-like 5 (*CDKL5*, OMIM 300203) gene, encoding for a serine/threonine protein kinase that belongs to the CMGC family of serine/threonine kinases. The highest levels of CDKL5 occur in the brain, especially during early postnatal stages, in parallel with brain development and maturation. This is in accordance with its involvement in neurodevelopmental alterations, suggesting its role in brain maturation and function. Protein kinases are enzymes that modify the activity, localization, and stability of other proteins by attaching phosphate groups to the target protein. A single protein kinase is generally expected to have multiple substrates/phosphorylation sites and thereby regulates a wide variety of cellular functions. Given the importance of protein kinases in cellular physiology, it is not surprising that deregulation of protein kinase activity has been found to underlie many pathological processes. Autosomal recessive kinase mutations are the predominant cause of disparate neurological diseases, ranging from degenerative and encephalopathic disorders to epilepsies and ataxia. Since kinase function alterations are associated with several pathologies, cancers, and also neurological disorders, these proteins can be both valuable biomarkers and potential drug targets for disease prognosis and treatment. Unfortunately, the poor clinical understanding of the pathological mechanism of CDD highlights the need to characterize CDKL5 biological function and identify effective therapies targeted toward slowing or reversing the progression of the disease. Screening for targets of a specific kinase is necessary in order to understand the signaling networks in which the protein kinase participates and, more importantly, to identify potential substrates for drug therapy approaches. Here we took advantage of a phospho-specific-antibody-microarray technology to identify potential direct CDKL5 substrates in a mouse model of the disorder. An overview of the dataset highlighted the misregulated pathways suggesting the potential involvement of the kinase in signaling transduction, immune system, neuronal maturation and function, cell-cycle regulation,

apoptosis and DNA damage repair. Among the potential CDKL5 targets, SMAD3, a primary mediator of TGF- β action, has been identified as a direct CDKL5 phosphorylation substrate, and its CDKL5-dependent phosphorylation promotes protein stability. Importantly, restoration of SMAD3 signaling through TGF- β 1 treatment normalized defective neuronal survival and maturation in *Cdkl5* knockout (KO) neurons, suggesting that TGF- β /SMAD3 signaling deregulation plays a key role in the etiology of the CDKL5 pathological phenotype. Moreover, we demonstrated that *Cdkl5* KO neurons are more vulnerable to neurotoxic/excitotoxic stimuli. Indeed, TGF β signaling through SMAD3 is a critical regulator of key events in brain development and it is also known to have a neuroprotective effect against various toxins and injurious agents. Both *in vitro* and *in vivo* treatment with TGF- β 1 prevents increased NMDA-induced cell death in hippocampal neurons from *Cdkl5* KO mice and in CDKL5 KO mice respectively. This finding suggests that SMAD3 signaling deregulation is involved in the neuronal susceptibility to excitotoxic injury found in *Cdkl5* KO mice.

This finding has revealed a new CDKL5 substrate and its crucial role in the neuronal response to stress stimuli while also providing a panel of potential CDKL5 substrates for future studies aimed at increasing the definition of the signaling networks in which the protein kinase participates. In addition, our results have shown the first evidence of a new function of CDKL5 in neuronal survival, that could have important implications for susceptibility to neurodegeneration in patients with CDD.

In conclusion, this study contributes to a better understanding of the molecular pathomechanism underlying the clinical phenotype of CDD and raises important implications of absence of CDKL5 function in the potential susceptibility to neurodegeneration in patients with CDD.

INTRODUCTION

Protein Kinases

Protein kinases belong to a class of cellular enzymes that catalyze the transfer of a phosphate group PO_4^{3-} from a high-energy, phosphate-donating molecule, usually nucleotide triphosphate (ATP or GTP), to specific substrate residues in polypeptide chains. This process, called phosphorylation, results in a covalent modification of the target which produces a structural change, thereby modifying its activity and function (Huse and Kuriyan, 2002, Endicott et al., 2012).

Known as the most abundant protein post-translational modification, phosphorylation, and its phosphatase-mediated counterpart dephosphorylation, allow for a reversible mechanism of substrate modification that plays a crucial role in cellular function regulation. The complicated and sophisticated system of protein kinase activity is used in cellular transport, cell signaling, metabolism, protein regulation, secretory processes, and other cellular pathways, providing a critical tool for controlling and influencing many biological processes (Krebs, 1985, Hamilton, 1998, Shchemelinin et al., 2006).

The importance of protein kinases in cellular physiology is also evidenced by the wide distribution of these enzymes in all 6 kingdoms of life: in eukaryotic cells they constitute 2% of the genes (Huse and Kuriyan, 2002), while in humans they account for 1.7% of the entire genome, representing the third most populous protein family (Endicott et al., 2012).

Classification and function

Due to the wide range of proteins and their broad spectrum of actions, eukaryotic kinases have been classified according to several schemes, depending on which of the many different parameters such as function or structure was examined. The first classification scheme was proposed in 1995 (Hanks and Hunter, 1995) and then largely extended or adapted; it has been continuously revised with additional research studies, discoveries, and new kinome sequencing. Therefore, the main classification now in use is a hybrid classification that aims to be of practical use rather than conforming to general rules.

Considering this, kinases can be divided into large groups and subdivided into families and subfamilies, accordingly to their functions, sequence and structure similarity, and evolutionary history (Manning et al., 2002). Kinases are sorted into groups according to site specificity, by the identification of the specific phosphorylated residues (serine/threonine, tyrosine, histidine) or the general consensus site (e.g., proline adjacent to the phosphorylated residue). A more precise analysis of biological functions and amino acid sequence homology, with a particular focus on the catalytic domains, allows for a division into family groups, which are sometimes further subdivided into subfamilies in relation to their conservation among phyla (Manning et al., 2002).

Aside from “atypical” proteins that do not share similarities with most of the eukaryotic kinases, some of the main known and studied “conventional” protein kinase groups are, for example, Tyrosine Kinases, that phosphorylate almost exclusively tyrosine residues, as opposed to Serine/Threonine Kinases, which make up the majority of kinases, and target serine/threonine amino acids. One of the main families is the AGC that derives from the name of the core intracellular signaling kinases PKA, PKG and PKC, whose activities are responsive to the presence of messenger molecules such as calcium, phospholipids, and cyclic nucleotides; CMGC represents another large group of well-known families CDK, MAPK, CLK, GSK3, which are critical for a broad spectrum of cellular processes (cell cycle control, MAPK growth- and stress-response, splicing, metabolic control, and many other unknown functions) (Manning et al., 2002).

Protein kinases can act downstream of a number of different cellular pathways, influencing many biological activities. Depending on the input signal and the cellular context, individual members of the family can phosphorylate different protein targets. The specificity of target recognition allows for a tight control of the cellular activities and responses to different stimuli. This specificity mainly depends on the type of kinase-substrate interaction, which is based either on the direct recognition of the consensus amino acid sequence by the catalytically active site of the kinase or on the interaction between docking sites, structural motifs or domains distant from both the substrate phosphorylation site and the active site of the kinase (Cheng et al., 2011). The consequent phosphorylation of the substrate influences its function by inducing conformational changes in the protein or by modifying its structural surfaces for protein-protein interactions. This post-translational modification has profound effects on protein function, resulting, for example, in enzyme activation/inhibition or formation/disruption of the interaction with protein partners, thus

leading to activation or inactivation of specific pathways for intra- and extra-cellular signal transmission to the nucleus (Endicott et al., 2012).

Although protein kinases play a major role in protein phosphorylation, they can also have non-catalytic activities. Indeed, only recently with new emerging evidence, increasing attention is being given to activity such as DNA binding, competition for protein interactions, or scaffolding of protein complexes (Rauch et al., 2011). Interestingly, these functions can be autonomous and independent of the kinase catalytic activity, or can be complementary to the main phosphotransfer activity, for example by increasing substrate specificity or coordinating the phosphorylation event (Rauch et al., 2011).

The physiological functions of protein kinases are mediated by their target substrates. Whereas genome projects allowed for the discovery of the organism kinome profile, the identification of the cellular target of protein kinases now represents the major challenge to elucidating their physiological function. Alongside a direct approach for the discovery of new kinase substrates, researchers must investigate the structural basis of target recognition in order to expedite the identification of potential substrates.

Structure and regulation

The understanding of the biological functions of kinases along with the tight regulation of their activity come also through an in-depth comprehension of their structure. Structural studies on protein kinases have provided insight into the phosphorylation mechanism, kinase scaffolding, target selection, domain interactions, kinase activation/inactivation (Endicott et al., 2012), highlighting molecular details that have turned out to be crucial for proper kinase function and regulation.

Kinases exist in two different states which are dependent on the different structural folding of the enzyme. In fact, active and inactive configurations are reflected by an open and closed conformation, respectively, and the switching between these two states provides a tool for the control of kinase activity in response to environmental and external stimuli (Huse and Kuriyan, 2002, Shchemelinin et al., 2006, Endicott et al., 2012). Catalytically competent conformation is attained by correct positioning of the catalytic residues in the active site; indeed, proper kinase

pocket formation is mandatory for the allocation and orientation of ATP and the substrate for the phosphoryl transfer mechanism to be successfully completed (Endicott et al., 2012). On the contrary, inactive configuration does not require catalytic constraints to protein fold. Thus, while the ATP-binding pocket adopts a catalytically active structure that is strikingly similar among kinases, the inactive state reveals a notable plasticity of the protein for a more diverse structure (Huse and Kuriyan, 2002, Shchemelinin et al., 2006, Endicott et al., 2012). Indeed, the absence of the structural constraints needed for the correct formation of the peptide phosphorylation platform is responsible for more flexibility that allows kinases to assume different conformations. Nevertheless, they share common domains or structural motifs for mutual biological activities, protein interactions, or substrate recognition.

Many kinases undergo transition from the inactive state to the active conformation as a consequence of phosphorylation on peptide motifs that triggers structural changes, responsible for folding the rest of the domain. However kinases can also be activated as a result of interactions with accessory proteins (such as cyclins for CDKs), as opposed to removing restraining interactions with extra domains or separate subunits (for example in the Src kinase, or AMP-activated kinases); dimerization can also activate kinases (as first observed with the receptor tyrosine kinase subfamily) (Endicott et al., 2012).

Once activated, kinases catalyze the phosphorylation of serine, threonine, or tyrosine in the substrate. The specificity for the target proteins is defined by the capability of the phosphorylation site-containing region to fit the kinase pocket and establish stable interactions between critical residues. Thanks to their intrinsically more disordered nature, these target regions are able to be structurally resolved to fit the kinase catalytic site and at the same time can function, upon phosphorylation, as interaction motifs for several proteins (Endicott et al., 2012). Considering the flexibility of the target region and the similarity of active sites of the kinases, remote docking sites are useful in order to increase substrate selection and specificity of phosphorylation events. Being distant from the active pocket and located on different domains or subunits of the kinase, these sites increase the stability of the association with the substrate, whereas in the catalytic region this configuration is transient, thus raising the affinity for protein targets (Endicott et al., 2012).

A combination of these multiple mechanisms allows kinase function to be dependent on, and modulated by, multiple layers of control. Since protein kinases play a key role in fundamental

cellular processes and signaling transduction in response to extracellular stimulation, the tight regulation of their activity is critical for the integration of multiple input signals and the correct maintenance of cellular biological functions (Huse and Kuriyan, 2002, Shchemelinin et al., 2006). Coordination of this system allows protein kinases to function downstream of different pathways in a concerted network of interactions. From gene transcription to protein degradation, kinase control is operated in a spatial and temporal way over many different aspects. Interacting protein partners, protein post-translational modifications, and cellular localization are just some of the most common methods employed in cells for kinase activity regulation (Hamilton, 1998, Huse and Kuriyan, 2002, Endicott et al., 2012). Apart from being necessary for integrating different biological processes, interaction with other proteins or kinases is the basis of activation of kinase signaling cascades, a peculiar feature of many signaling pathways that allows for a hierarchical organization of signal transduction. Protein interactions not only contribute to activation or inhibition of kinase activity via allosteric control or protein biochemical modifications, but also provide a tool for spatial allocation of phosphorylation events (Hamilton, 1998, Huse and Kuriyan, 2002). Subcellular localization of kinases, also determined by structural motifs that work as localization signals, limits accessibility of substrates and activators or influences the availability spectrum of interacting partners in selectively activating specific physiological functions (Hamilton, 1998). In addition to spatial control, stringent temporal regulation through inactivation or destruction of kinases after phosphorylation events is also mandatory for cellular growth and development (Huse and Kuriyan, 2002, Shchemelinin et al., 2006).

This system modularity is as complex as it is sophisticated and it is of central importance for establishing the subtle regulation over the cellular machinery and the proper stimulus-response coupling.

Pathological implication of kinase malfunction

Given the precise regulation of the kinase system and its significant impact on cellular physiology, deregulation of protein kinase activity can be directly correlated to pathological processes. Kinase function alterations are associated with a number of disorders and cancers; their deregulation also results in neurological disorders (Shchemelinin et al., 2006, Chico et al., 2009, Cheng et al., 2011, Rauch et al., 2011, Endicott et al., 2012). Epigenetic and genetic modification such as mutations or

chromosomal rearrangement can affect kinase genes directly, usually having a higher impact when they involve the kinase domain, or indirectly, through alteration of the molecular mechanisms that are involved in their codification, time and space distribution, activity regulation, and protein interactions. As a result, some kinases are both biomarkers and potential drug targets for disease prognosis and treatment.

One of the most common kinase families involved in disorders is that of tyrosine receptor kinases. Since activation of these kinases, upon ligand binding to the extracellular domain, promote interconnected phosphorylation events that trigger multiple signaling cascades, their deregulation affects several biological processes and cellular responses (Choura and Rebai, 2011). For example, the kit receptor tyrosine kinase is expressed in many different tissues and promotes pleiotropic effects through different pathways such as PI3K/Akt and Ras/MAPK or the JAK/STAT and Src family (Shchemelinin et al., 2006). Reported loss- and gain-of-function mutations of c-kit result in decreased activity due to receptor truncation or permanent activation in the absence of ligand, thus inducing uncontrolled cell proliferation, cell survival, and other cellular responses; these alterations lead to defects in melanogenesis, gametogenesis, or hematopoiesis, and in a variety of malignancies (Shchemelinin et al., 2006). Improper functioning of many receptors belonging to the well-studied families of EGFR, IR, FGFR, VEGFR are known to be involved in breast, colorectal, ovarian, and prostate cancers. Truncations of the extracellular domain or receptor overexpression are the most common alterations that promote cell proliferation, fostering tumor growth and malignancies (Choura and Rebai, 2011).

Besides receptor kinases, non-receptor tyrosine kinases are also implicated in human diseases. Bcr-Abl is a deregulated, constitutively activated enzyme generated by the fusion of the Bcr and Abl proteins as a consequence of chromosomal rearrangement, t(9;22), known as Philadelphia chromosome. Multiple pathways are activated by the deregulated tyrosine kinase activity of this aberrant protein, resulting in a chronic myeloid leukemia (Deininger et al., 2000, Shchemelinin et al., 2006).

In addition to tyrosine kinases, many serine-threonine kinase misfunctions are reported to be related to cancers and disorders. CDKs are involved in colorectal cancer, lung cancer, and in various types of sarcomas, whereas alterations affect either the kinase itself or its cognate activating cyclin or specific inhibitor (Shchemelinin et al., 2006). In addition, MAPK family

members such as p38 or JNKs have crucial roles in inflammatory processes, brain cytoarchitecture, and development, and their abnormal activities have been found in several pathological conditions like acute ischemic damage or rheumatoid arthritis, as well as CNS disorders like Huntington's, Parkinson's and Alzheimer's diseases, Down's syndrome, and tauopathies (Shchemelinin et al., 2006, Chico et al., 2009). Among this group of kinases GSK3 is another serine-threonine kinase worthy of mention. Due to its involvement in a wide range of cellular processes and the complexity of its regulation, GSK3 has been linked to numerous human diseases such as diabetes, stroke, Alzheimer's disease, sleep disorders, and neuropsychiatric and mood disorders (Chico et al., 2009).

Kinase	Type	Disease indication
AMPK	S-T	Multiple sclerosis, Cerebral ischaemia
BCR-ABL	Y	Glioma
CDK	S-T	Traumatic brain injury, Cerebral ischaemia
DAPK1	S-T	Acute brain injury, Alzheimer's disease
EGFR1 and EGFR2	Y	Glioma
FLT3	Y	Meningioma
GSK3	S-T	Alzheimer's disease, Amyotrophic lateral sclerosis, Bipolar disorder, Cerebral ischaemia, Depression, HIV-associated dementia, Parkinson's disease, Neurocognitive deficits, cranial irradiation, Shock, Spinal cord injury, Traumatic brain injury
JAK3	S-T	Amyotrophic lateral sclerosis
JNK1	S-T	Subarachnoid haemorrhage, Parkinson's disease, Cerebral ischaemia
KIT	Y	Glioma, Neurofibromatosis type 1, Meningioma, Von Hippel-Lindau-related haemangioblastoma
MEK1 and MEK2	S-T	Behavioral disorders and drug abuse, Cerebral ischaemia, Traumatic brain injury, Neuropathic pain
MLK1, MLK2 and MLK3	S-T	Excitotoxic injury, Hearing loss, Huntington's disease, Motor neuron disease, Parkinson's disease
MLCK	S-T	Cerebral vasospasm
mTOR	Y	Autism, Huntington's disease, Tuberous sclerosis, Glioma
p38 α	S-T	Alzheimer's disease, Neuropathic pain
MAPK		Amyotrophic lateral sclerosis, Cerebral ischaemia, Neuropathic pain, Parkinson's disease, Spinal cord injury, Cerebral ischaemia, Traumatic brain injury
PDGFR β	Y	Glioma, Neurofibromatosis type 1, Meningioma, Von Hippel-Lindau-related haemangioblastoma
PDHK	S-T	Glioma
PKA	S-T	Alzheimer's disease, Memory impairment, Morphine tolerance, Neuropathic pain
PKC	S-T	Alzheimer's disease, Bipolar disorder, Brain tumours, Cerebral ischaemia, Cerebral vasospasm, Neuropathic pain, Opioid dependence, Parkinson's disease
PLK2	S-T	Parkinson's disease
RAF	S-T	Glioma, Neurofibromatosis type 1
ROCK	S-T	Alzheimer's disease, Cerebral ischaemia, Multiple sclerosis, Epilepsy, Spinal canal stenosis, Pain, Spinal cord injury, Raynaud's phenomenon
SNRPE	S-T	Cerebral ischaemia
SRC	Y	Brain injury, Intracerebral haemorrhage
VEGFR1	Y	Glioma, Von Hippel-Lindau-related haemangioblastoma, Meningioma, Neurofibromatosis type 1,
TGF β R	Y	Glioblastoma

Table 1
Protein kinase in CNS disorders and cancers (Adapted from (Chico et al., 2009)).

Since protein kinases are regarded as important effectors in human pathology, they are intensively studied and have become major targets for therapy. Therefore, kinase inhibitors represent potential therapeutic agents for the development of selective and specific targeted therapies.

CDKL5 deficiency disorder: an overview

CDKL5 deficiency disorder (CDD) is an early infantile epileptic encephalopathy and is a very severe and chronically debilitating disorder. It is an X-linked monogenic disorder that mostly affects girls with an incidence of 1:42000 live birth (Symonds et al., 2019). The history of CDD started very recently when, in 2003, Vera Kalscheuer and colleagues showed that a balanced translocation causing a truncation of the X-linked cyclin-dependent kinase-like 5 (*CDKL5/STK9*) gene was responsible for the profound developmental delay and infantile spasms exhibited by two unrelated girls (Kalscheuer et al., 2003). Due to many overlapping clinical features, such as neurodevelopmental delay, stereotypic hand movements, hypotonia, and impaired psychomotor development (Artuso et al., 2010), patients diagnosed with the “early seizure variant” of RTT, also known as “Hanefeld variant”, were studied and found to be positive for *CDKL5* mutations (Tao et al., 2004, Weaving et al., 2004). RTT is a severe childhood neurological disorder, most often caused by mutations in the X-linked gene of the methyl-CpG-binding protein 2 (MeCP2), with a frequent clinical picture characterized by impairment of motor and cognitive functions, spinal problems (scoliosis), epilepsy, loss of communication ability, and characteristic stereotypic hand movements. Nevertheless, CDD has only recently been proposed as a distinct clinical entity with its unique features such as the early drug-resistant epilepsy starting within the first 6 months of life and the consequent lack of normal development (Fehr et al., 2013).

Ever since, a full clinical overview of the CDD has improved, as the number of patients has increased, allowing for a better definition of the clinical symptoms and diagnostic criteria. In the past few years, a more detailed phenotypic spectrum has been described, spanning from a milder form to a more severe form (Guerrini and Parrini, 2012). Once the early-onset seizures were established as the core feature of the CDKL5-related phenotype, screenings for *CDKL5* mutations were also extended to cohorts of patients with an undefined diagnosis of West syndrome, epileptic encephalopathy, or infantile spasms, resulting in high positive scores (Intusoma et al., 2011). CDD is a very severe encephalopathy that strongly impairs the quality of life of patients and their families, and for which there are no available cures at the moment.

CDD is caused by pathogenic variants and loss of function of cyclin-dependent kinase-like 5 (*CDKL5*) (Kalscheuer et al., 2003, Tao et al., 2004, Weaving et al., 2004), a serine/threonine protein kinase that belongs to the CMGC family of serine/threonine kinases. Despite the wide expression

among different tissues in the body, the highest levels of CDKL5 occur in the brain, especially during early postnatal stages, in parallel with brain development and maturation (Rusconi et al., 2008). This is in accordance with its involvement in neurodevelopmental alterations, suggesting its role in brain maturation and function.

CDD clinical features and phenotype-genotype correlation

CDD phenotype is variable, with differently distributed clinical symptoms. Bahi-Buisson and colleagues tried to define the clinical profile of 20 patients with *CDKL5* mutations screened among 183 females with early seizure encephalopathy. The core symptoms were early-onset seizures in the first six months of life, neurocognitive development, and severe hypotonia, commonly followed by the repetitive hand movements as the hallmark of the disease (Bahi-Buisson et al., 2008b, Fehr et al., 2013). Despite seizures being prominent and usually severe, they include a wide range of expression depending on the progression of the disease, including infantile spasms, myoclonic seizures, tonic-clonic seizures, and, most particularly, epileptic encephalopathy. Consequently, a three-stage evolution trend in epilepsy has been described based on age. Stage I characterizes younger patients (1-10 weeks old) with early epilepsy and frequent prolonged tonic-clonic seizures occurring 2-5 times a day; epileptic encephalopathy with infantile spasms and hysarrhythmia is identified as Stage II (from 6 months to 3 years of age); finally, in Stage III about half of the patients may experience seizure remission, whereas the remainder continue to present refractory epilepsy with tonic seizures and myoclonia (Bahi-Buisson et al., 2008a).

Other common and less common clinical features are autistic behavior, sleep and respiratory disturbances, absent language skills, limited hand use, poor developmental skills, including poor sucking and poor eye contact, cardiorespiratory dysrhythmias, gastroesophageal reflux, and scoliosis (Bahi-Buisson et al., 2008b, Artuso et al., 2010, Pini et al., 2012, Fehr et al., 2013) (Figure 1).

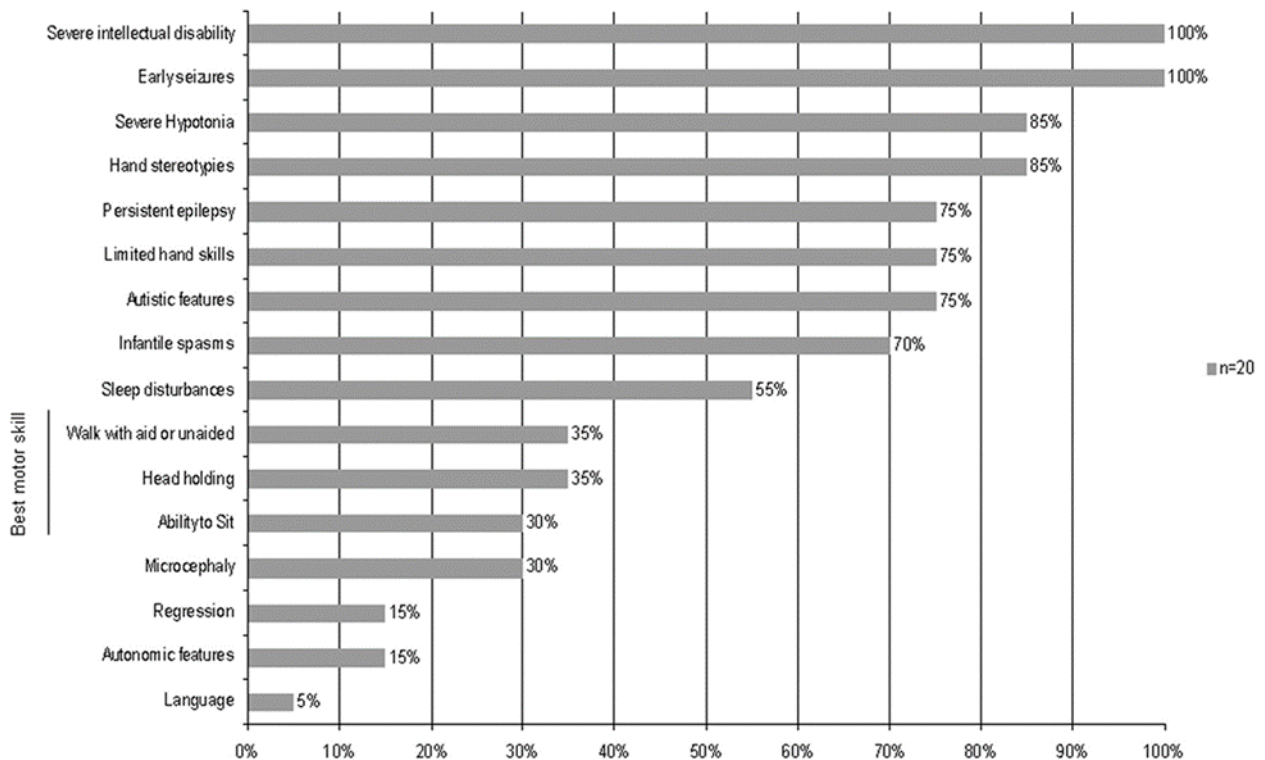


Figure 1

Prevalence of 18 clinical features in 20 CDKL5 mutation patients (Bahi-Buisson et al., 2008b).

Most of the affected patients are girls, although a few boys with this disorder have also been identified and a reported ratio of 4:1 have emerged (Olson et al., 2019). Male hemizygous patients (YX⁻) with just one mutated copy of *CDKL5* were initially reported to show a more severe phenotype compared to heterozygous females (XX⁻), who usually have a wild-type copy of the gene that was thought to be responsible for the milder form of the pathology (Fehr et al., 2015, Liang et al., 2019). However, recently, a clinic-based study by the International Foundation for CDKL5 Research Centers of Excellence (COEs) suggested that no striking differences were observed between genders and that males also show milder phenotype (Olson et al., 2019).

Nevertheless, considering the physiological process of dosage compensation of the X chromosome expression through random X-inactivation, female cells may express either the mutated copy or the normal copy. The resulting variable mosaic pattern among different tissues in the body is suggested to be responsible for the different phenotypic outcome of the disorder (Zhou et al., 2017), but the influence of somatic CDKL5 mosaicism on clinical phenotype is still unknown (Olson et al., 2019). Nevertheless, the big clinical heterogeneity is also being explained by the wide CDKL5 mutational spectrum identified in patients, accounting for the severe to profound alterations in

CDKL5 protein function (Bahi-Buisson et al., 2008a, Fehr et al., 2016). Therefore, patients span from a milder form of the disorder with independent ambulation and controlled epilepsy to severe forms that include intractable refractory seizures, absolute microcephaly, and no motor milestones. This heterogeneous clinical presentation is also strengthened by the report of two twin CDD patients showing a significant discordant phenotype (Weaving et al., 2004). Since both girls were characterized by random X-inactivation, this observation emphasizes the idea that epigenetic or environmental factors may also play a role in influencing the phenotypic outcome of the pathology (Kilstrup-Nielsen et al., 2012). Considering the above discussion, the genotype-phenotype correlation still remains limited.

Given the above considerations and the small number of cases, further studies are necessary to increase the clinical understanding of CDD. These limitations highlight the need to characterize CDKL5 biological function, to understand the mechanisms underlying CDKL5-related disorder, and identify effective therapies targeted toward slowing or reversing the progression of the disease.

CYCLIN-DEPENDENT KINASE-LIKE 5 (CDKL5)

CDKL5 gene and protein isoforms

The human CDKL5 kinase was initially identified through a positional cloning study aimed at identifying disease gene mapping on the X-chromosome. Sequence homologies and protein signatures that are common to the serine-threonine protein family led the authors to name the gene *STK9* (Serine Threonine Kinase 9) [Montini et al. 1998]. Given the strong similarity to some cell division protein kinases, the *STK9* gene was subsequently renamed cyclin-dependent kinase-like 5, *CDKL5*.

The cyclin-dependent kinase-like 5 (*CDKL5*) human gene is located on the Xp22, spanning around a 240kb region. It comprises 27 exons which are combined in five major transcript isoforms containing distinct coding regions (Hector et al., 2016) (Figure 2). Although all the isoforms appear to have the same ATG start codon from exon 2, the first 6 untranslated exons contain alternative transcriptional start sites (TSS) reflecting differences in the 5'UTR of the different transcribed mRNAs. On the contrary, the last exons (19-22) codify for a very large 3'UTR (>6,6kb), suggesting

their importance in the potential additional regulation of *CDKL5* transcripts, while the remaining exons (2-19) stand for the coding region of the different protein isoforms (Hector et al., 2016).

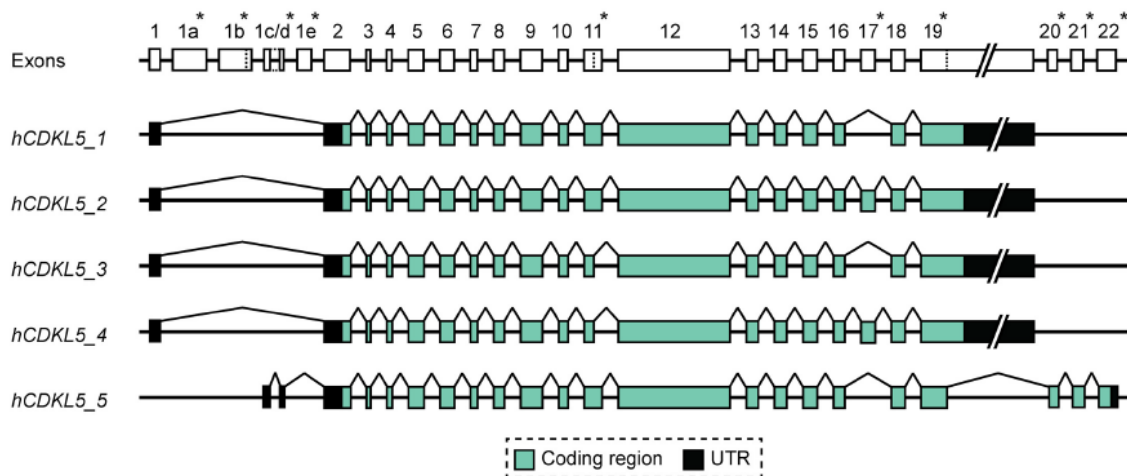


Figure 2

Human *CDKL5* gene and transcript isoforms (Hector et al., 2016). Lines linking exons indicate splicing events while asterisks indicate exon differences across transcript isoforms.

It is worth noting that the *hCDKL5_1* and *hCDKL5_5* transcripts encode for the two main known *CDKL5* protein isoforms, the *CDKL5₁₀₇* and the *CDKL5₁₁₅*, respectively. The latter was the first to be reported and studied (Kalscheuer et al., 2003, Tao et al., 2004), while the first was later found to be the most abundant in the brain (Williamson et al., 2012). The differing weights (107kDa and 115kDa) revolve around the different C-terminal regions that are suggested to be involved in activity regulation, localization, and protein interaction (Lin et al., 2005, Rusconi et al., 2008). Other 3 *CDKL5* transcripts *hCDKL5_2*, *hCDKL5_3*, and *hCDKL5_4*, that are very similar to *hCDKL5_1*, have been identified, but vary depending on either the addition of exon 17, truncation of exon 11 due to an alternative splicing site, or a combination of the two. While exon 17 does not contain known functional elements, truncation of exon 11 results in the loss of a putative nuclear localization signal. The corresponding coded proteins have not yet been characterized, probably due to the lower abundance of their transcripts (Hector et al., 2016).

Pathological *CDKL5* mutations

With the exception of one instance of familial occurrence, likely due to gonadal mosaicism, all reported cases of CDD are sporadic, with mutations occurring de novo in the germline (Weaving et

this, overexpression of mutated derivatives in non-neuronal cell culture lines have been used to investigate the molecular effects of these mutations, along with some of the most recurrent modifications observed in patients (Lin et al., 2005, Bertani et al., 2006, Rusconi et al., 2008). From these studies it emerged that the C-terminal region exerts multiple regulatory functions on the protein, negatively regulating its phosphorylating activity and localizing the protein in the subcellular compartments. Considering the kinase localization-related functions, this mislocalization could contribute to the pathogenic phenotype of the disorder.

Since loss-of-function mutations are usually associated with catalytic impairment, it has been suggested that they correlate with a more severe form of the pathology. On the contrary, gain-of-function alterations, that usually preserve kinase function while altering its control and modulation, have been proposed to have less impact on the phenotypic outcome (Rusconi et al., 2008, Fehr et al., 2016). Indeed, two well-known RTT *CDKL5* derivatives, R781X and L879X, are proposed to cause neurological phenotypes due to the kinase mislocalization into the nucleus and the increased autocatalytic activity observed in vitro (Bertani et al., 2006). However, the correct in vivo expression of this mutant still to be addressed.

Nevertheless, large duplication events involving the *CDKL5* gene have also been identified in several studies (Szafranski et al., 2015). However the duplicated regions reported (spanning 8–21 Mb) included as many as 80 genes making the interpretation of gene-specific overexpression effects in such circumstances problematic (Hector et al., 2017). Although more evidence is required to conclude that there is a well-defined *CDKL5* duplication syndrome, as is found in the closely-related genes *MECP2* and *FOXP1*, the importance of a gene dosage effect might be taken into consideration.

Continued evaluation of cases investigating both genotypic and phenotypic expressions as well as diagnoses of copy number variations involving *CDKL5* may help to elucidate pathological aspects of *CDKL5* mutations.

Mouse *CDKL5* isoforms and mouse models of CDD

The majority of the *CDKL5* coding region is orthologous and well-conserved between humans and mice. A detailed analysis of mouse *Cdkl5* transcripts has also been carried out. A total of 23

identified exons were combined with exon boundaries and chromosomal sequence coordinates demonstrating the existence of five major transcript isoforms containing distinct coding regions (Hector et al., 2016). The murine isoforms *mCdkl5_1-2* are orthologous of their human counterparts while, in contrast, the remaining 3 isoforms show more differences and therefore have been termed as *mCdkl5_6*, *mCdkl5_7* and *mCdkl5_8*.

Human and mouse *CDKL5_1* are the most abundant isoforms in the brain; they have a very similar expression profile and show a very high degree of nucleotide and amino acid sequence similarity. Altogether this homology renders *Cdkl5* mouse models of significant relevance when studying CDKL5 functions. Although animal models cannot completely recapitulate the pathology, they provide an excellent tool for studying the molecular mechanisms underlying the development and progression of the disease and identifying potential therapeutic intervention for treatment of patients. For this reason, *Cdkl5* constitutive knockout mice have been developed in order to address how CDKL5 dysfunction leads to neurological defects in CDD. Some conditional KO mouse models have also been generated to isolate *Cdkl5* deletion to a specific cellular type and study the connection to the pathological outcomes. By using the site-specific recombinase technology of Cre-Lox recombination, exons 6 (Wang et al., 2012, Jhang et al., 2017, Tang et al., 2017), exon 4 (Amendola et al., 2014), and exon 2 (Okuda et al., 2017) have been targeted both in conditional and constitutive KO mouse models to generate a premature stop codon within the N-terminal kinase domain, thus mimicking a loss-of-function mutation (Figure 4).

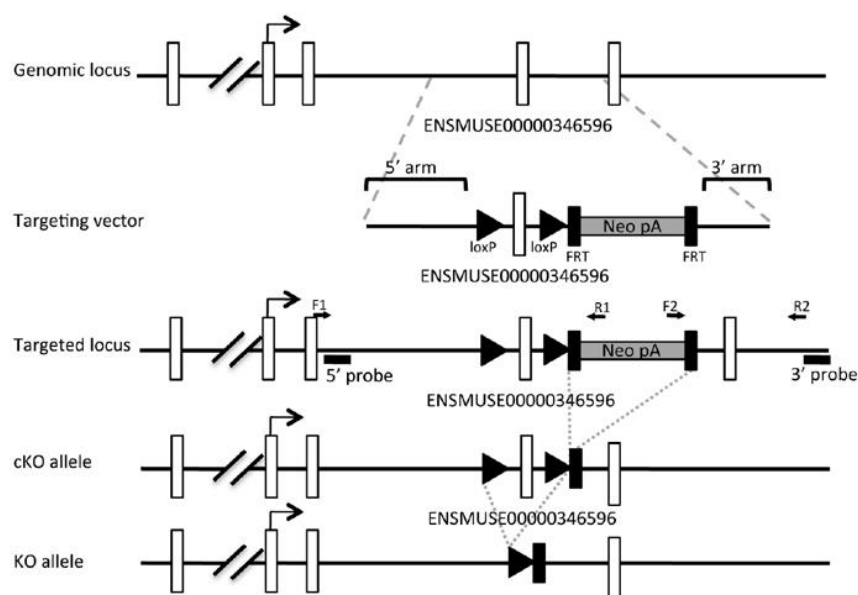


Figure 4
Generation of *Cdkl5* knockout mice (Adapted from (Amendola et al., 2014)).

The first constitutive *Cdkl5* knockout mice studied by Wang and colleagues displayed hyperactivity, motor defects, reduced anxiety, decreased sociability, and impaired learning and memory. They recapitulated several core features observed in CDKL5 patients, such as absence of hand skills, intellectual disability, hyperactivity, and poor response to social interactions. Sensory information processing measured as an event-related potential (ERP) showed impaired neuronal connectivity, although EEG monitoring revealed an absence of spontaneous seizures (Wang et al., 2012).

Deletion of exon 4 by Amendola and colleagues also revealed abnormal claspings of hind-limbs, a decrease in locomotion, and hippocampus-dependent learning and memory impairment (Amendola et al., 2014). These deficits are associated with neuroanatomical defects and are similar to previous findings from Wang's group. As reported by Wang et al., spontaneous seizure or epileptiform activity in mutant mice was not detected, but an abnormal EEG response to convulsant, as PTZ and KA, has been described (Amendola et al., 2014).

Conditional knockouts of *Cdkl5* in glutamatergic cortical neurons (cortical interneurons, striatal medium spiny neurons) with *Emx1::Cre* and GABAergic forebrain neurons (cortical and hippocampal pyramidal neurons) with *Dlx5/6::Cre* had been reported (Amendola et al., 2014). These models revealed that behavioral phenotypes can be mapped to diverse forebrain neuronal populations (Amendola et al., 2014). In fact, while limb claspings and head tracking are associated with cortical motor and visual circuits, non-cortical regions control the hypolocomotion phenotype. The study of a similar forebrain excitatory neuron-specific *Cdkl5* knockout line demonstrated the glutamatergic origins of impaired hippocampal-dependent memory, along with context-dependent hyperactivity and hindlimb claspings (Tang et al., 2017). This study also showed that the altered neuronal morphology corresponds to an increased spontaneous excitatory and inhibitory synaptic activity in the CA1 microcircuit, that is crucial for learning and memory.

A further exon 6 *Cdkl5* KO mouse model was characterized by Jhang et al., confirming previous studies by Wang and colleagues, and introducing new features resembling core symptoms of attention-deficit hyperactivity disorder (ADHD) and autism such as impulsivity, aggressiveness, increased digging stereotypy and the disruption of dopamine synthesis and sociocommunication-associated gene expression in the corticostriatal areas (Jhang et al., 2017).

A significant recent study on a CDKL5 exon 2-targeted KO mouse model revealed an aberrant gain-of-function effect on postsynaptic NMDARs in the hippocampus and identified hyperexcitability in response to NMDA (Okuda et al., 2017). In this study, the same authors found that behavioral characterization of these mice also showed significant enhancement of anxiety- and fear-related behaviors and impairment in both acquisition and long-term retention of spatial reference memory (Okuda et al., 2018).

Although most CDD patients are female, male hemizygous knockout mice have mostly been studied, in order to avoid the potential confound introduced by mosaic CDKL5 protein expression due to random X-inactivation. Nevertheless, a new study recently demonstrated that heterozygous *Cdkl5* knockout female mice show several aspects of CDD, including autistic-like behaviors, defects in motor coordination and memory performance, and breathing abnormalities (Fuchs et al., 2018).

Mouse model	Regions targeted	Neuronal morphology		Behavior							Reference
		Dendrite	Spine	Clasping	Locomotion	Motor coordination	Anxiety	Social interaction	Learning & memory	Spontaneous seizures	
<i>Cdkl5^{-/-}</i>	Whole body	–	–	Yes	Hyperactivity	Impaired	Decreased	Impaired	Impaired	No	Wang <i>et al.</i> (2012)
<i>CDKL5^{-/-}</i>	Whole body	Reduced arborization	Increased immature spine	Yes	Hypoactivity	Impaired	–	–	Impaired	No	Amendola <i>et al.</i> (2014) Fuchs <i>et al.</i> (2014) Sivilia <i>et al.</i> (2016)
<i>CDKL5^{-/-}</i>	Whole body	Reduced arborization	Increased immature spine	–	Hypoactivity	Impaired	Increased	Impaired	Impaired	No	Okuda <i>et al.</i> (2017) Okuda <i>et al.</i> (2018)
<i>CDKL5^{-/-}</i>	Whole body	–	–	–	Hyperactivity	Impaired	–	Impaired	Impaired	No	Jhang <i>et al.</i> (2017)
<i>Cdkl5^{fllox}/y</i> Nex-Cre	Forebrain	Reduced complexity	Increased density (trend)	Yes	Hyperactivity	–	–	–	Impaired	No	Tang <i>et al.</i> (2017)

Five CDKL5 knockout mouse lines have been developed: four constitutive knockouts and one forebrain specific knockout. The phenotypes of neuronal morphogenesis and behavior in each mouse line are listed. We only present mouse lines that have been well characterized in the literature.

Figure 5

Summary of the neuronal morphology and behavior of the *Cdkl5* constitutive and conditional KO mouse line (Zhu and Xiong, 2019).

To sum up, mice lacking CDKL5 recapitulate the core symptoms of CDKL5-related disorders such as the severe intellectual disability and autistic-like features, but not the early-onset seizures. Indeed, the absence of spontaneous seizures observed in the *Cdkl5* KO mice may reflect a significantly different mechanism of epilepsy development in humans and mice. Nevertheless, all things

considered, mouse models are a very useful tool for revealing pathological mechanisms and testing therapeutic interventions for CDD.

CDKL5 protein structure

CDKL5 is a Ser/Thr protein kinase that belongs to the CMGC family of serine/threonine kinases, which include cyclin-dependent kinases (CDKs), glycogen synthase kinases (GSKs), mitogen-activated protein kinases (MAP kinases), and CDK-like (CDKL) kinases (Montini et al., 1998). The protein is characterized by an N-terminal catalytic domain (aa 13-297) that is homologous to that of the other CDKL-family members, and a long unique C-terminal tail (over 600 a.a.), that is highly conserved among the several CDKL5 orthologues that differ only for the extreme C-terminus (Figure 6).

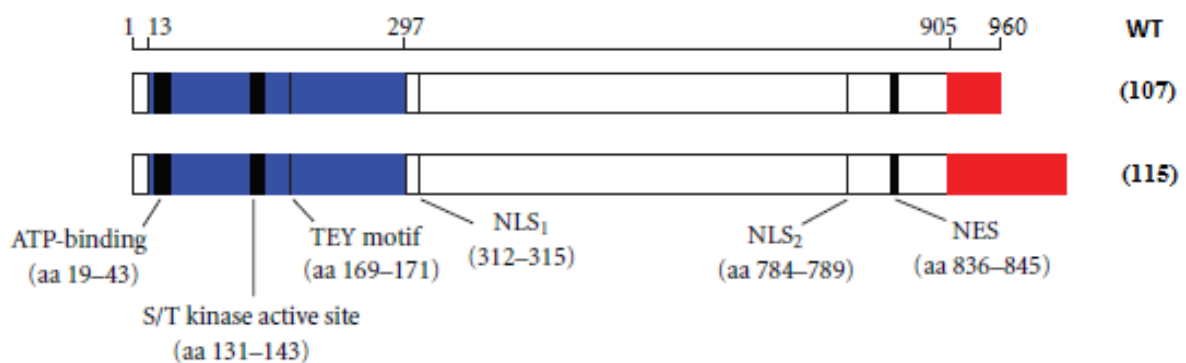


Figure 6

Schematic view of the CDKL5_1 and CDKL5_5 protein isoforms structure (Adapted from (Kilstrup-Nielsen et al., 2012)).

The catalytic domain contains the ATP-binding region, the kinase active site, and the typical TEY motif (Thr-Asp-Tyr) of the MAPK proteins, whose dual phosphorylation usually induces protein kinase activation. Interestingly, CDKL5 itself is capable of autophosphorylating this motif (Lin et al., 2005, Bertani et al., 2006), as are some of the other CMGC protein kinases.

On the contrary, the large C-terminal region presents a unique sequence that includes two nuclear localization signals (NLSs) and one nuclear export signal that are involved in protein import/export from the nucleus. Indeed, the COOH-tail is crucial for protein subcellular localization (Lin et al., 2005, Rusconi et al., 2008). In addition, it is suggested that the C-terminal includes the interacting

regions of some of the few characterized CDKL5 substrates (Mari et al., 2005, Sekiguchi et al., 2013), highlighting its role in protein-protein interactions. As suggested from transcript studies, CDKL5 protein isoform differences occur in the C-terminal region and mostly in the extreme C-terminal tail. This structural variability could reflect different needs for CDKL5 regulation and function in a time- and spatial-dependent manner.

CDKL5 expression profile: stage-, tissue- and cell type-specificity

Expression levels and tissue specificity of CDKL5 proteins have also been investigated. Expression studies have shown that *CDKL5* mRNAs are at their highest in the brain, accordingly to their suggested function based on the pathological phenotype of the disorder (Williamson et al., 2012). Nevertheless, the kinase has been found to be widely expressed among different tissues in the body and its mRNAs can easily be detected in testis, lung, spleen, prostate, uterus, and placenta, whereas they are almost undetectable in heart, kidney, liver, and skeletal muscle (Williamson et al., 2012).

A detailed study in the developing mouse brain reported a temporal and spatial diversity of the CDKL5 protein (Rusconi et al., 2008). In fact, CDKL5 levels appear to be different between the individual regions of the adult mouse and human brain, showing a higher expression in forebrain structures like the hippocampus and cortex. It has also been found in the thalamus and striatum, albeit at lower levels, but it is barely present in the cerebellum and hypothalamus (Rusconi et al., 2008). Superficial cortical layers such as the motor, cingulate, pyriform, and entorhinal cortices, areas that are involved in higher functions like language and information processing, showed a notably higher CDKL5 expression compared to other cortical areas, evidencing the importance of the kinase for the physiology of these brain districts (Kilstrup-Nielsen et al., 2012). Also in the hippocampus, high levels of CDKL5 have been found in all CA fields, but not in the dentate gyrus, where neurogenesis is more prominent in adulthood (Kilstrup-Nielsen et al., 2012). Considering the expression profile, it has been assumed that glutamatergic and GABAergic neurons are the primary cell types that express CDKL5, since no to little expression was observed in dopaminergic and noradrenergic areas.

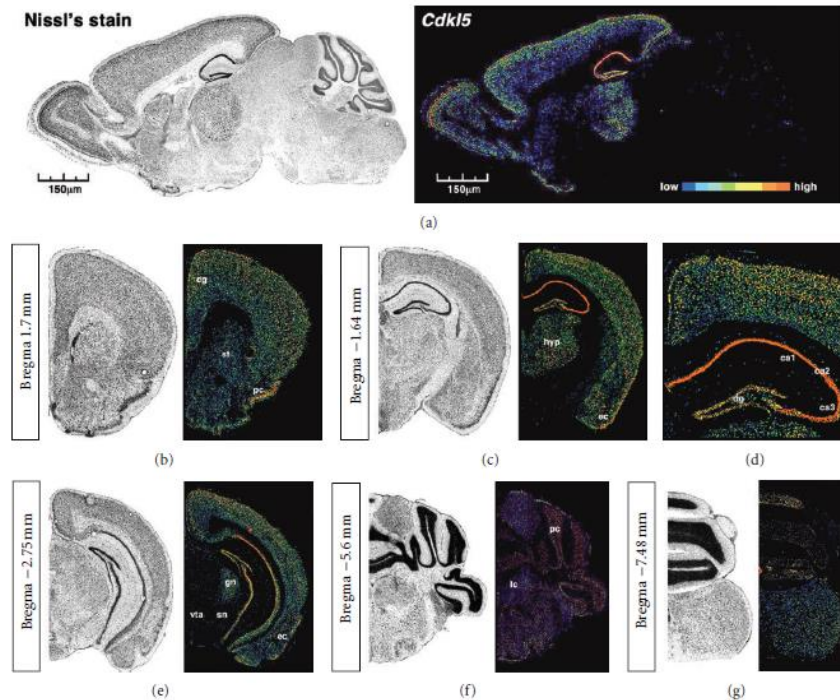


Figure 7
CDKL5 expression profile in the mouse brain (Kilstrup-Nielsen et al., 2012).

Given the strong similarity of CDD to RTT and considering the developmental expression profile of MeCP2, a correlation between neuronal maturation and CDKL5 expression has been considered. Indeed, while CDKL5 is reduced in embryonic stages, it starts to be expressed in perinatal stages, with a strong induction in early postnatal days, showing a tight CDKL5 expression modulation during pre- and postnatal development (Rusconi et al., 2008).

Along with increasing available information, further studies have better defined the spatial and temporal expression profiles in relation to the different human and mouse *CDKL5* transcripts (Hector et al., 2016). This detailed analysis showed individual transcript level changes during development, highlighting a more complex and dynamic developmental regulation of CDKL5 expression in relation to the different isoforms (Hector et al., 2016). Nevertheless, the functional implications of this tight spatial and temporal isoform-dependent modulation still need to be assessed.

At the cellular level CDKL5 is easily detectable in the majority of the neuronal fractions, while it is expressed at very low levels in the glia, indicating an essential role in neuronal development and function. In addition to the variances in protein levels between the different brain areas, the

specific distribution of the protein between the cellular compartments also differs, suggesting that the protein plays multiple roles and regulates distinct signaling pathways depending on its localization, therefore making subcellular localization another key mechanism for CDKL5 activity control. Neuronal CDKL5 protein is expressed in both the nucleus and the cytoplasm, with a ratio that varies depending on the brain areas and stage of development (Rusconi et al., 2008). In fact, during embryonic stages the CDKL5 protein predominantly localizes in the cytoplasm, but from perinatal and postnatal stages, during which protein expression is induced in concomitance with neuronal maturation, until adult stages, CDKL5 progressively accumulates in the nucleus. However, this differential localization changes only in the hippocampus, cortex, and thalamus, where the nuclear fraction accounts for 40% of the total protein, while in the striatum and cerebellum it remains around 20% (Rusconi et al., 2008).

Studies in non-neuronal cell culture revealed that exogenous CDKL5 translocation is mediated by an active export mechanism. This process is controlled by the receptor CRM1/Exportin 1, that is dependent on the recognition of nuclear export signals that are present in the C-terminal domain of the protein (Rusconi et al., 2008). Similarly, the domain also includes a nuclear localization signal on the presence of which depends the nuclear import of the protein. Indeed, CDKL5 phosphorylation close to its NLS by the dual specificity tyrosine-phosphorylation-regulated kinase 1A (DYRK1A) localized the kinase in the cytosolic subcellular compartment of cultured neuronal cells (Oi et al., 2017). Additional studies confirmed the primary role of the C-terminal region in mediating the subcellular localization of the exogenously expressed CDKL5 protein isoforms (Lin et al., 2005, Bertani et al., 2006, Williamson et al., 2012). Interestingly, in primary murine hippocampal neurons CDKL5 was localized both in nucleus and cytoplasm, but it did not undergo constitutive shuttling between these compartments as did proliferating cells. On the contrary, a glutamatergic stimuli induced the translocation and accumulation of the kinase in the perinuclear cytoplasm (Rusconi et al., 2011). Moreover, prolonged treatment promoted CDKL5 proteasomal degradation, showing that expression and localization are modulated by the activity of extrasynaptic N-methyl-d-aspartate receptors (NMDARs).

All things considered, the coordination of this network through the integration of multiple layers of control over the CDKL5 protein is critical for proper regulation of its activity and for the correct time and spatial maintenance of cellular biological functions.

CDKL5 substrates and functions

As already mentioned, the expression profile of the CDKL5 protein suggests that the protein plays a main role in brain development and function. Nevertheless, it has been found to be implicated in several physiological processes, suggesting its involvement in many cellular biological functions. Both *in vivo* and *in vitro* studies, using mouse models, neuronal hippocampal cultures, and non-neuronal cell lines, have shown that CDKL5 coordinates multiple signaling cascades at the cellular level through the direct and indirect interaction with protein partners and molecular machineries.

➤ *Neuronal proliferation, differentiation and cell cycle control*

CDKL5 was found to affect proliferation and differentiation in a study that used neuroblastoma cells as cellular model (Valli et al., 2012). Neuroblastoma cells share several features with normal neurons and are therefore considered a good model with which to study the biochemical and functional properties of neuronal cells. Showing the regulation of pro-proliferative MYCN on the CDKL5 gene, Valli and colleagues proved that CDKL5 inhibits proliferation, promoting cell cycle exit and subsequently inducing cell differentiation, suggesting that the kinase has a crucial role in interconnecting proliferation and differentiation processes in neuronal precursors. Another study correlates CDKL5 with neuronal differentiation in CDKL5 patient-derived induced pluripotent stem cells (iPSCs) (Livide et al., 2015). In fact, GRID1, encoding for glutamate D1 receptor (GluD1), a member of the δ -family of ionotropic glutamate receptors, and important for inducing the differentiation of presynaptic inhibitory neurons, has been found to be altered in CDKL5-mutated iPS cells.

Considering the homology of CDKL5 with MAPKs and CDKs, the role of the kinase in cell cycle progression has been further investigated. Increased proliferation rate of neuronal precursor cells (NPC) was observed in the hippocampus of adult Cdkl5 KO mice with an increase in apoptotic cell death of post-mitotic granule neuron precursors (Fuchs et al., 2014b). Interestingly, it is suggested that CDKL5 exerts the modulation of this balance between survival/proliferation and differentiation of hippocampal postnatal neurogenesis through the control of the AKT/GSK-3 β signaling pathway, known to be involved in diverse developmental events in the brain, including neurogenesis, neuron survival and differentiation (Luo, 2012). Moreover, the AKT/mTOR/rpS6 signaling cascade has also been found to be disrupted in two mouse models of the disorder (Wang et al., 2012, Amendola et al., 2014). The implication regarding the regulation of cell cycle

progression has been further confirmed by a recent study in proliferating cells where CDKL5 was found to localize at the midbody and contribute to faithful cell division, mediating the correct formation of mitotic spindle and regulating cytokinesis (Barbiero et al., 2017b).

➤ *Neuronal maturation and morphology: actin and microtubule associated functions*

As mentioned above, the localization of CDKL5 at the midbody for a cell cycle control might reflect the involvement of the kinase in the interactions with microtubules and actin networks. Processes of cytoskeletal remodeling such as migration and cell polarity, proliferation, vesicle transport, and intracellular signaling are fundamental for correct neuronal maturation. Multiple potential partners of CDKL5 that are important for the correct assembly and function of the microtubule cytoskeleton have recently been determined. By using a chemical genetics method and phosphoproteomic screening, respectively, two independent studies have identified murine microtubule-associated targets MAP1S (microtubule-associated protein 1S), EB2 (microtubule-associated protein EB family member 2) and ARHGEF2 (Rho guanine nucleotide exchange factor 2) (Baltussen et al., 2018), and human MAP1S, CEP131 (Centrosomal Protein 131) and DLG5 (Discs Large MAGUK Scaffold Protein 5) (Munoz et al., 2018), proteins that are fundamental for microtubule establishment, cilia based signaling and cell polarity.

The clear involvement of CDKL5 in regulating cytoskeletal dynamics has also been described (Barbiero et al., 2017a). Barbiero et al. demonstrated that a loss of CDKL5 negatively regulates the IQGAP-Rac1-CLIP170 complex formation, which is necessary for microtubule stability and microtubule growth, with a consequent disruption of proper cell morphology. However, a series of experiments by Chen et al. provided preliminary evidence of the CDKL5 link to the actin cytoskeleton. They showed that CDKL5 plays a critical role in neuronal morphogenesis and dendritic arborization in a BDNF-Rac1 dependent manner. Brain-derived neurotrophic factor (BDNF) is found to induce phosphorylation of CDKL5 that colocalized with F-actin in the peripheral domain of growth cones and formed a protein complex with Rac1, a Rho GTPase involved in the remodeling of the actin and microtubule cytoskeleton. It is suggested that disruption of this interaction causes neuronal migratory defects that may be implicated in early seizures in patients with CDKL5 mutations (Chen et al., 2010). In addition, when overexpressed in cultured neurons, CDKL5 increased the total dendritic length in a kinase activity-dependent manner, showing that the kinase is not only required, but is sufficient to promote dendrite growth. It is worth noting that

Rac1 signaling is also important for Shootin1 function, a brain-specific protein acting as a determinant of axon formation. The interaction with CDKL5 concurs to regulate neuronal polarization regulation and proper axon specification and elongation in mouse primary hippocampal neurons (Nawaz et al., 2016).

A microtubule-based organelle called primary cilium also plays a main role in neurogenesis, and has emerged as an essential signaling hub in many cells, including neural progenitors and differentiating neurons (Lepanto et al., 2016). In fact, ciliopathies are associated with a large variety of manifestations that often include distinctive neurological findings (Valente et al., 2014). In addition to deleterious effects on postnatal development, a lack of primary cilia in adult progenitor cells resulted in a reduction in hippocampal neurogenesis and a deficit in spatial learning in mice. These findings support a potential pathomechanism for intellectual disability associated with ciliary dysfunction. Indeed a specific branch of CMGC kinases, including CDKL5 protein, is known to be involved in ciliary functions (Canning et al., 2018). Interestingly, CDKL5 has been found to impair ciliogenesis when overexpressed, and CDKL5 patient mutations modeled in *C. elegans* CDKL-1 caused localization and/or cilium length defects (Canning et al., 2018). This suggested functional activity of cilium structure and length control may be relevant for neurological disorders and especially for elucidating CDD pathological mechanisms.

All these data reinforced the evidence observed in CDKL5 mouse models in which neuroanatomical defects pointed to CDKL5 having a crucial role in the correct morphological development of neurons. Several studies, aimed at characterizing neuroanatomical aspects of the mouse models, showed that the loss of CDKL5 protein in the KO mouse negatively impacts on proper neuronal maturation (Amendola et al., 2014, Fuchs et al., 2014b, Tang et al., 2017, Okuda et al., 2018). Cortical and hippocampal pyramidal neurons showed a reduction in dendritic arborization and immature spine development. In particular, the dendritic complexity of CA1 pyramidal neurons was decreased in different KO mice, with an overall reduction in branching and a reduction also in length in one mouse line. Reduced dendritic arborization results in a significant reduction in thickness of cortical and hippocampal layers (Amendola et al., 2014).

➤ *Neuronal function: dendritic spine structure and synapse activity*

It has been demonstrated that CDKL5 also contributes to correct spine structure and synapse activity. A synapse is a structure that mediates the communication between two neurons. Synapses are mostly formed on specialized dendritic protrusions called dendritic spines. Abnormal spine morphology is observed in patients with intellectual disability (Purpura, 1974). In dendritic spines, CDKL5 is highly enriched in the postsynaptic density (PSD), a dense protein complex composed of the key proteins for synaptic transmission, signal transduction, and cell adhesion, suggesting its role in synapse development and function (Ricciardi et al., 2012, Zhu et al., 2013). Even though RNAi experiments in cultured neurons showed either an increase in the number of dendritic protrusions and immature spines (filopodia-like and thin-headed spines) or a reduction in spine size and density, probably depending on the different stages of neuronal differentiation, the number of functional spines was generally reduced. In fact, a reduction in synaptic markers such as PSD-95 and Homer was observed (Ricciardi et al., 2012, Zhu et al., 2013, Pizzo et al., 2016), and a corresponding reduction in miniature excitatory postsynaptic current (mEPSC) was measured (Ricciardi et al., 2012, Zhu et al., 2013, Pizzo et al., 2016). Although these defects are also confirmed in a constitutive KO mouse model (Della Sala et al., 2016, Trazzi et al., 2018), they are in contrast with the increase in spine density and mEPSC identified in a conditional KO mouse model, in which CDKL5 is ablated from forebrain excitatory neurons only (Tang et al., 2017). Interestingly, miniature inhibitory postsynaptic current (mIPSC) was unaffected in initial experiment with CDKL5 silenced neurons (Ricciardi et al., 2012), further indicating the relationship of CDKL5 with excitatory neurons. However later *in-vivo* investigations of the synaptic activity of different conditional CDKL5 knockout mice showed different results. While a selective loss of CDKL5 in GABAergic neurons did not affect mIPSC (Tang et al., 2019), an enhancement of the inhibitory signaling was observed in CA1 pyramidal neurons of a mouse model with a selective loss of CDKL5 in glutamatergic neurons (Tang et al., 2017). All these inconsistencies raise the possibility that compensatory mechanisms might take place when CDKL5 is ablated from a specific group of cells only, complicating the interpretation of its function. Nevertheless, CDKL5 is found to be required for ensuring a correct number of well-shaped spines in developing and mature neurons.

Excitation and inhibition in the CNS are mediated mainly by the neurotransmitters glutamate and γ -amino butyric acid (GABA), respectively. The type of synapses formed depends on the specific neurotransmitter released and related receptors expressed, respectively, by the axonal terminal

and the postsynaptic dendrites that make contact. The direct binding of CDKL5 to palmitoylated PSD95 has been found to promote kinase targeting to excitatory synapses for dendritic spine development (Zhu et al., 2013). Recruitment of specific molecules may then regulate the type of neurotransmitter receptors recruited at these sites. Indeed, the study by Okuda and colleagues in the hippocampus of a mouse model of the disorder has revealed that CDKL5 has a crucial role in controlling postsynaptic localization of GluN2B-containing NMDARs (Okuda et al., 2017). In concordance with this result, electrophysiological analysis in the hippocampal CA1 region revealed an increased ratio of NMDA/AMPA receptor-mediated excitatory postsynaptic currents (EPSCs), abrogated by a GluN2B-selective antagonist. This molecular pathomechanism underlying the NMDA-induced hyperexcitability of Cdkl5 KO mice is suggested to be the primary underlying cause of epileptogenesis associated with the loss of CDKL5. Previous findings had already linked CDKL5 function to glutamate stimulation, showing that extrasynaptic NMDAR activation induces cytoplasmic translocation of CDKL5 and its proteasomal degradation (Rusconi et al., 2011). Moreover a recent study in a conditional CDKL5 KO mouse demonstrated that selective loss of CDKL5 in GABAergic neurons leads to autistic-like phenotypes in mice accompanied by excessive glutamatergic transmission, hyperexcitability, and increased levels of postsynaptic NMDA receptors (Tang et al., 2019). Alongside accumulation and overactivation of NMDA receptors, an *in vitro* reduction in GluA2-containing AMPAR expression (Tramarin et al., 2018, Ren et al., 2019) and an overall *in vivo* AMPAR dysregulation (Yennawar et al., 2019) have been observed as a consequence of CDKL5 loss of function. Taken together, all these studies showed that the loss of CDKL5 induces an apparent imbalance in glutamate receptors subunit composition.

In recent years, it has become clear that dendrites and spines are dynamic structures that, during early postnatal development, undergo a significant remodeling, involving processes such as formation, elongation, stabilization, and retraction, all of these necessary for synapse function and plasticity. As development proceeds to adulthood, spines continue to be remodeled in response to diverse stimuli such as LTP and LTD; these changes are considered of high relevance for learning and memory. Recently, Della Sala and collaborators monitored structural dynamics of dendritic spines by applying an *in vivo* two-photon microscopy of the somatosensory cortex of Cdkl5 KO mice. Their data showed that CDKL5 absence results in a specific deficit of dendritic spine stabilization that was prominent in juvenile mice and that persisted in adults. New spines were generated normally but failed to stabilize and were eliminated at an abnormally high rate in the

absence of CDKL5. Their loss led to a strong decrease in spine density associated with a reduced number of postsynaptic constituents and defective LTP, accompanied by a consistent reduction in the frequency of miniature EPSCs (Della Sala et al., 2016). These results reinforced the idea of the involvement of CDKL5 in the stabilization of mature mushroom-shaped spines rather than in the formation of new spines. Indeed, at the molecular level, CDKL5 interacts with the netrin-G1 ligand (NGL-1), a synaptic cell adhesion molecule (CAMs) that exerts a regulatory role in synapse formation and homeostasis. NGL-1 spine-inducing capability is promoted by targeting PSD-95 to new-forming dendritic protrusions and the stabilization of this interaction seems to be reinforced by CDKL5 phosphorylation of NGL-1, ensuring excitatory synapse stability (Ricciardi et al., 2012). CDKL5 coupling with NGL-1 may be required for stabilization rather than formation of nascent contacts, a critical process for the development of fully functional synapses.

Moreover, a new paradigm that has come to light indicates that differential association of proteins modulates the balance between excitatory and inhibitory synapses (Levinson and El-Husseini, 2005). In this regard, molecules that control retention of these cell adhesion molecules at a particular synapse type may eventually determine the specificity of stabilized synapses. Relative levels of scaffolding proteins that regulate excitatory synapse maturation may modulate the excitation/inhibition (E/I) ratio by sequestering members of the neuroligin family to excitatory synapses at the expense of inhibitory contacts. The number of excitatory versus inhibitory contacts that a single neuron receives dictates neuronal excitability and function. Thus, precise control systems must be established in each neuron to maintain appropriate numbers of excitatory and inhibitory synapses. In fact, Pizzo and colleagues investigated the organization of excitatory and inhibitory synapses in the cerebral cortex of Cdkl5 KO mice showing the E/I balance disruption in the Cdkl5-null brain. CDKL5 deletion produces an opposite impact on excitatory and inhibitory transmission in cortical circuits, with an increase in PV⁺ inhibitory contacts and a perturbation of glutamatergic synapses, consistent with previous findings (Pizzo et al., 2016). Another work carried out on the cerebellar area of CDKL5 KO adult mice brains demonstrated that a greater reduction in spontaneous GABA efflux, as opposed to glutamate efflux, leads to a significant increase in the spontaneous glutamate/GABA efflux ratio (Sivilia et al., 2016). The disruption of the postsynaptic machinery at glutamatergic synapses, along with the enhancement of GABAergic transmission, conceivably results in an alteration of the E/I balance and reflects

activity-dependent plastic modifications that may be required for rebalancing dynamic changes in the neuronal network.

Finally, another line of evidence of the crucial role of CDKL5 functional activity over synapse function comes from the direct interaction of the kinase with its endogenous substrate AMPH1 (Sekiguchi et al., 2013). AMPH1 is a brain-specific protein that plays important roles in neuronal transmission and synaptic vesicle recycling through clathrin-mediated endocytosis, thus suggesting that CDKL5 has a potential role in the fine control of endocytotic processes in neuronal cells.

Thus, CDKL5 exerts important functions not only in the correct structure formation of mature spines but also in the maintenance, function, and plasticity of the neuronal network.

➤ *Nuclear activity: transcriptional regulators and epigenetic and splicing factors*

In addition to these cytoplasmic activities, the CDKL5 kinase has been found to regulate important nuclear processes through interaction with epigenetic and splicing factors, and transcriptional regulators. Indeed, since mutations in *MeCP2* and *CDKL5* genes lead to similar genetic disorders, it was deemed important to investigate the relationship between the two. *MeCP2* gene, mapped to the Xq28 chromosome, encodes for the methyl-CpG-binding protein 2, a transcriptional regulator capable of binding specifically to methylated DNA. MeCP2 is important for the correct function of nerve cells, and its mutations have been linked to RTT. Different groups have suggested that CDKL5 and MeCP2 work in common molecular pathways, after it was shown that the two genes are activated simultaneously during development and share a similar expression pattern (Mari et al., 2005, Bertani et al., 2006, Carouge et al., 2010). Nevertheless, whether or not CDKL5 is able to directly phosphorylate MeCP2 in vitro, influencing its activation and function, still needs to be confirmed (Lin et al., 2005).

On the contrary, Kameshita et al. have shown the in vitro capability of CDKL5 to bind and phosphorylate the N-terminal region of DNMT1, an enzyme that maintains a correct DNA methylation pattern, even though this interaction has not yet been confirmed in vivo (Kameshita et al., 2008).

Ricciardi et al. reported that in both cell lines and tissues CDKL5 localizes and is associated with the splicing factor SC35 that is clustered in specific nuclear foci that are referred to as nuclear speckles. These are sub-nuclear structures traditionally considered as storage/modification sites of

pre-mRNA splicing factors. By providing evidence that CDKL5 regulates the dynamic behavior of nuclear speckles, the authors suggested that the kinase was indirectly involved in pre-mRNA processing (Ricciardi et al., 2009).

Lastly, the histone deacetylase 4 (HDAC4) has been reported to be a direct phosphorylation target of CDKL5. Trazzi and colleagues found that in the *Cdkl5* knockout mouse model hypophosphorylated HDAC4 translocates to the nucleus of neural precursor cells where it binds to chromatin and transcription factors, leading to histone deacetylation and altered neuronal gene expression.

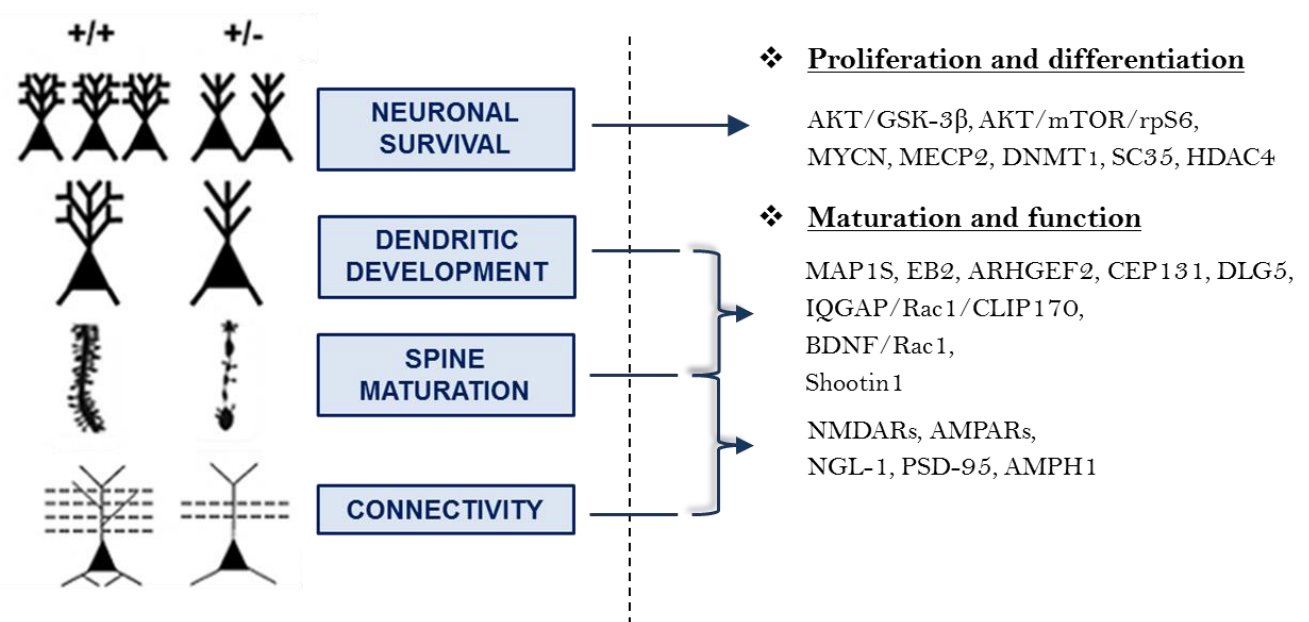


Figure 8
Graphical representation of CDKL5 KO pathological phenotype in neurons and its related direct/indirect interactors.

These data show that different CDKL5-signaling cascades are involved in brain development and function, and act on neuronal development, maturation and transmission; they elucidate, in part, how a lack of CDKL5 may contribute to the typical neuronal phenotype of CDD.

CDKL5 consensus motif and phospho-proteomic analysis

The pathological phenotype of the disorder depends on kinase substrates, therefore studies aimed at the identification of direct and indirect partners of CDKL5 will help to define its functions and could lead to the identification of relevant targets for therapeutic approaches.

As already stated, target phosphorylation mainly depends on the recognition of the consensus amino acid sequence by the catalytically active site of the kinase. CDKL5 belongs to a unique group of kinases that share homology with proline-directed kinases, CDKs and MAPKs. Indeed, sequence analysis revealed that the presence of a critical arginine residue in the kinase subdomain VIII suggests that CDKL5 might be a proline-directed kinase. This residue is highly conserved among proline-directed kinase subfamilies and is required for the selectivity toward substrates containing a proline at the P+1 position, relative to the phosphate acceptor (Tao et al., 2004). Later, the newly discovered CDKL5 interactor AMPH1, and its non-phosphorylated homologue AMPH2, were used *in vitro* to investigate the molecular mechanisms of substrate recognition. In the study in question, RPXSX emerged as a putative consensus sequence (Katayama et al., 2015).

More recently, two independent works identified new multiple CDKL5 substrates using two different mass spectrometry (MS)-based phosphoproteomics approaches, converging on a subset of substrates related both through shared subcellular function(s) and conserved consensus site(s) of CDKL5 phosphorylation (Eyers, 2018). A minimal CDKL5 phosphorylation consensus emerged in both papers as the amino acid sequence RPX[S/T][A/P], confirmed biochemically with model peptide substrates. Interestingly, this is the first *in vitro* evidence that CDKL5 is also able to phosphorylate Thr residue, albeit to a much lesser extent.

It is worth noting that CDKL5_5, but not CDKL5_1, shows this motif in the unique extreme distal C-terminal part of the protein that differs from the other CDKL5 isoforms. This additional potential auto-phosphorylation site could account for a more consistent role of this unique C-terminus in the regulation of subcellular localization and, especially, kinase activity of this isoform. Indeed, a slight change in the subcellular compartmentalization has been observed and a higher auto-phosphorylation activity has been measured compared to CDKL5_1 isoform (Williamson et al., 2012). Since studies on the C-terminal tail have been performed on the CDKL5_5 isoform that contains this RPXSX site, in light of this recent finding it would be interesting to assess the role of the CDKL5_1 C-terminus in more detail. Considering that the different isoforms are also differently

expressed during development in the context of the same tissue (Hector et al., 2016), the cytoplasmic preference of CDKL5_1 could account for a more structural neuron-specific function, while its homologue CDKL5_5, mainly expressed in the fetal stage of the brain, could be crucial for cell cycle and proliferation control of neuronal precursor cells. Future studies will investigate these time and spatial isoform-dependent differences that may be crucial for the development of effective therapeutic strategies.

The CDKL5 consensus represents a preliminary solution to the identification of other CDKL5 targets, but the lack of this motif in other CDKL5 substrates described in literature highlights the need for further studies to better understand the molecular interactions underlying kinase substrate phosphorylation. Surprisingly, many substrates are phosphorylated on residues that are not within linear consensus motifs. Therefore, strategies aimed at screening for interactors based on primary amino acid sequences using the predicted linear consensus might fail to identify a large subset of substrates. Apart from the already-mentioned substrate docking sites in the kinase that are distant from the catalytic site and are also important in enhancing substrate-kinase interactions, the phosphorylated residues are often found in flexible structures, such as loops; it has been proposed that these structures conformationally adapt to the catalytic site (Johnson, 2011). In fact, a recent work demonstrated that in “structurally formed” consensus motifs, amino acids that are present in a distant part of the primary sequence come close to the phosphorylated residue in the folded protein, thereby producing a structurally formed consensus motif. This study showed that structurally formed consensus motifs are common and that analysis of linear sequences surrounding phosphorylation sites may reveal only a subset of substrates (Duarte et al., 2014).

Therefore, complementary approaches are needed to further increase possibilities for CDKL5 protein phosphorylation profiling and expedite a better definition of the molecular pathways regulated by CDKL5. Together with consensus-based bioinformatic analysis, antibody microarrays represent an interesting method for profiling experiments on tissue samples with the aim of discovering a panel of candidate CDKL5 phosphorylation targets. This technique would not only permit simultaneous screening of large protein sets but would also be more sensitive and rapid than other screening methods. Notably, since proteins used in the antibody array assays are not denatured, their tertiary folding structures are intact, thereby this technique allows not only

taking into consideration threonine phosphorylation and structurally formed consensus motifs, but also providing an overview on indirect targets and overall dysregulated pathways.

Indeed, a preliminary Phosphoproteomic analysis using specific Antibody Microarray-based phosphoprotein profiling was recently performed by Trazzi and colleagues using extracts from CDKL5 overexpressing SH-SY5Y neuroblastoma cells. The direct CDKL5 target HDAC4 was found and further validated, confirming the reliability and efficacy of this technique for CDKL5 substrate screening (Trazzi et al., 2016). Interestingly, this target is one of the few validated targets containing the RPXSX consensus site.

Increasing knowledge of the molecular targets of CDKL5 may help identify substrates for pharmacological intervention.

MATERIALS and METHODS

Colony

Mice were handled according to protocols approved by the Italian Ministry for Health (approval number DGSAF 114/2018). The mice used in this work derive from the *Cdkl5* KO strain in the C57BL/6N background developed in (Amendola et al., 2014) and backcrossed in C57BL/6J for three generations. Mice for testing were produced by crossing *Cdkl5* +/- females with *Cdkl5* -/Y males and *Cdkl5* +/- females with +/Y males; animals were genotyped by PCR of genomic DNA using GoTaq® DNA Polymerase from Promega and the following primers spanning *Cdkl5* exon 4: LoxUp 5'-ACGATAGAAATAGAGGATCAACCC-3', LoxDown 5'-TGGAAAGGGGTATACTTGGG-3', and *Cdkl5*flp_Rw 5'-TCTCTAGCCCCTAGTCACAG-3'. The day of birth was designated as postnatal day (P) zero and animals with 24 h of age were considered as 1-day-old animals (P1). Mice were housed 3-5 per cage on a 12 h light/dark cycle in a temperature-controlled environment with food and water provided *ad libitum*.

Antibody microarray

Six phospho explorer antibody microarrays (PEX100; Full Moon BioSystems) were labeled according to the manufacturer's protocol, starting from cortex protein extracts from 3 *Cdkl5* +/Y and 3 *Cdkl5* -/Y mice aged P20. Briefly, proteins were extracted with non-denaturing lysis buffer, and biotinylation of protein samples was performed with the antibody array assay kit (Full Moon BioSystems). The antibody microarray slides were first blocked in a blocking solution for 30 min at room temperature, then rinsed 10 times with Milli-Q grade water for 3-5 min. The slides were then incubated with the biotin-labeled cell lysates (100 µg of protein) in coupling solution at room temperature for 2 h. The array slides were washed 4 to 5 times with 1x Wash Solution and rinsed extensively with Milli-Q grade water before detection of bound biotinylated proteins using Cy3-conjugated streptavidin. Fluorescence intensity of each array spot was quantified and the average signal intensity of replicate spots was calculated. Raw data were normalized as follows: (Average Signal Intensity – Average Background intensity)/Median Signal. Median Signal is the median value of Average Signal Intensity for all antibodies on the array. For total protein, the fold change was calculated as a ratio between the *Cdkl5* -/Y and *Cdkl5* +/Y mean signals. Phospho site-specific signals were firstly normalized on the corresponding site-specific signals of the same protein and

then the fold change was calculated based on the following equation: Phosphorylation ratio = (phosphoA/unphosphoA)/(phosphoB/unphosphoB) where phosphoA or phosphoB and unphosphoA or unphosphoB referred to signals of the phosphorylated and unphosphorylated proteins, respectively, from the experimental samples: (A) *Cdkl5* -/Y (B) *Cdkl5* +/Y samples.

Plasmids

The following plasmids were used: pHA-hCDKL5 (Lin et al., 2005) and phCDKL5-3xFLAG (Trazzi et al., 2016), carrying the first characterized CDKL5 isoform that generates a protein of 1030 amino acids (115 kDa; (Lin et al., 2005)); pCS2-FLAG-SMAD2 (Addgene), pCS2-FLAG-SMAD3 (Inui et al., 2011), pCS2-FLAG-SMAD3-MH1, pCS2-FLAG-SMAD3-MH2 and pCS2-FLAG-SMAD3-L-MH2 (Inui et al., 2011). SMAD3 deletion mutant plasmids were produced by whole around PCR using pCS2-FLAG-SMAD3 plasmid as a template and the indicated primers: Fw 5'-TAGGAATTCAAGGCCTCTCGAG-3' and Rev 5'-AGGTAGAAGTGGTGTCTCTACTCTC-3' for MH1; Fw 5'-TGGTGCTCCATCTCTACTACG-3' and Rev 5'-CTTGTCATCGTCGTCCTGTAGTC-3' for MH2. pCS2-FLAG-SMAD3 plasmid was provided by Prof. Stefano Piccolo (University of Padova, Italy) (Inui et al., 2011), (CAGA)₁₂-luc plasmid, reporter gene for SMAD3 activity, was provided by Caroline Hill (Lincoln's Inn Fields Laboratories) (Levy et al., 2007), and pTKRL plasmid was obtained from Promega.

Quantitative Real Time PCR and Standard Reverse Transcription-PCR

Total RNA was isolated from the hippocampus and cortex of wild-type +/Y and *Cdkl5* -/Y male mice with TRI reagent (Sigma-Aldrich), according to the manufacturer's instructions. cDNA synthesis was achieved with 5 µg of total RNA using iScript™ Advanced cDNA Synthesis Kit (Bio-Rad), according to the manufacturer's instructions. We used the primers that gave an efficiency that was close to 100%. Real-time PCR was performed using SsoAdvanced Universal SYBR Green Supermix (Bio-Rad, CA, USA) in an iQ5 Real-Time PCR Detection System (Bio-Rad). The primer sequences used were as follows: glyceraldehyde-3-phosphate dehydrogenase (GAPDH; E = 95.0%), Fw 5' GAACATCATCCCTGCATCCA 3', Rv 5' CCAGTGAGCTTCCCGTTCA 3'; SMAD3 (E = 97.1%), Fw 5' GTTGAAGAAGGGCGAGCAG 3', Rv 5' ATCCAGTGCCTGGGGATGGTA 3'. Relative quantification was performed using the $\Delta\Delta C_t$ method.

Co-immunoprecipitation assays

HEK293T cells were transfected with HA-CDKL5 alone or co-transfected with HA-CDKL5 and SMAD3-FLAG or SMAD3 mutants using Metafectene Easy Plus (Biontexas). Twenty-four h after transfection, cells were lysated in lysis buffer (50 mM Tris-HCl, pH 7.4, 150 mM NaCl, 0.1% NP40, 1 mM dithiothreitol), supplemented with 1 mM PMSF and 1% protease and phosphatase inhibitor cocktail (Sigma-Aldrich), and cleared by centrifugation (10,000 x g, 30 min). One mg of protein lysate was added to 40 μ l of EZview™ Red ANTI-FLAG® M2 Affinity Gel (Sigma-Aldrich) and incubated overnight at 4°C. For endogenous SMAD3 co-immunoprecipitation, SH-SY5Y cells were infected with CDKL5-FLAG adenovirus particles (Ad-CDKL5) or GFP adenovirus particles as a control (Ad-GFP; Vector BioLabs) at 100 multiplicities of infection (MOI). Twenty-four h after transfection, cells were lysed in lysis buffer, and 2 mg of total protein lysate was added to 20 μ l of resin. Twenty μ g was kept for input. After 6 washing steps in lysis buffer, loading buffer was added to the resin and boiled for 10 min at 95°C. For CDKL5 and SMAD3 immunodetection the immunoprecipitates were subjected to Western blotting as described below.

In vitro phosphorylation assay

Two mg of protein lysate from HEK293T cells transfected with SMAD3-FLAG or SMAD3 mutants was added to 20 μ l of EZview™ Red ANTI-FLAG® M2 Affinity Gel (Sigma-Aldrich) and incubated overnight at 4°C. 3xFLAG peptide was used to elute purified protein according to the manufacturer's instructions (Sigma-Aldrich). For recombinant CDKL5 kinase assay, CDKL5 Δ C protein (rCDKL5 1-498aa, Aurogene) was incubated with 2 mM cold ATP, 1x kinase buffer (20 mM HEPES, pH 7.4, 10 mM MgCl₂, 10 mM NaCl), 10 μ Ci of [γ -³²P]-ATP (Perkin Elmer), and SMAD3 purified proteins at 32°C for 60 min. The reaction was terminated by the addition of 15 μ l loading buffer and boiled at 95°C for 10 min. For the wild-type CDKL5 kinase assay, 2 mg of protein lysate from HEK293T cells transfected with hCDKL5-FLAG was immunoprecipitated on an EZview™ Red ANTI-FLAG® M2 Affinity Gel (Sigma-Aldrich). Beads were washed 3 times with 1x kinase buffer. Twenty μ l of CDKL5-bound beads were pre-incubated with 2 mM cold ATP and 1x kinase buffer at 32°C for 30 min to activate the kinase. Beads were washed twice with 1x kinase buffer and a kinase assay was performed with the addition of 2 mM cold ATP, 10 μ Ci of [γ -³²P]-ATP (PerkinElmer) and

SMAD3-FLAG or SMAD2-FLAG purified proteins. The kinase assays were carried for 1 h at 32°C and terminated by the addition of loading buffer. Western blotting was performed as described below and membrane was exposed to an autoradiographic film. After the decay of radioactivity, membranes were stained with PonceauS or immunostained with anti- SMAD3 and SMAD2 antibodies.

Primary hippocampal cultures

Primary hippocampal neuronal cultures were prepared from P1 *Cdkl5* ^{+/Y} and *Cdkl5* ^{-/Y} mice. Briefly, hippocampi were dissected from mouse brains under a dissection microscope and treated with trypsin (Sigma-Aldrich) for 15 min at 37°C and DNase (Sigma-Aldrich) for 2 min at room temperature before triturating mechanically with a fire-polished glass pipette to obtain a single-cell suspension. Approximately 1.2×10^5 cells were plated on coverslips coated with poly-L-lysine in 6-well plates and cultured in Neurobasal medium supplemented with B27 (Invitrogen) and glutamine (Invitrogen). Cells were maintained *in vitro* at 37 °C in a 5% CO₂-humified incubator and processed for further experiments as described below.

TGF-β1 treatment –1 ng/ml TGF-β1 (ReliaTech GmbH) was added to the conditioned medium on alternate days starting from day 2 postplating (DIV2). Cells were fixed on DIV4 for apoptotic studies and on DIV10 for SMAD3 and P-SMAD (Ser213) expression studies and morphological analysis. For P-SMAD experiments, 1h TGF-β1 treatment was performed. For luciferase experiments, 5ng/mL TGF-β1 was used.

CDKL5 re-expression studies - Primary hippocampal neurons were infected on DIV3 with CDKL5-Flag (Ad-CDKL5) or GFP (Ad-GFP) adenovirus particles (Vector BioLabs) at 100 multiplicities of infection (MOI). Cells were fixed on DIV4 for apoptotic studies and on DIV10 for SMAD3 expression studies and morphological analysis.

Neurotoxicity studies - Primary hippocampal neurons were treated at DIV10 for 10 min with 100 μM NMDA in a Mg²⁺-free, HEPES-buffered saline containing 146 mM NaCl, 5 mM KCl, 1 mM CaCl₂, 10 mM glucose, 10 mM Hepes, 10 μM glycine, pH 7.42. During this time, cells were kept in the incubator at 37°C. After NMDA treatment, hippocampal cultures were washed several times and returned to the original medium. After the washing steps, some cultures were treated with 1 ng/ml TGF-β1 (ReliaTech GmbH), fixed after 24 h and processed for immunocytochemistry analysis. On DIV10 primary hippocampal neurons were exposed for 18 h to 100 μM H₂O₂. Some

H₂O₂-treated cultures were co-treated with 1 ng/ml TGF- β 1 (ReliaTech GmbH). Cell cultures were fixed and processed for immunocytochemistry analysis at DIV10.

Immunocytochemistry

Hippocampal cultures were fixed in 4% paraformaldehyde + 4% sucrose in 100mM phosphate buffer, pH 7.4. Fluorescent images were acquired using a Nikon Eclipse TE600 microscope equipped with a Nikon Digital Camera DXM1200 ATI System (Nikon Instruments Inc.).

SMAD3 and P-SMAD3 (Ser213) nuclear intensity – Primary hippocampal neurons were fixed after 10 days in culture DIV10 and immunostaining was performed using a primary anti-SMAD3 antibody (rabbit polyclonal anti-SMAD3 Ab, 1:200, Cell Signaling) or a primary anti-Phospho-SMAD3 antibody (Ser213) (rabbit polyclonal anti-phospho-SMAD3 Ab, 1:200; Full Moon Biosystem Inc) and a Cy3-conjugated anti-rabbit IgG (1:200, Jackson ImmunoResearch) secondary fluorescent antibody. Nuclei were counterstained with Hoechst-33342 (Sigma-Aldrich), and fluorescence images were acquired at the same intensity. To assess SMAD3 or P-SMAD3 nuclear intensity Hoechst and SMAD3 or P-SMAD3 images of the same cell were processed. The perimeter of the nucleus was traced using Hoechst counterstaining as a guide to define the nuclear area of each cell, and the intensity of Cy3-staining corresponding to the SMAD3 or P-SMAD3 signal was quantified by determining the number of positive (bright) pixels of the cell and within the nucleus. A total of 200 cells for each condition were quantified for SMAD3 signal intensity. A total of 50 cells for each condition were quantified for P-SMAD3 signal intensity.

Apoptotic cell death - To assess apoptotic cell death primary hippocampal cultures were fixed on DIV4 or DIV10-12 (after exposure to different neurotoxic stimuli as above described) and double-stained with the following primary antibodies: anti- α -tubulin (mouse monoclonal anti- α -tubulin Ab, 1:500, Sigma-Aldrich) and anti-cleaved caspase-3 antibody (rabbit polyclonal anti-cleaved caspase-3 Ab, 1:200, Cell Signaling). Detection was performed with a FITC-conjugated anti-mouse IgG (1:200, Jackson ImmunoResearch) and a Cy3-conjugated anti-rabbit IgG (1:200, Jackson ImmunoResearch) antibody. The number of cleaved caspase-3 positive neurons (α -tubulin positive cells with a neuronal phenotype) was counted manually and expressed as a percentage of the total number of neurons. A total of 100 cells for each condition were counted.

Neuronal maturation – In order to assess axon elongation and neuritic outgrowth primary hippocampal neurons were fixed on DIV10 and stained with the following primary antibodies: anti-

TAU1 (mouse monoclonal anti-TAU1 Ab, 1:200, Merck Millipore) and anti-MAP2 (rabbit polyclonal anti-MAP2 Ab, 1:100, Merck Millipore). Detection was performed with a Cy3-conjugated anti-mouse IgG (1:200, Jackson ImmunoResearch) and a FITC-conjugated anti-rabbit IgG (1:200, Jackson ImmunoResearch) antibody. Neurites with a significant intensity of TAU1 staining increasing along the proximal to distal axis were counted as axons. Axon and dendritic length was analyzed by tracing along each neuronal projection using the image analysis system Image Pro Plus (Media Cybernetics, Silver Spring, MD, USA). The starting point of a dendrite was defined as the point at the midline of the dendrite that intersected the curvature of the soma. For our measures, protrusions emerging from the cell soma with all its branches were counted as a single dendrite, tracing the entire dendritic arbor. The average neurite length per cell was calculated by dividing the total neurite length by the number of cells counted in the areas. A total of 50 neurons for each condition were evaluated for axon elongation and neuritic outgrowth.

To assess the degree of synaptic innervation primary hippocampal neurons were fixed on DIV10 and stained with the following antibodies: anti-synaptophysin (mouse monoclonal anti-SYN Ab, 1:500, clone SY38, Merck Millipore) and anti-MAP2 (rabbit polyclonal anti-MAP2 Ab, 1:100, Merck Millipore). Detection was performed with a Cy3-conjugated anti-mouse IgG (1:200, Jackson ImmunoResearch) and a FITC-conjugated anti-rabbit IgG (1:200, Jackson ImmunoResearch) antibody. The degree of synaptic innervation was evaluated by counting the number of synaptic puncta (SYN-positive) along the proximal dendrites and expressed as the number of SYN puncta per 10 μm of dendritic length. In order to evaluate spine density fluorescence images (MAP2-positive protrusions) were acquired using a Leica TCS confocal (Leica Microsystems) 63x oil immersion lens at a 0.6 μm intervals at 1.024 x 1.024 pixels resolution with a 1x zoom. Spine density was measured by counting the number of dendritic protrusions (spines) on proximal dendrites and expressed as the number of spines per 10 μm of dendritic length. A total of 50 neurons for each condition were evaluated for the number of synaptic puncta and number of spines.

Luciferase assay

SMAD3 activity in SH-SY5Y cells and primary hippocampal cultures was monitored through luciferase assays using a p(CAGA)₁₂-luc reporter plasmid. SH-SY5Y cells were plated 24 h before transfection in 24-well plates (10^5 cells/well) and co-transfected with phCDKL5-FLAG (1000 ng),

p(CAGA)₁₂-luc (800ng) and Renilla pTKRL (16ng), as an internal control to normalize for transfection efficiency, using Metafectene Easy Plus (Biontex). Cells were treated with 5 ng/ml TGF- β 1 (ReliaTech GmbH) or 10 μ M SB431542 (Sigma-Aldrich), or left untreated. For the luciferase assay in primary hippocampal neurons, cultures were co-transfected on DIV2 with p(CAGA)₁₂-luc (800 ng) and pTKRL (16ng), using Metafectene Easy Plus (Biontex). SB431542 (10 μ M, Sigma-Aldrich) was added immediately after transfection to the medium. After 24 h some cultures were extensively washed with PBS and then treated with 5ng/ml TGF- β 1 (ReliaTech GmbH) for an additional 6h. Luciferase activity was measured with Dual-Luciferase[®] Reporter Assay System Kit (Promega) according to the manufacturer's instructions. Firefly luciferase activity was normalized for each sample by dividing for the Renilla luciferase activity in the same sample. Luciferase activity was measured with GloMax[®] Discover Microplate Reader (Promega, USA).

Western blot analysis

Total proteins from SKNBE cells transfected with wild-type CDKL5 or CDKL5 Δ N, SH-SY5Y cells infected with CDKL5-FLAG (Ad-CDKL5) or GFP (Ad-GFP) adenovirus particles, and primary hippocampal cultures at DIV10 were lysed in ice-cold RIPA buffer (50 mM Tris-HCl, pH 7.4, 150 mM NaCl, 1% Triton-X100, 0.5% sodium deoxycholate, 0.1% SDS) supplemented with 1mM PMSF, and with 1% protease and phosphatase inhibitor cocktail (Sigma-Aldrich). Total proteins from the hippocampus and cortex of 9-12-week-old *Cdkl5* $-/\gamma$ and *Cdkl5* $+/\gamma$ male mice were homogenized in ice-cold RIPA buffer. Protein concentration for both cell and tissue extracts was determined using the Lowry method (Lowry et al., 1951) and equivalent amounts (50 μ g) of protein were subjected to electrophoresis on a 4-12% Mini-PROTEAN[®] TGX[™] Gel (Bio-Rad) and transferred to a Hybond-ECL nitrocellulose membrane (Amersham - GE Healthcare Life Sciences). The following primary antibodies were used: anti-HA antibody (rabbit polyclonal anti-HA Ab, 1:1000, Cell Signaling Technology), anti-FLAG M2 antibody (mouse monoclonal anti-FLAG M2 Ab, 1:1000, Sigma-Aldrich), anti-SMAD3 antibody (rabbit polyclonal anti-SMAD3 Ab, 1:1000; Cell Signaling Technology), anti-SMAD2 antibody (rabbit polyclonal anti-SMAD3 Ab, 1:1000; Cell Signaling Technology), anti-Phospho-SMAD3 antibody (Ser423/425) (rabbit polyclonal anti-phospho-SMAD3 Ab, 1:1000; Cell Signaling Technology), anti-Phospho-SMAD3 antibody (Ser425) (rabbit polyclonal anti-phospho-SMAD3 Ab, 1:1000; Full Moon Biosystem Inc), anti-Phospho-SMAD3 antibody (Ser213) (rabbit polyclonal anti-phospho-SMAD3 Ab, 1:1000; Full Moon Biosystem Inc), anti-GFP

antibody (rabbit polyclonal anti-green fluorescent protein Ab, 1:1000; Thermo Fisher scientific), anti-CDKL5 antibody (rabbit polyclonal anti-green fluorescent protein Ab, 1:500, Sigma-Aldrich), and anti-GAPDH antibody (rabbit polyclonal anti-GAPDH Ab, 1:5000; Sigma-Aldrich). Densitometric analysis of digitized images was performed using Chemidoc XRS Imaging Systems and Image Lab™ Software (Bio-Rad).

In vivo experiments

NMDA and KA treatment- Experiments were carried out on a total of 46 *Cdkl5* ⁻/_Y and 38 *Cdkl5* ⁺/_Y mice. Seizures were induced in 10-12-week-old mice by intraperitoneal administration of 60 mg/kg NMDA (Sigma-Aldrich) or 35 mg/kg KA (Sigma-Aldrich) in phosphate-buffered saline (PBS). Seizure grades were scored according to (Wu et al., 2005) and recorded in a 120-min observation period. NMDA- or KA-induced seizures were scored as follows: 0 – no abnormalities; 1 – exploring, sniffing, and grooming ceased, with mice becoming motionless; 2 – forelimb and/or tail extension, appearance of rigid posture; 3- myoclonic jerks of the head and neck with brief twitching movements, or repetitive movements with head-bobbing or “wet-dog shakes”; 4 – forelimb clonus and partial rearing, or rearing and falling; 5 – forelimb clonus, continuous rearing and falling; 6 – tonic-clonic movements with loss of posture tone, often resulting in death.

Rescue experiments with TGF-β1 – Rescue experiments with TGF-β1 (ReliaTech GmbH) were performed 60 min after drug injections on 5 *Cdkl5* ⁻/_Y mice. Animals were injected under general anesthesia (2% isoflurane in pure oxygen) with an intracerebroventricular internal cannula (diamenter 26 G, C313I, Plastics One). The following stereotaxic coordinates were used to place the tip of the cannula in the lateral ventricle: 0.6 mm posterior and 1.2 mm lateral to bregma, 2 mm depth from the bone surface. The internal cannula was connected to a Hamilton syringe and 5 microliters of TGF-β1 (10 ng/μl) was injected at a flow rate of 1 μl/min using an infusion pump (Harvard Apparatus). Analgesic (Carprofen 5 mg/kg) and antibiotic (12500 UI/kg Benzylpenicillinbenzathine + 5 mg/kg dihydrostreptomycinsulphate) were given subcutaneously to each mouse. After TGF-β1 injection the cannula was removed and the skin was sutured.

Animals were sacrificed 24 h after NMDA and 8-days after KA injection and were preceded for immunohistochemical and histological procedures as described below.

Immunohistochemical and histological procedures

For immunolabeling experiments animals were deeply anesthetized with isoflurane (4% in pure oxygen) and sacrificed by cervical dislocation. Brains were quickly removed, cut along the midline and hemispheres were fixed by immersion in 4% paraformaldehyde in 100 mM phosphate buffer, pH 7.4. Brains were stored in fixative solution for 48 h, kept in 20% sucrose in phosphate buffer for an additional 24 h and then frozen with cold ice. Brains were cut with a freezing microtome into 30- μ m-thick coronal sections that were serially collected. One out of 6 sections from the somatosensory cortex and the hippocampal formation were used for immunohistochemistry. Brain sections were incubated overnight with a primary anti-SMAD3 antibody (rabbit polyclonal anti-SMAD3 Ab, 1:200, Cell Signaling) or anti-cleaved caspase-3 antibody (rabbit polyclonal anti-cleaved caspase-3 Ab, 1:200, Cell Signaling). Sections were then incubated for 2 h at room temperature with a Cy3-conjugated anti-rabbit IgG (1:200, Jackson ImmunoResearch) secondary fluorescent antibody, mounted on gelatin-coated glass slides, and nuclei were counterstained with Hoechst-33342 (Sigma-Aldrich). Fluorescent images were acquired using a Nikon Eclipse TE600 microscope equipped with a Nikon Digital Camera DXM1200 ATI System (Nikon Instruments Inc.). SMAD3-positive cells were manually counted using the point tool in Image Pro Plus (Media Cybernetics) in one out of 6 sections of the somatosensory cortex and expressed as a percentage of the total cells. The analysis of nuclear SMAD3 intensity was performed under constant microscope settings. The perimeter of the nucleus was traced using the Hoechst counterstaining as a guide to define the nuclear area of each cell, and the intensity of Cy3 staining corresponding to the SMAD3 signal was quantified by determining the number of positive (bright) pixels within the nucleus. Hoechst 33342 staining was used to identify cell nuclei and pyknotic cells in CA1. To assess cell damage the density of apoptotic (cleaved caspase-3 positive) and pyknotic cells in CA1 was established as cells/mm³.

Statistical analysis

Values are expressed as means \pm standard error (SE). The significance of results was obtained using Student's t test and one-way or two-way ANOVA followed by Fisher's LSD post-hoc test. A probability level of $P < 0.05$ was considered to be statistically significant.

RESULTS

Protein expression and phosphorylation profiling in the brain of *Cdkl5* KO mice

To search for CDKL5 target proteins, cortex protein *extracts* from 3 *Cdkl5* $-/\gamma$ and 3 wildtype ($+/\gamma$) mice were applied onto Phospho Explorer antibody microarrays (Figure 1). These microarrays consist of 1318 site-specific and phospho site-specific antibodies against proteins related to multiple signaling pathways and biological processes.

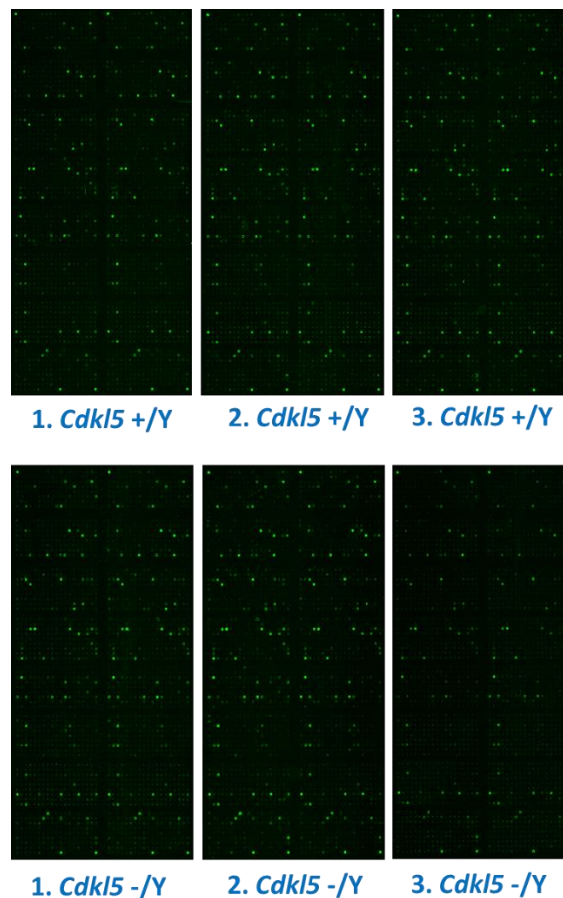


Figure 1

Differential CDKL5-dependent phosphorylation profile.

Representative images of the Phospho Explorer Antibody Microarrays. Microarrays were labeled as described in Materials and Methods section, starting from cortical protein extracts from 3 *Cdkl5* $+/\gamma$ and 3 *Cdkl5* $-/\gamma$ mice aged P20.

The comparative analysis of KO- and wild type- data resulted in a panel of proteins misregulated in their total ($n=36$) and/or phosphorylated forms ($n=14$). Reactome, a tool for

analysis of biological pathways (Fabregat et al., 2017), provided an interesting visualization and interpretation of the datasets, with a functional relationships among identified protein in known pathways (Figure 2). Pathway analysis considers the connectivity between molecules, grouping all of them in sub-pathway branches. Proteins in the analyzed dataset are then matched to this pathway steps, giving an indication of the proportion of the pathways that matches the data. Among the different pathways (see Discussion), a clear involvement of CDKL5 in signal transduction emerged. Of note, SMAD family members resulted misregulated in the absence of Cdkl5. SMADs comprise a family of structurally similar proteins that are the main signal transducers for receptors of the transforming growth factor beta (TGF- β) superfamily. Since SMAD-dependent canonical TGF-signaling is critical for multiple aspects of neurodevelopment, including adult neurogenesis and neuroprotection (Moustakas and Heldin, 2009, Ueberham and Arendt, 2013, Caraci et al., 2015), we decided to focus our study on this signaling.

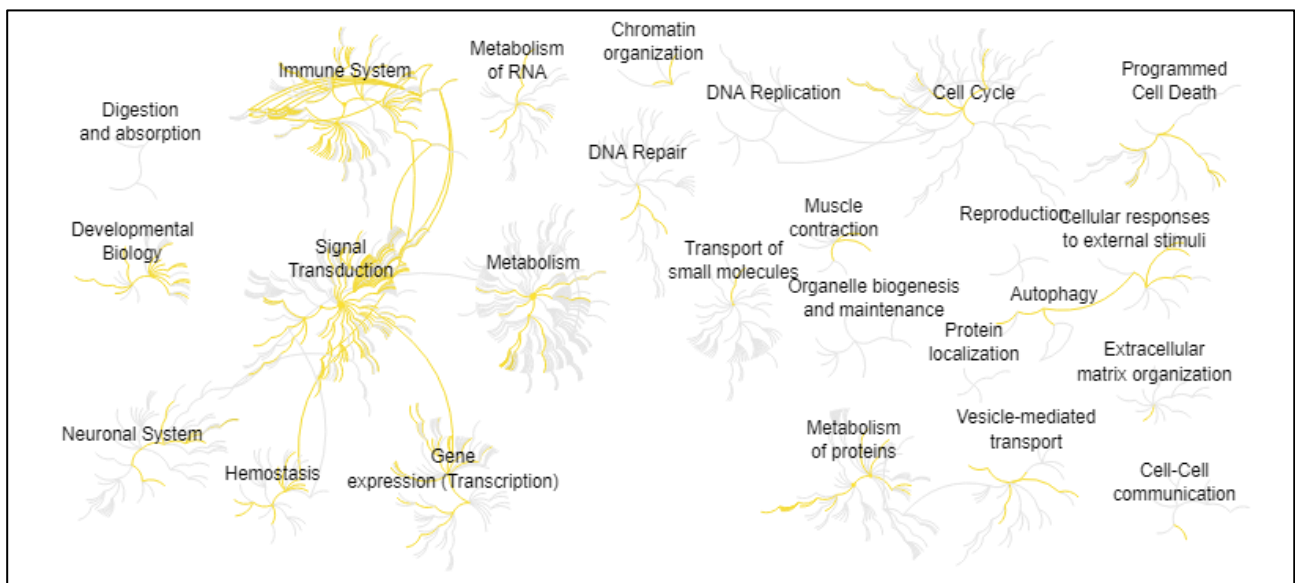


Figure 2

CDKL5-dependent pathway overview.

Graphical visualization of Reactome Pathway analysis obtained using Phospho Explorer Antibody Microarray datasets. A yellow color is applied to pathway branches for evidencing dataset coverage.

Reduced SMAD3 protein levels in the brains of *Cdk15* KO mice

Among the antibodies against the SMAD family proteins, array data obtained with the site-specific antibody against SMAD2 (Smad2 Ab-245) and that against SMAD3 (Smad3 Ab-204) suggested reduced SMAD2 and SMAD3 protein levels in the absence of *Cdk15* (Table 1). No difference in SMAD protein phosphorylation levels between *Cdk15* $-/Y$ and $+/Y$ mice was highlighted by the SMAD phospho site-specific antibodies on the array (Table 1).

PhosphoExplorer Antibody Microarray - SMAD family signals					
	KO/WT ratio	Pvalue		KO/WT ratio	Pvalue
Smad1 (Ab-187)	0,94 ± 0,10	0,560	Smad1		
Smad1 (Ab-465)	1,17 ± 0,11	0,202	P-Ser187/Smad1 (Ab-187)	1,16 ± 0,13	0,238
Smad1-mean	1,05 ± 0,12		P-Ser465/Smad1 (Ab-465)	0,70 ± 0,15	0,183
Smad2 (Ab-220)	1,13 ± 0,22	0,555	Smad2		
Smad2 (Ab-245)	0,86 ± 0,05	0,047*	P-Ser250/Smad2 (Ab-250)	0,94 ± 0,09	0,619
Smad2 (Ab-250)	0,89 ± 0,05	0,173	P-Ser467/Smad2 (Ab-467)	1,33 ± 0,29	0,286
Smad2 (Ab-255)	0,96 ± 0,11	0,732	P-Thr220/Smad2 (Ab-220)	0,91 ± 0,13	0,544
Smad2 (Ab-467)	0,83 ± 0,08	0,120	Smad2/3		
Smad2-mean	0,93 ± 0,05		P-Thr8/Smad2/3 (Ab-8)	1,13 ± 0,15	0,385
Smad2/3 (Ab-8)	0,83 ± 0,13	0,320	Smad3		
Smad3 (Ab-179)	0,96 ± 0,02	0,117	P-Ser204/Smad3 (Ab-204)	1,08 ± 0,08	0,309
Smad3 (Ab-204)	0,75 ± 0,07	0,054(*)	P-Thr213/Smad3 (Ab-213)	1,00 ± 0,17	0,972
Smad3 (Ab-213)	0,88 ± 0,13	0,480	P-Ser425/Smad3 (Ab-425)	0,93 ± 0,12	0,645
Smad3 (Ab-425)	1,02 ± 0,08	0,819	P-Thr179/Smad3 (Ab-179)	0,92 ± 0,06	0,315
Smad2-mean	0,90 ± 0,06				

Table 1

Profile of SMAD family members expression and phosphorylation in the cortex of *Cdk15* KO mice.

A summary of Phospho Explorer Antibody Microarray results for the SMAD family of proteins is presented with corresponding antibodies. *Cdk15* $-/Y$ (KO, n=3) versus *Cdk15* $+/Y$ (WT, n=3) ratio of total SMAD proteins and their phospho-isoforms are indicated with fold change, error and P value. (Unpaired t-test).

Western blot analyses were used to confirm array data. While we did not find reduced SMAD2 levels in the cortex of *Cdk15* $-/Y$ mice in comparison with $+/Y$ mice (Figure 4A), we

confirmed that SMAD3 levels are reduced both in the cortex (Figure 4B) and hippocampus (Figure 4C) of *Cdk15* $-/\gamma$ mice.

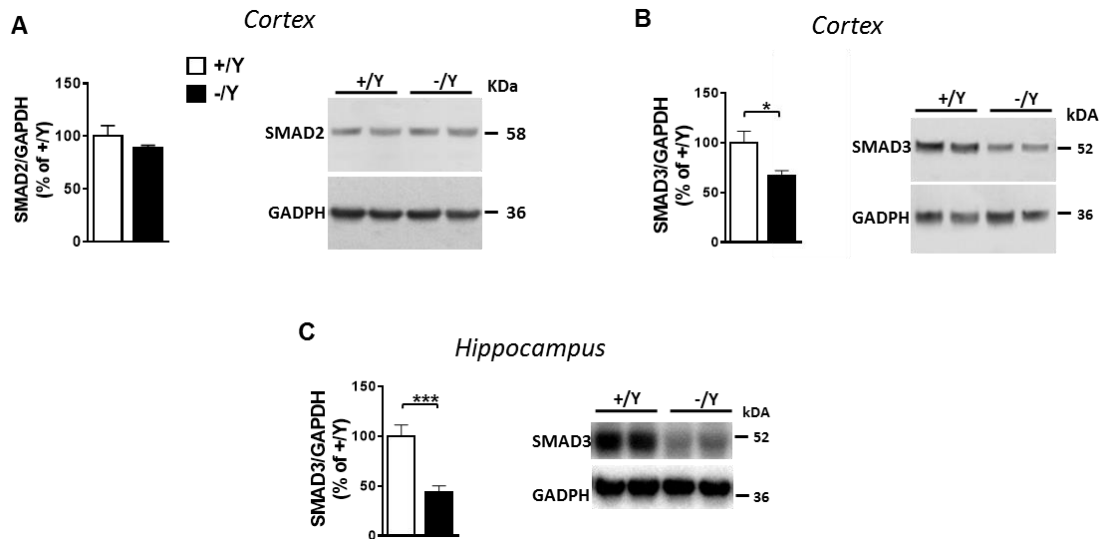


Figure 4

SMAD2 and SMAD3 levels in the cortex and hippocampus of *Cdk15* KO mice.

A: Western blot analysis of SMAD2 levels normalized to GAPDH levels in the somatosensory cortex of wild-type (+/Y; n=4) and *Cdk15* $-/\gamma$ (n=4) adult mice. **B,C:** Western blot analysis of SMAD3 levels normalized to GAPDH levels in the somatosensory cortex (B) of wild-type (+/Y; n=3) and *Cdk15* $-/\gamma$ (n=4) adult mice and in the hippocampus (C) of wild-type (+/Y; n=7) and *Cdk15* $-/\gamma$ (n=8) adult mice. Immunoblots are examples from two animals of each experimental group. Values are represented as means \pm SE. *p<0.05; **p<0.01; ***p<0.001 (Unpaired t-test).

Immunohistochemistry analyses showed that in *Cdk15* $-/\gamma$ mice, in all cortical layers, the number of SMAD3 positive cells were reduced compared to wild-type (+/Y) mice (Figure 5A,C). These latter mice exhibited a strong SMAD3 immunopositivity, whereas *Cdk15* $-/\gamma$ mice showed a moderate SMAD3 immunopositivity both in the cortex (Figure 5A,D) and hippocampus (Figure 5B,D).

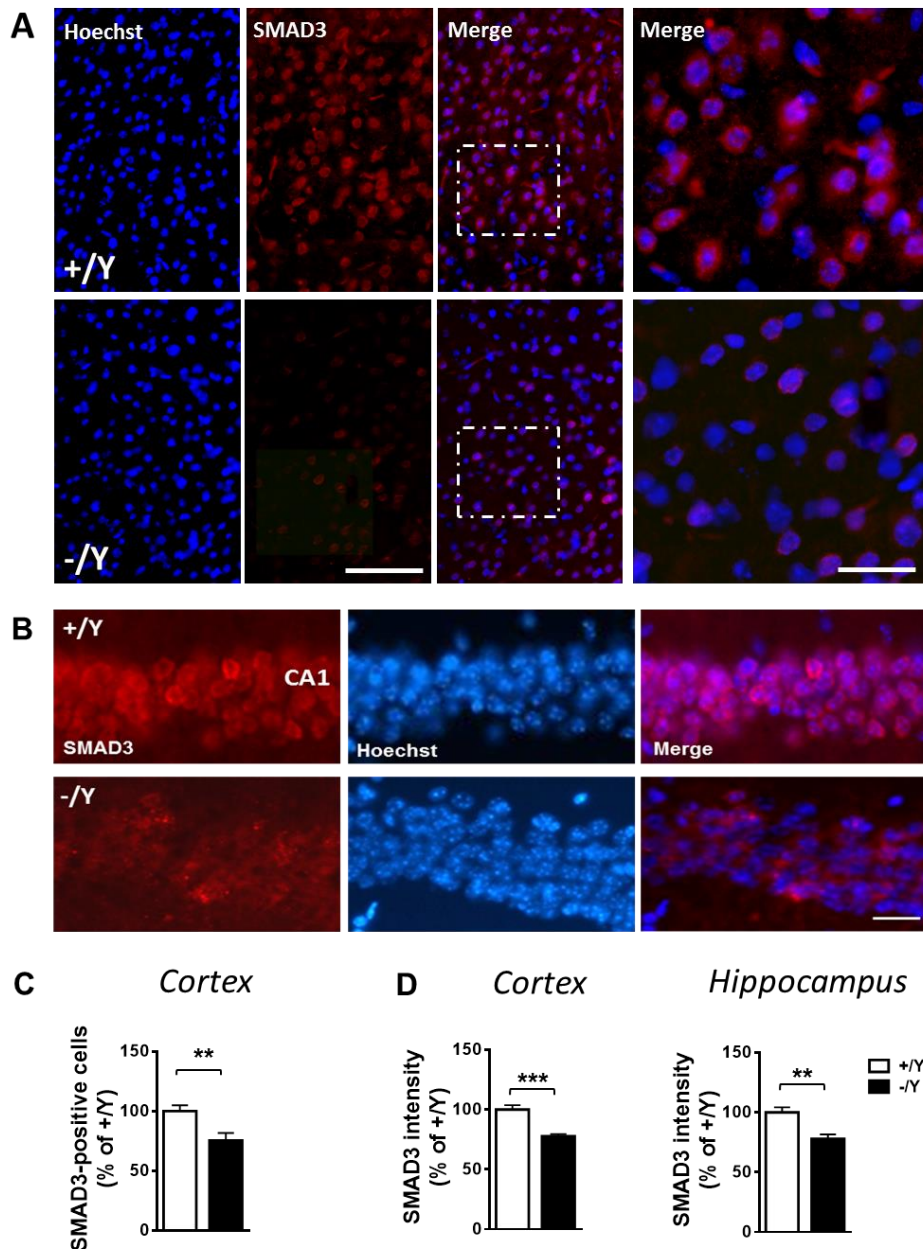


Figure 5

Reduced SMAD3 levels in the cortex and hippocampus of *Cdk15* KO mice.

A,B: Representative images of cortical sections (A) and hippocampal sections at the CA1 field level (B) processed for fluorescent SMAD3 immunostaining of wild-type (+/Y) and *Cdk15* -/Y mice. The dotted boxes indicate the regions shown at a higher magnification. (A) Scale bar = 50 μ m lower magnification, 15 μ m higher magnification. (B) Scale bar = 40 μ m. **C:** Number of SMAD3 positive cells in the somatosensory cortex of wild-type (+/Y; n=10) and *Cdk15* -/Y (n=7) adult mice. **D:** SMAD3 nuclear signal intensity in the cortex and hippocampus of wild-type (+/Y; n=4, n=8 respectively) and *Cdk15* -/Y (n=4, n=8 respectively) mice. Values are represented as means \pm SE. **p<0.01, ***p<0.001 (Unpaired t-test).

As suggested by the array data (Table 1), we did not observe a difference in SMAD3 phosphorylation levels at Ser213 and Ser425 in the cortex of *Cdkl5* $-/Y$ mice in comparison with $+/Y$ mice (Figure 6A,B).

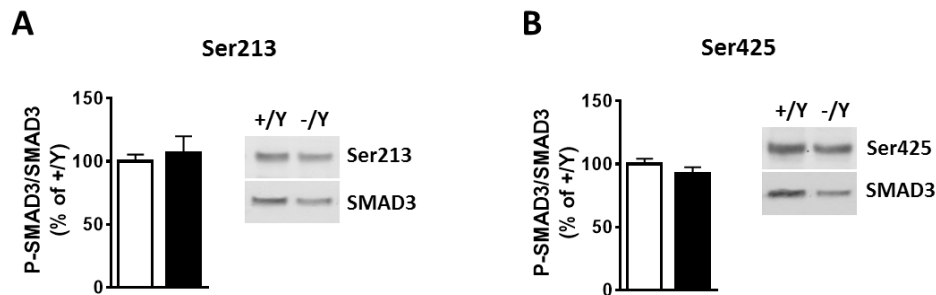


Figure 6

SMAD3 phosphorylation levels at Ser213 and Ser425 in the cortex of *Cdkl5* $-/Y$ mice.

A,B: Western blot analysis of P-SMAD3 (Ser213 (A) and Ser425 (B)) levels normalized to SMAD3 levels in the somatosensory cortex of wild-type ($+/Y$; n=4) and *Cdkl5* $-/Y$ (n=4) adult mice. Immunoblots are examples from one animal of each experimental group. Values are represented as means \pm SE. (Unpaired t-test).

SMAD3 is regulated at the mRNA level and at the level of protein stability (Poncelet et al., 2007, Daly et al., 2010). No differences in SMAD3 mRNA levels were observed between *Cdkl5* $-/Y$ and $+/Y$ mice in either the cortex (Figure 7A) or hippocampus (Figure 7B), suggesting a CDKL5-dependent post-transcriptional regulation of SMAD3.

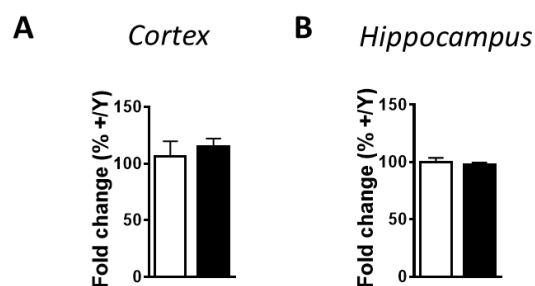


Figure 7

SMAD3 mRNA levels in the cortex and hippocampus of *Cdkl5* $-/Y$ mice.

A,B: Quantification by RT-qPCR of *SMAD3* expression in the somatosensory cortex (A) and hippocampus (B) of wild-type ($+/Y$; n=5, n=8 respectively) and *Cdkl5* $-/Y$ (n=6, n=8 respectively) mice. Data are expressed as a percentage of the values of *Cdkl5* $+/Y$ mice. Values are represented as means \pm SE. (Unpaired t-test).

SMAD3 physically interacts with CDKL5

SMAD3, together with SMAD2, is one of the primary mediators of TGF- β action (Feng and Derynck, 2005, Hill, 2009, Macias et al., 2015). Upon phosphorylation by the TGF- β receptors, the SMAD proteins translocate into the nucleus, where they regulate transcription (Inman, 2005).

To establish whether SMAD3 and CDKL5 physically interact *in vivo*, we performed co-immunoprecipitation assays from cell lysates of HEK293T cells transfected with both HA-CDKL5 and SMAD3-FLAG. Using an anti-FLAG antibody, we found co-immunoprecipitation of SMAD3 and CDKL5, indicating their interaction (Figure 8B; lane 4 arrow). SMAD3 consists of two highly conserved MAD homology domains, in the amino (MH1) and carboxyl (MH2) termini, that are connected by a proline-rich non-conserved linker region (Figure 8A). To identify the SMAD3 domain that interacts with CDKL5, FLAG-tagged SMAD3 deletion constructs (Figure 8A), FLAG-MH1 (amino acids 1–136) and FLAG-L-MH2 (amino acids 136–425), were co-transfected with HA-CDKL5 into HEK293T cells. As shown in figure 8B, CDKL5 interacted with the SMAD3 deletion construct MH1 (Figure 8B; lane 6 arrow), but not with the L-MH2 construct (Figure 8B; lane 8), indicating that the association of CDKL5 and SMAD3 in cells is mediated via the N-terminal MH1 domain of SMAD3. To confirm the interaction of CDKL5 with SMAD3 in cells, we also performed co-immunoprecipitation experiments with endogenous SMAD3 protein in SH-SY5Y cells, a neuroblastoma cell line that exhibits relatively high basal levels of SMAD3 (Figure 8C,D). We infected SH-SY5Y cells with CDKL5-FLAG adenovirus particles (Figure 8C) or transfected SH-SY5Y cells with CDKL5-FLAG plasmid (Figure 8D) and precipitated the overexpressed protein from the cell extracts with anti-FLAG antibodies (Figure 8C,D). Subsequent immunoblotting with an anti-SMAD3 antibody revealed that endogenous SMAD3 co-precipitated with overexpressed CDKL5-FLAG (Figure 8C,D). As control of IPs we used GFP (Fig. 8C) or an empty vector (data not shown).

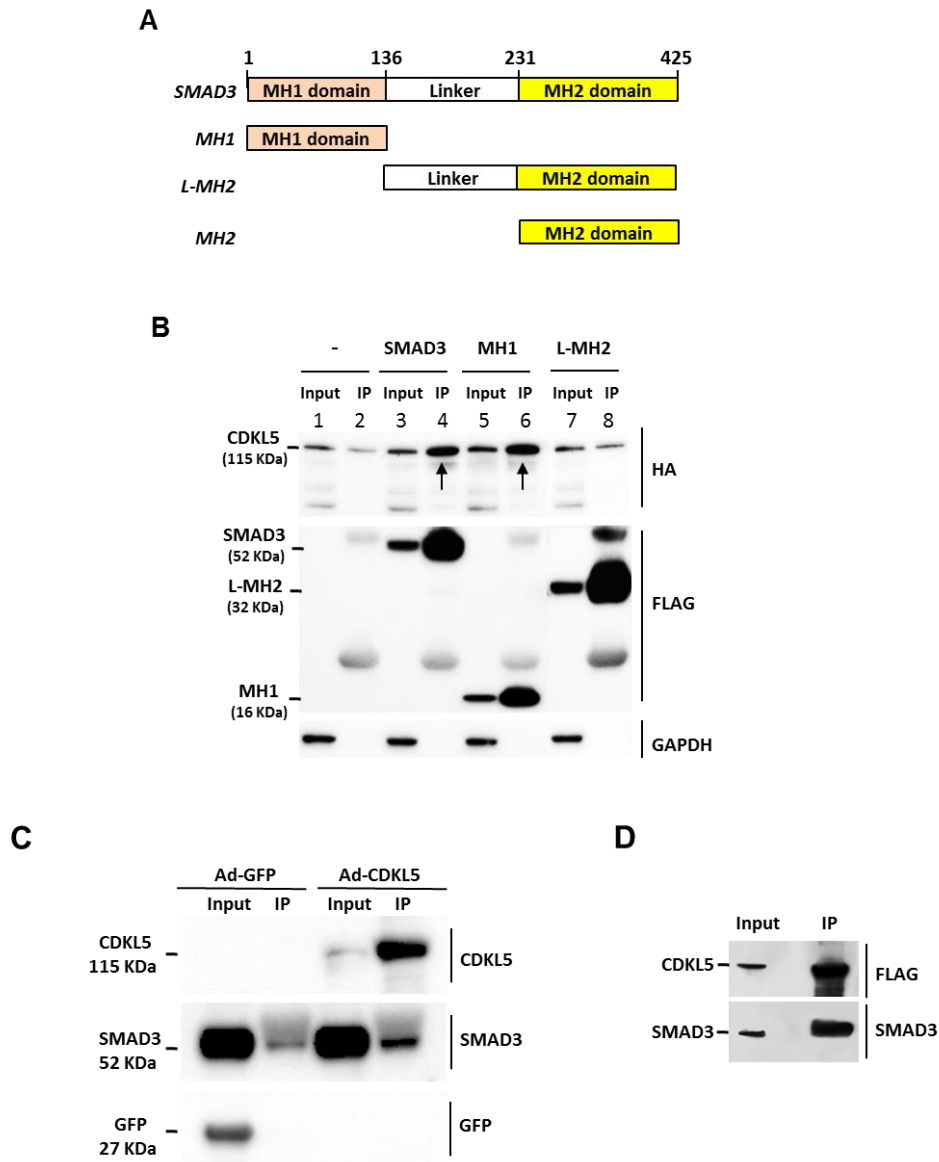


Figure 8

CDKL5 interacts with SMAD3 protein.

A: Schematic representation of SMAD3 and mutant SMAD3 domains. The locations of MH1 domain (brown), linker region, and MH2 domain (yellow) are shown. **B:** Interaction between CDKL5 and SMAD3. HEK293T cells were co-transfected with HA-CDKL5 and wild-type SMAD3-FLAG or the indicated SMAD3 mutant-FLAG plasmids, and cell lysates (Input) were immunoprecipitated with anti-FLAG antibodies (IP). GAPDH was used as an internal control for Input. Immunoprecipitated proteins were detected by anti-HA (CDKL5) and anti-FLAG antibodies (SMAD3 and SMAD3 mutants). Arrows indicate co-immunoprecipitated CDKL5. Lysates of cells overexpressing only HA-CDKL5 (Input; lane 1) were immunoprecipitated with anti-FLAG antibodies as a control (IP; lane 2). **C,D:** SH-SY5Y cells were infected with CDKL5-FLAG adenoviral particles or GFP adenoviral particles as control in C, and SH-SY5Y cells were transfected with CDKL5-FLAG vector in D. Cells were lysed (Input) and immunoprecipitated with anti-FLAG antibodies (IP). Immunoprecipitated CDKL5, SMAD3 and GFP were detected by anti-CDKL5, anti-SMAD3 and anti-GFP antibodies, respectively.

SMAD3 is a phosphorylation target of CDKL5

To determine whether SMAD3 is a direct phosphorylation substrate for CDKL5, we immunoprecipitated overexpressed SMAD3 from transfected HEK293T cells and incorporated it into a reaction mixture containing [γ -³²P] ATP, in the presence of increasing concentrations of the CDKL5 kinase domain (amino acids 1-498; CDKL5 Δ C). We observed a CDKL5 Δ C dose-dependent increase in SMAD3 phosphorylation (Figure 9A), indicating that SMAD3 is a direct CDKL5 phosphorylation target. To determine the critical domain in SMAD3 phosphorylated by CDKL5, the SMAD3 deletion constructs MH1, L-MH2, and MH2 were incubated with CDKL5 Δ C. While L-MH2 and MH2 were not phosphorylated in the presence of CDKL5, MH1 was highly phosphorylated (Figure 9A). Confirming previous evidence (Lin et al., 2005, Bertani et al., 2006), we found that CDKL5 Δ C exhibits autophosphorylation activity, which increased in the presence of a target protein (Figure 9A). The increased efficiency of the MH1 domain phosphorylation by CDKL5 could be explained by the absence of structural constraints in the MH1 domain that could allow for a more open conformation of the domain compared to the one in the full-length SMAD3 protein (Kurisaki et al., 2001). At the same time, the increased association between CDKL5 and the target could then trigger a proximity effect of CDKL5 kinase monomers that could explain the higher CDKL5 autophosphorylation signal (Beenstock et al., 2016).

SMAD3 and SMAD2 are closely related TGF- β downstream effectors with 92% amino acid sequence similarity (Brown et al., 2007). To investigate whether CDKL5 specifically phosphorylates SMAD3 and not SMAD2, we compared the effect of wild-type CDKL5 kinase activity on SMAD3 and SMAD2. Full-length CDKL5 phosphorylated SMAD3, similarly to CDKL5 Δ C, but did not phosphorylate SMAD2 (Figure 9B), indicating a specific CDKL5/SMAD3 interaction.

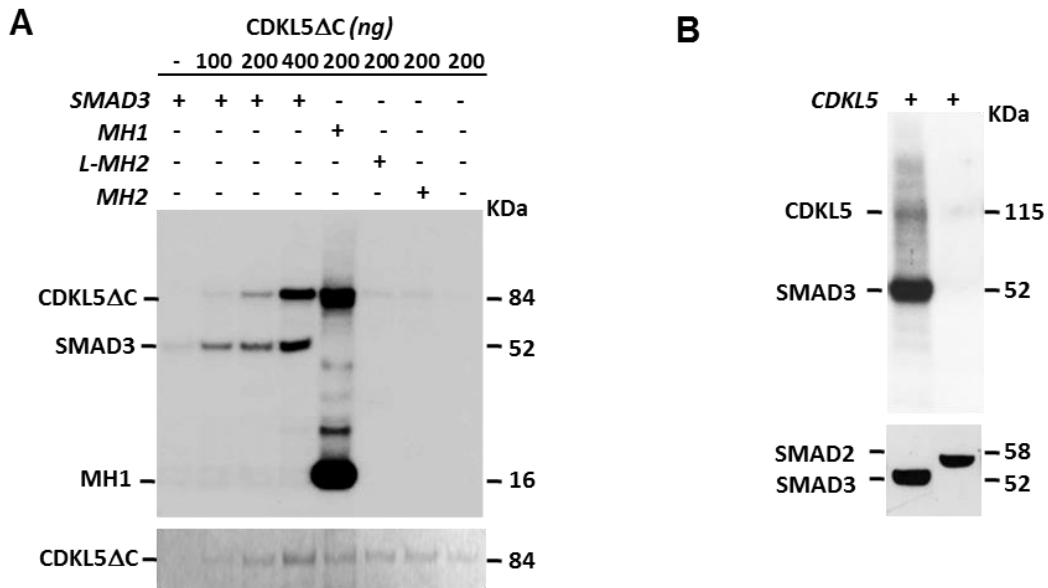


Figure 9
CDKL5 phosphorylates SMAD3.

A: CDKL5 phosphorylates SMAD3 at the MH1 domain. Kinase assays were conducted with purified CDKL5ΔC (1-498aa) and SMAD3 or SMAD3 mutants (Fig. 8A). Samples were resolved by SDS-PAGE, transferred onto nitrocellulose membrane and exposed to film by autoradiography. CDKL5ΔC was detected with PonceauS staining (lower panel). **B:** Immunoprecipitated FLAG-tagged wild-type CDKL5 was subjected to an *in vitro* kinase assay to test its ability to phosphorylate purified SMAD3 and SMAD2 (see Materials and Methods). Samples were resolved by SDS-PAGE, transferred onto nitrocellulose membrane and exposed to film by autoradiography. The same membrane was subjected to immunoblot analyses using anti- SMAD3 and SMAD2 antibodies.

CDKL5-mediated phosphorylation of SMAD3 is required for SMAD3 protein stability

Various types of phosphorylation of SMAD3, mediated by protein kinases and phosphatases, have been reported to affect its activity, stability, and localization in cells (Wrighton et al., 2009, Tarasewicz and Jeruss, 2012, Xu et al., 2012). SMAD3 regulates transcription of genes by binding to specific sequences within the promoter of target genes and by interacting with other proteins (Shi and Massague, 2003). To explore whether CDKL5-dependent phosphorylation affects the transcriptional activity of SMAD3, we performed assays with a luciferase reporter that is sensitive to SMAD3 (Figure 10A). CAGA(12)-luc reporter, containing CAGA elements in the

promoter which bind activated SMAD3 (Dennler et al., 1998), was transfected into SH-SY5Y cells. Expression of CDKL5 did not modify luciferase activity in SH-SY5Y cells (Figure 10A), indicating that CDKL5 does not directly affect SMAD3 transcriptional activity. Treatment with TGF- β 1 strongly increased SMAD3 transcriptional activity (Figure 10A), while treatment with SB431542 (SB), a potent and specific inhibitor of TGF- β receptor, decreased SMAD3 transcriptional activity (Figure 10A), indicating the presence of a functional TGF- β /SMAD3 signaling in SH-SY5Y cells.

Since phosphorylation levels could affect SMAD3 basal turnover and protein stability (Inoue et al., 2004, Waddell et al., 2004, Kim et al., 2005, Guo et al., 2008) we hypothesized that CDKL5-dependent phosphorylation of SMAD3 might affect SMAD3 protein levels. To support this hypothesis, we over-expressed CDKL5 or GFP as a control in SH-SY5Y neuroblastoma cells. We found higher SMAD3 protein levels in cells expressing CDKL5, compared to SH-SY5Y cells that were not infected or expressing GFP (Figure 10B). Similarly, in a neuroblastoma cell line, SKNBE, that does not express endogenous CDKL5 (Valli et al., 2012), we found that the stability of co-expressed SMAD3 protein was affected by whether it was CDKL5 or CDKL5 lacking the kinase domain (CDKL5 Δ N) that was expressed (Figure 10C). We found higher SMAD3 protein levels in SKNBE cells expressing CDKL5, compared to cells expressing CDKL5 Δ N (Figure 10C).

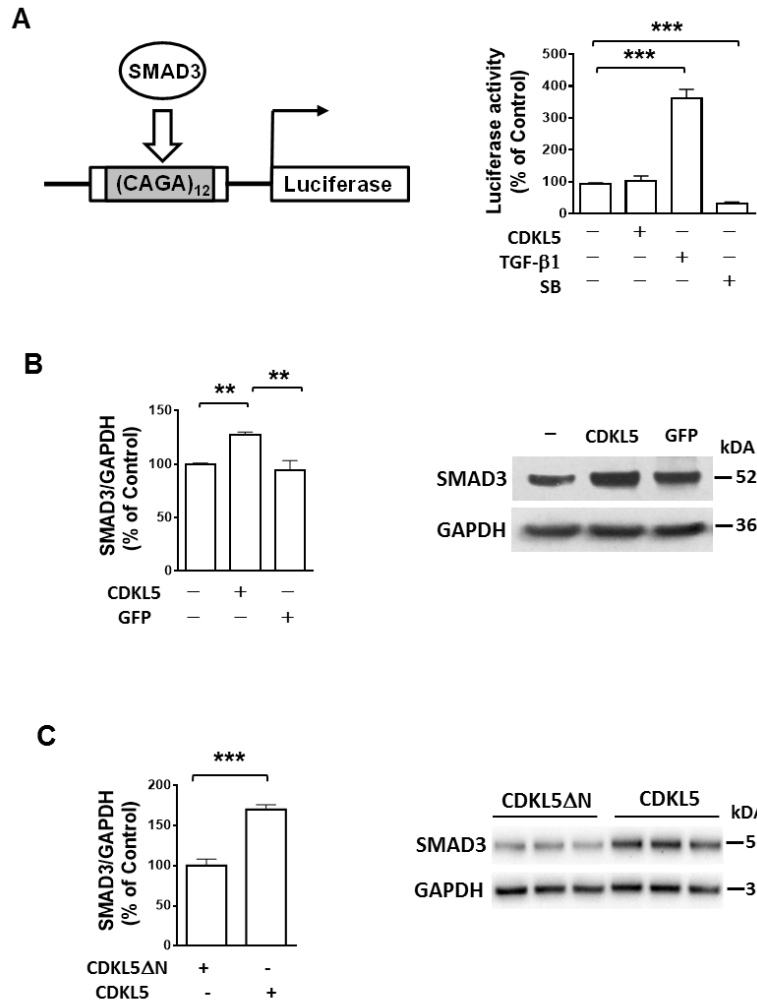


Figure 10

CDKL5 regulates SMAD3 protein levels.

A: Luciferase reporter analysis of SMAD3-dependent promoter (CAGA₁₂-luc reporter; schematic representation in the upper panel) in SH-SY5Y cells transfected with CDKL5 or treated with TGF-β1 (5 ng/ml) or SB431542 (SB; 10 μM). **B:** Western blot analysis of SMAD3 levels normalized to GAPDH levels in SH-SY5Y cells infected with CDKL5 adenoviral particles (Ad-CDKL5; n=3), with GFP adenoviral particles (Ad-GFP; n=3), or not infected (n=3). Immunoblots (upper panel) are examples from each experimental group. **C:** Western blot analysis of SMAD3 levels normalized to GAPDH levels in SKNBE cells co-transfected with CDKL5ΔN (n=4) or wild-type CDKL5 (n=4) and SMAD3. Immunoblots (upper panel) are three examples from each experimental group. Data are expressed as a percentage of the values of control samples. Values are represented as means ± SE. **p<0.01; ***p<0.001 (Unpaired t-test in C; Fisher's LSD after ANOVA in A,B).

Reduced SMAD3 protein levels in hippocampal neurons from Cdkl5 KO mice

As observed *in vivo* in *Cdkl5* $-/Y$ mice (Figure 5), we found reduced SMAD3 levels in hippocampal cultures from *Cdkl5* $-/Y$ mice compared to wild-type mice (Figure 11A-C), which were paralleled by a reduced SMAD3 nuclear intensity (Figure 11D). Re-expression of CDKL5 in *Cdkl5* $-/Y$ neurons restored SMAD3 protein levels (Figure 11B,C) and, consequently, its nuclear intensity (Figure 11D), suggesting a CDKL5-dependent regulation of SMAD3 protein levels. In a similar way, treatment with TGF- β 1 was able to restore SMAD3 nuclear intensity in *Cdkl5* $-/Y$ hippocampal neurons (Figure 11E).

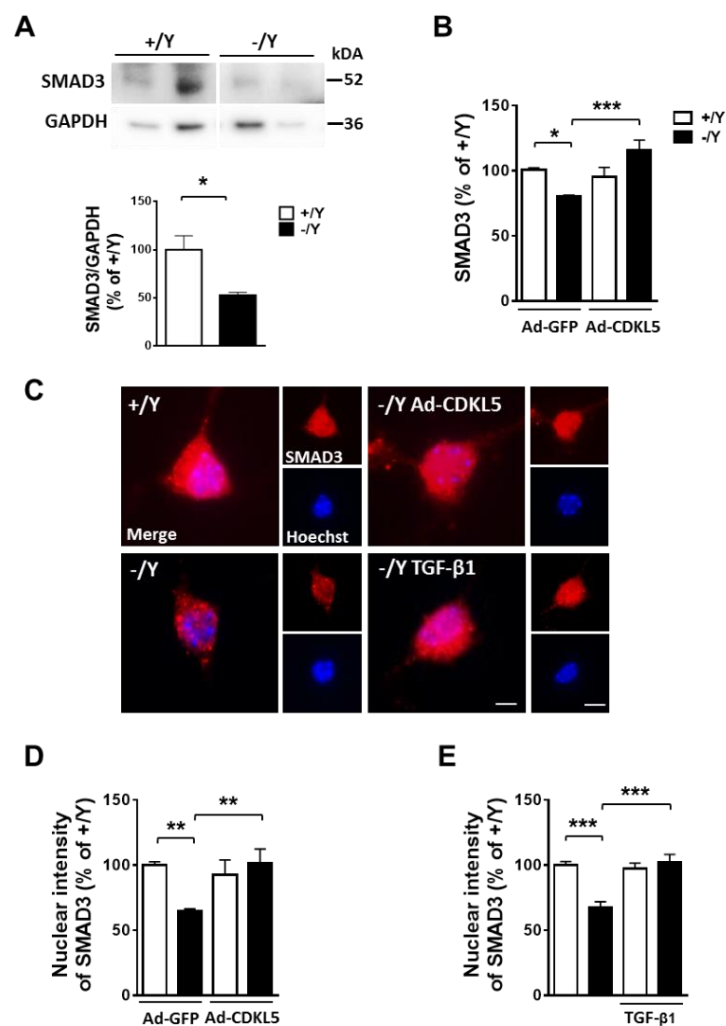


Figure 11

Reduced SMAD3 protein levels in hippocampal neurons from *Cdkl5* $-/Y$ mice.

A: Western blot analysis of SMAD3 levels in 10-day (DIV10) differentiated hippocampal neurons from wild-type (+/Y, n=5) and *Cdkl5* $-/Y$ (n=6) mice. Immunoblots (upper panel) are

two examples from each experimental group. **B:** Quantification of SMAD3 signal intensity in hippocampal neurons infected with adenoviral particle for GFP (Ad-GFP; +/Y n=5, -/Y n=4) or CDKL5 (Ad-CDKL5; +/Y n=5, -/Y n=4). **C:** Representative fluorescent images of 10-day (DIV10) differentiated hippocampal neurons from wild-type (+/Y) and *Cdkl5* -/Y mice immunopositive for SMAD3 and counterstained with Hoechst. SMAD3 localizes both in the nucleus and in the cytoplasm. *Cdkl5* -/Y hippocampal cultures were infected with adenoviral particle for CDKL5 (Ad-CDKL5) or GFP as a control (Ad-GFP) on DIV3, or treated with TGF- β 1 (1 ng/ml) administered on alternate days starting from DIV2. Scale bar = 1.5 μ m higher magnification, 6 μ m lower magnification. **D,E:** Quantification of SMAD3 nuclear signal intensity in hippocampal neurons infected with adenoviral particles for GFP (Ad-GFP ; +/Y n=5, -/Y n=4) or CDKL5 (Ad-CDKL5; +/Y n=5, -/Y n=4) in D and untreated (+/Y n=5, -/Y n=5) or treated with TGF- β 1 (+/Y n=4, -/Y n=5) in E. Data are expressed as a percentage of the values of control samples. Values are represented as means \pm SE. *p<0.05; **p<0.01; ***p<0.001 (Unpaired t-test in A; Fisher's LSD after ANOVA in B,D,E).

In agreement with reduced SMAD3 nuclear levels, we found a decreased SMAD3-dependent transcriptional activity in hippocampal cultures from *Cdkl5* -/Y mice compared to wild-type mice (Figure 12A). Treatment with TGF- β 1 in *Cdkl5* -/Y neurons restored SMAD3 activity to control levels (Figure 12A).

Increased TGF- β 1-induced SMAD3 transcriptional activity is mediated by TGF- β type I receptor-induced SMAD3 phosphorylation at the Ser213 site in the linker region (Bruce and Sapkota, 2012). As expected we found increased SMAD3 phosphorylation at Ser213 in hippocampal cultures from both *Cdkl5* KO and wild-type mice treated with TGF- β 1 (Figure 12B,C).

Differently, as observed *in vivo* in *Cdkl5* -/Y mice (Figure 6A), a lack of *Cdkl5* did not affect SMAD3 phosphorylation at Ser213 in hippocampal cultures (Figure 12B,C), suggesting that TGF- β 1 furthers SMAD3 activity through a CDKL5-independent pathway.

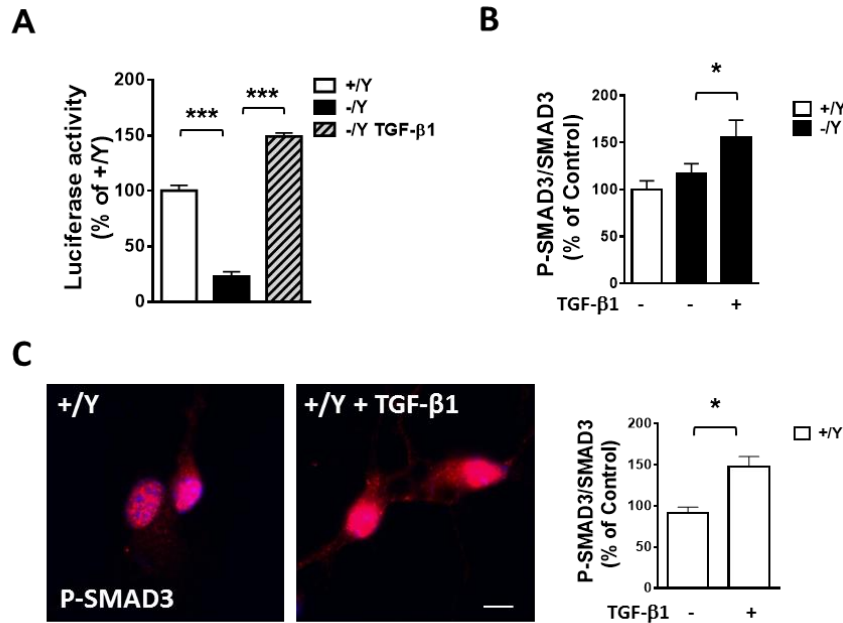


Figure 12

Decreased SMAD3-dependent transcriptional activity in *Cdkl5* KO hippocampal neurons is restored by treatment with TGF-β1.

A: Luciferase reporter analysis of SMAD3-dependent promoter in primary hippocampal neurons from wild-type (+/Y, n=5) and *Cdkl5* -/Y (n=5) mice and in *Cdkl5* -/Y cultures treated with TGF-β1 (5 ng/ml; n=5). **B:** Western blot analysis of P-SMAD3 (Ser213) levels normalized to SMAD3 levels in untreated hippocampal cultures (+/Y = 9; -/Y = 14) or treated for 1h with TGF-β1 (-/Y = 8). **C:** Representative fluorescent images of 10-day (DIV10) differentiated hippocampal neurons from wild-type (+/Y) mice immunopositive for P-SMAD3 (Ser213) and counterstained with Hoechst. *Cdkl5* +/Y hippocampal cultures were treated with TGF-β1 (1 ng/ml) for 1h. Scale bar = 2.5 μm. Quantification of P-SMAD3 (Ser213) signal intensity in untreated (+Y n=2) or TGF-β1 treated (+Y n=2) hippocampal neurons. Values are represented as means ± SE. *p<0.05; ***p<0.001 (Unpaired t-test in C; Fisher's LSD after ANOVA in A,B).

Restoration of TGF-β/SMAD3 signaling in primary hippocampal neurons from *Cdkl5* KO mice recovers neuronal survival and maturation

Based on evidence that TGF-β/SMAD signaling regulates many physiological processes in the brain, including neuronal survival, development, and activity (Dobolyi et al., 2012), we sought to investigate whether restoration of TGF-β/SMAD3 signaling improves the neurodevelopmental alterations that characterize *Cdkl5* -/Y hippocampal neurons (Fuchs et al., 2014a, Fuchs et al., 2015, Trazzi et al., 2016).

The assessment of apoptotic cell death revealed that differentiating hippocampal neurons generated from *Cdkl5* $-/Y$ mice had more apoptotic (cleaved caspase-3 positive) cells compared to control cultures (Figure 13A). We found that treatment with TGF- β 1 restored the number of cleaved caspase-3 positive cells in hippocampal cultures from *Cdkl5* $-/Y$ mice (Figure 13A), suggesting that TGF- β /SMAD3 signaling plays a role in CDKL5-dependent neuronal survival. As expected, the re-expression of CDKL5 restored the number of apoptotic cells in hippocampal cultures from *Cdkl5* $-/Y$ mice (Figure 13B).

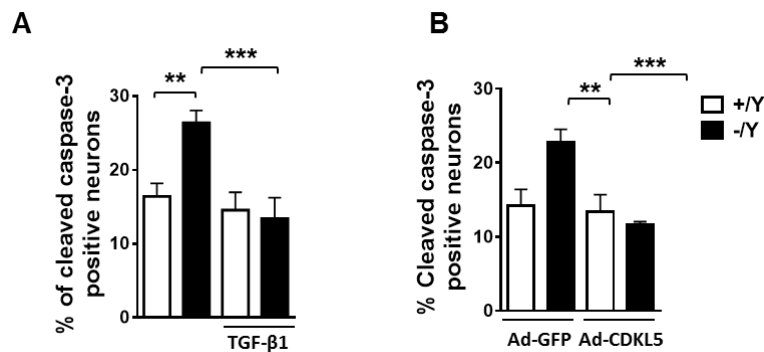


Figure 13

TGF- β 1 treatment and CDKL5 replacement restores *Cdkl5* KO hippocampal neuron survival.

A,B: Percentage of cleaved caspase-3 positive neurons in 4-day (DIV4) differentiated hippocampal neurons from wild-type (+/Y n=5) and *Cdkl5* $-/Y$ (n=5) mice treated with TGF- β 1 in A or infected with adenoviral particles for GFP (AdGFP) or CDKL5 (AdCDKL5) in B. Values are represented as means \pm SE. **p<0.01; ***p<0.001 (Fisher's LSD after ANOVA).

Hippocampal neurons from *Cdkl5* $-/Y$ mice are characterized by reduced axon (Figure 14A,B; (Nawaz et al., 2016)) and neurite (Figure 14C,D; (Trazzi et al., 2016)) outgrowth. We found that treatment with TGF- β 1 restored primary axon length in hippocampal neurons from *Cdkl5* $-/Y$ mice (Figure 14A,B), but did not improve the reduced neurite outgrowth (Figure 14A,D), suggesting that the TGF- β signal has a specific involvement in axonal development. The re-expression of CDKL5 restored both primary axon length and neurite outgrowth (Figure 14C,E).

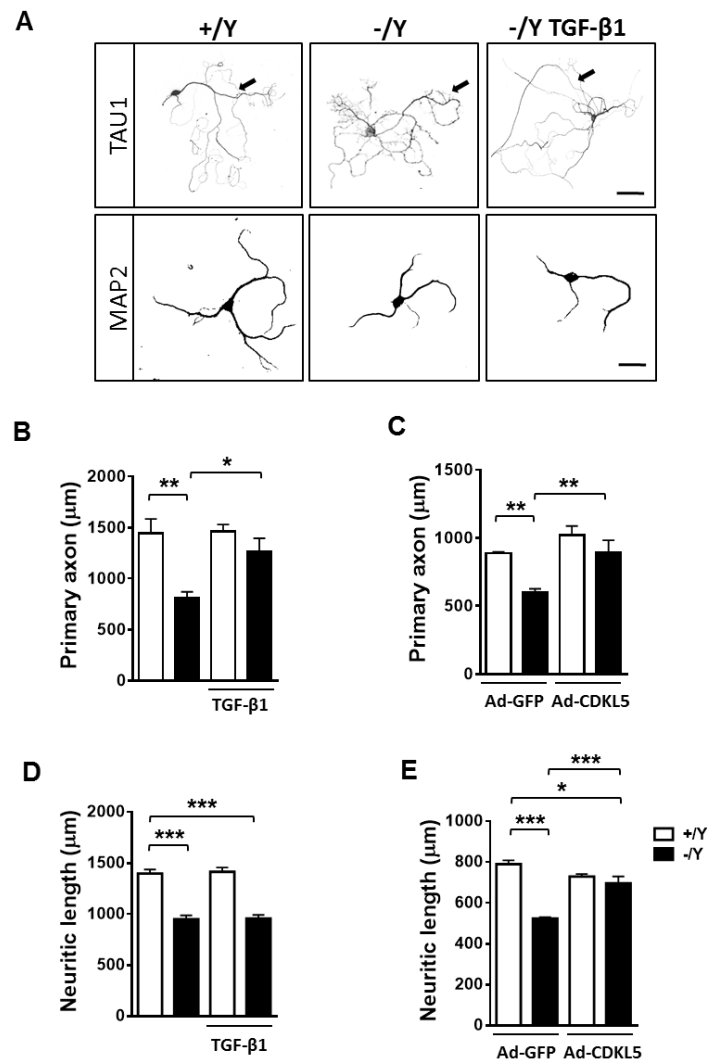


Figure 14

TGF-β1 treatment and CDKL5 replacement restores *Cdk15* KO hippocampal neuron maturation.

A: Representative images of 10-day (DIV10) differentiated +/Y and -/Y hippocampal neurons and -/Y hippocampal neurons treated with TGF-β1, immunopositive for the axon marker TAU1 (upper panel; scale bar = 50 μm, arrows indicate the primary axon), or microtubule-associated protein 2 (MAP2; scale bar = 30 μm). **B-E:** Quantification of the length of the primary axon (B,C, TAU1-positive; +/Y=4, -/Y=4), and the total length of MAP2-positive neurites (D,E, +/Y=6, -/Y=6), from differentiated hippocampal cultures from *Cdk15* +/Y and *Cdk15* -/Y mice. (B,D) Hippocampal culture were treated as in A or (C,E) infected with adenoviral particles for GFP (AdGFP) or CDKL5 (AdCDKL5). Values are represented as means ± SE. *p<0.05; **p<0.01; ***p<0.001 (Fisher's LSD after ANOVA).

As previously reported (Trazzi et al., 2016), the assessment of synaptophysin (SYN) puncta in neurites revealed that hippocampal neurons from *Cdk15* -/Y mice had a reduction in the number

of presynaptic connections (Figure 15A,B). Treatment with TGF- β 1 restored the number of SYN puncta in hippocampal neurons from *Cdkl5* -/Y mice (Figure 15A,B).

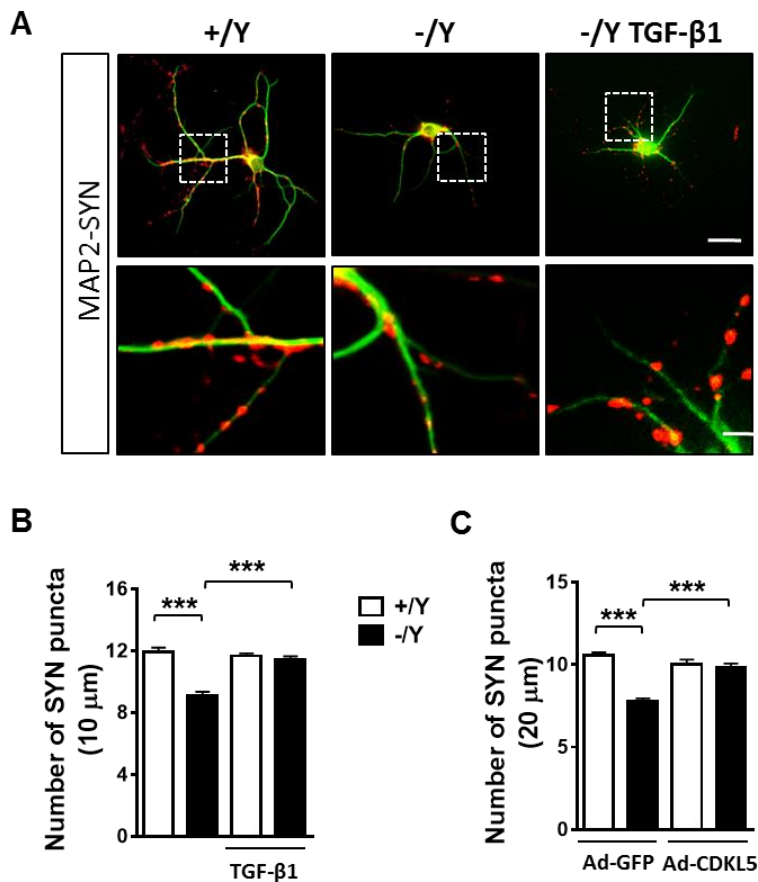


Figure 15

TGF- β 1 treatment and CDKL5 replacement restores *Cdkl5* KO hippocampal neuron connectivity.

A: Representative images of 10-day (DIV10) differentiated +/Y and -/Y hippocampal neurons and -/Y hippocampal neurons treated with TGF- β 1, immunopositive for microtubule-associated protein 2 (MAP2, green) plus synaptophysin (SYN, red). The dotted boxes indicate the regions shown at a higher magnification. Scale bar = 30 μ m lower magnification, 2.5 μ m higher magnification. **B,C:** Quantification of the number of SYN-immunoreactive puncta per 10 μ m in proximal dendrites (+/Y=6, -/Y=6) from differentiated hippocampal cultures from *Cdkl5* +/Y and *Cdkl5* -/Y mice. (B) Hippocampal cultures were treated as in A or (C) infected with adenoviral particles for GFP (AdGFP) or CDKL5 (AdCDKL5). Values are represented as means \pm SE. *** p <0.001 (Fisher's LSD after ANOVA).

To confirm the reduced number of synaptic connections, we evaluated the number of neuritic spine, labeled by MAP2 immunocytochemistry (Morales and Fifkova, 1989). We found a

reduced spine density in hippocampal neurons from *Cdkl5* $-/Y$ mice compared to those of control cultures (Figure 16A,B). Treatment with TGF- β 1 restored the density of dendritic spines in hippocampal neurons from *Cdkl5* $-/Y$ mice (Figure 16A,B). As expected, the re-expression of CDKL5 restored synaptic connections (Figures 15C and 16C). In control neurons treatment with TGF- β 1 or increased CDKL5 levels had no effect on neuronal survival (Figure 13B), axon and neurite growth (Figure 14B,D), or connectivity (Figures 15B and 16B).

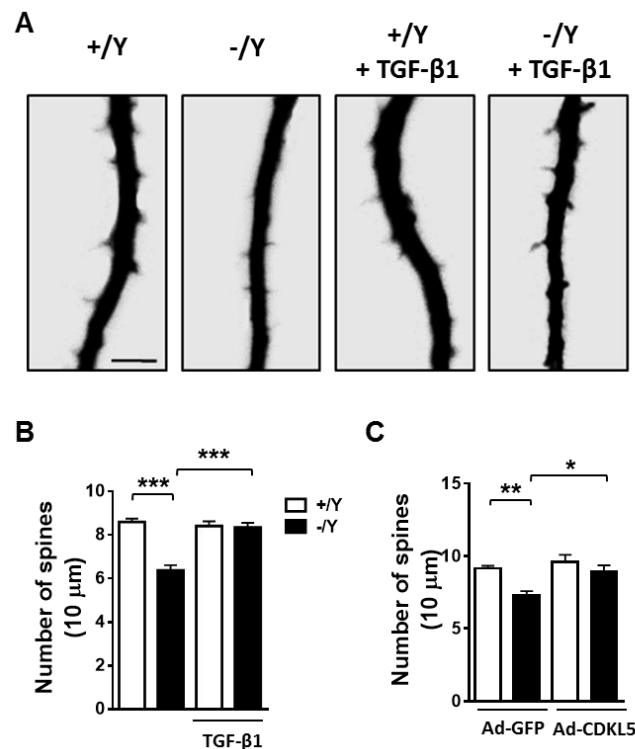


Figure 16

TGF- β 1 treatment and CDKL5 replacement restores spine density in *Cdkl5* KO hippocampal neuron.

A: Representative fluorescence images of proximal dendrite segments of hippocampal neurons treated with TGF- β 1 that were immunopositive for microtubule-associated protein 2 (MAP2) showing spine protrusions. Scale bar = 2.5 μ m. **B,C:** Quantification of the number of MAP2-positive spines ($+/Y=6$, $-/Y=6$) from differentiated hippocampal cultures from *Cdkl5* $+/Y$ and *Cdkl5* $-/Y$ mice treated with TGF- β 1 in B or infected with adenoviral particles for GFP (AdGFP) or CDKL5 (AdCDKL5) in C. Values are represented as means \pm SE. * $p<0.05$; ** $p<0.01$; *** $p<0.001$ (Fisher's LSD after ANOVA).

Increased susceptibility to neurotoxic stress in primary hippocampal neurons from *Cdkl5* KO mice is rescued by treatment with TGF- β 1.

Primary hippocampal neurons are known to be susceptible to excitotoxicity and oxidative stress, which lead to the induction of apoptotic cell death (Hwang et al., 2008, Chen et al., 2009, Wang et al., 2014, Calvo et al., 2015). Numerous studies have shown a protective effect of TGF- β signaling against various toxins and injurious agents in cultured neurons (Flanders et al., 1998, Unsicker and Kriegstein, 2000, Brionne et al., 2003). To test the hypothesis that CDKL5, with its function on TGF- β /SMAD3 signaling regulation, is required for neuronal apoptotic resistance, we exposed hippocampal neuronal cultures from *Cdkl5* $-/Y$ mice to an oxidative stress (100 μ M H₂O₂) or an excitotoxic stimulus (100 μ M NMDA). Apoptotic cell death was evaluated using cleaved caspase-3 immunocytochemistry or Hoechst staining to visualize pyknotic nuclei. Interestingly, neuronal vulnerability to H₂O₂- or NMDA-induced apoptosis was higher in hippocampal neurons from *Cdkl5* $-/Y$ mice in comparison with control neurons (Figure 17A-C). Treatment with TGF- β 1 after H₂O₂ or NMDA exposure prevented apoptosis in hippocampal neuronal cultures from *Cdkl5* $-/Y$ mice (Figure 17A-C).

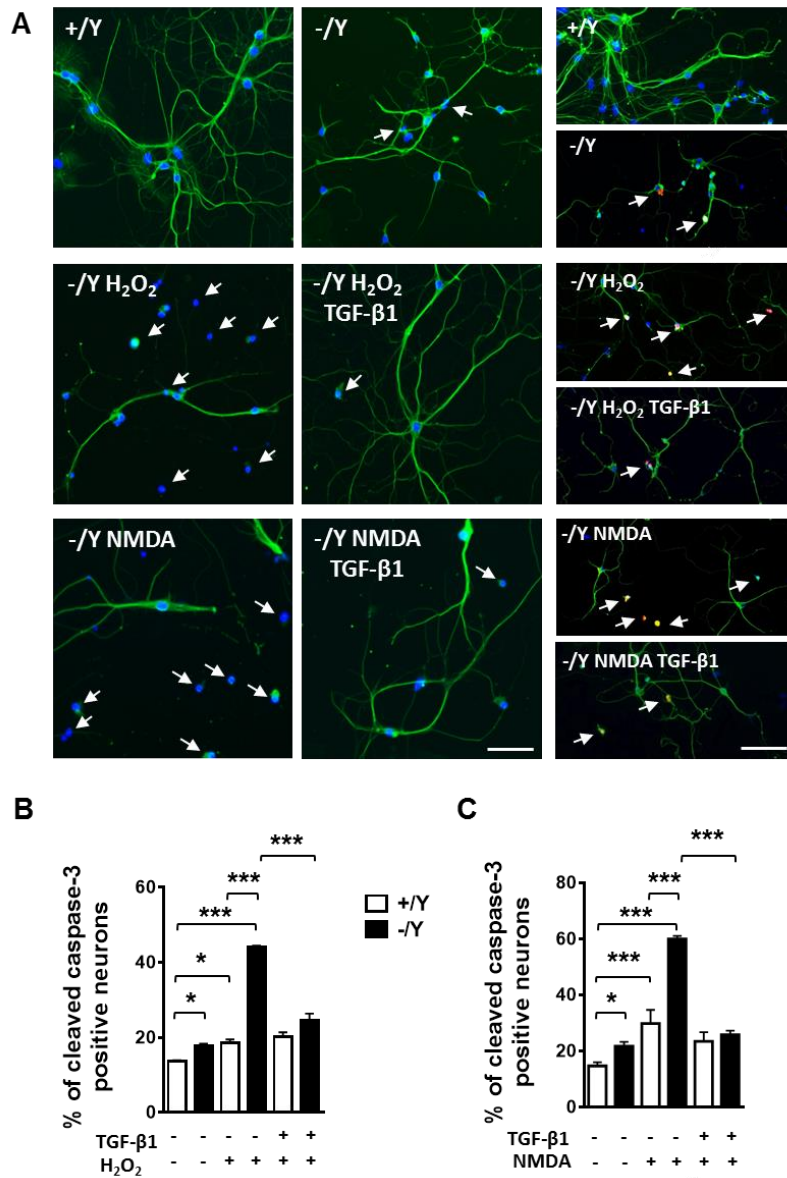


Figure 17

TGF-β1 treatment rescues the increased susceptibility to NMDA- and H₂O₂-induced stress of *Cdk15* KO hippocampal neurons.

Hippocampal cultures were treated on DIV10 with H₂O₂ (100 μM; +/Y n=4, -/Y n=4) or H₂O₂ + TGF-β1 (1 ng/ml; +/Y n=4, -/Y n=4) in B, and NMDA (100 μM; +/Y n=4, -/Y n=4) or NMDA + TGF-β1 (1 ng/ml; +/Y n=3, -/Y n=4) in C, and fixed after 24 h. **A:** Representative fluorescent images of differentiated hippocampal neurons from wild-type (+/Y) and *Cdk15* -/Y mice immunopositive for MAP2 (green), cleaved caspase 3 (red), and stained with Hoechst (blue). Higher magnification: white arrows indicate pyknotic nuclei, scale bar = 30 μm; Lower magnification: white arrows indicate apoptotic cells positive for cleaved caspase 3, scale bar = 40 μm. **B,C:** Percentage of cleaved caspase-3 positive neurons in primary hippocampal neurons from wild-type and *Cdk15* -/Y mice. Values are represented as means ± SE. *p<0.05; ***p<0.001 (Fisher's LSD after ANOVA).

In order to elucidate the mechanism underlying the higher neuronal vulnerability associated with *Cdkl5* loss of function, we investigated the effect of NMDA on TGF- β /SMAD3 signaling activation by evaluating SMAD3 nuclear-immunopositivity. NMDA-induced excitatory stimulation resulted in an increase in SMAD3 nuclear levels in control cultures (Figure 18). However, *Cdkl5* $-/Y$ neurons did not show a significant increase in SMAD3 levels after NMDA exposure (Figure 18), suggesting an impaired NMDA-induced SMAD3 activation in the absence of CDKL5. On the contrary, after TGF- β 1 treatment, similarly increased SMAD3 levels were detected in hippocampal neurons from *Cdkl5* $-/Y$ and control mice (Figure 18).

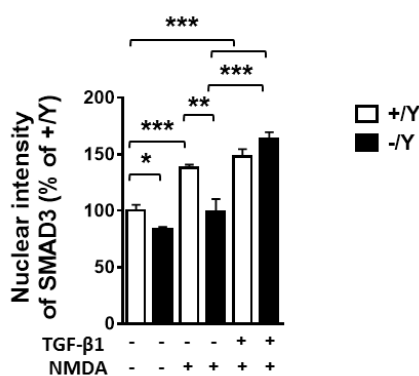


Figure 18

The increased susceptibility to neurotoxic stress of *Cdkl5* KO hippocampal neurons is due to an impaired SMAD3 activation.

Quantification of SMAD3 signal intensity in untreated (+/Y n=3, -/Y n=3), NMDA-treated (100 μ M; +/Y n=4, -/Y n=3), and NMDA + TGF- β 1-treated (1ng/ml; +/Y n=3, -/Y n=3) hippocampal neurons immunostained for SMAD3. Data are expressed as a percentage of the values of untreated +/Y. Values are represented as means \pm SE. *p<0.05; **p<0.01; ***p<0.001 (Fisher's LSD after ANOVA).

Treatment with TGF- β 1 protects CA1 pyramidal neurons from *Cdkl5* KO mice against NMDA-induced cell death

To determine whether *Cdkl5* KO neurons are also more susceptible to excitotoxic stimuli *in vivo*, we injected *Cdkl5* $-/Y$ and wild-type (+/Y) mice intraperitoneally with NMDA (60 mg/kg; Figure 19A) or Kainic acid (KA; 35 mg/kg; Figure 19A). No difference in seizure intensity was observed between *Cdkl5* $-/Y$ and wild-type (+/Y) mice in the 120 minutes following NMDA or KA administration. Seizure intensity reached a maximum of stage 3 on a 0 to 5 seizure scale, between 10 and 20 minutes following NMDA administration (Figure 19B), while seizure intensity reached a

maximum after 40 minute following KA administration and remains high for the next hour (Figure 19C). Similarly, a low mortality rate was observed in treated *Cdk15* ^{-/Y} and wild-type mice.

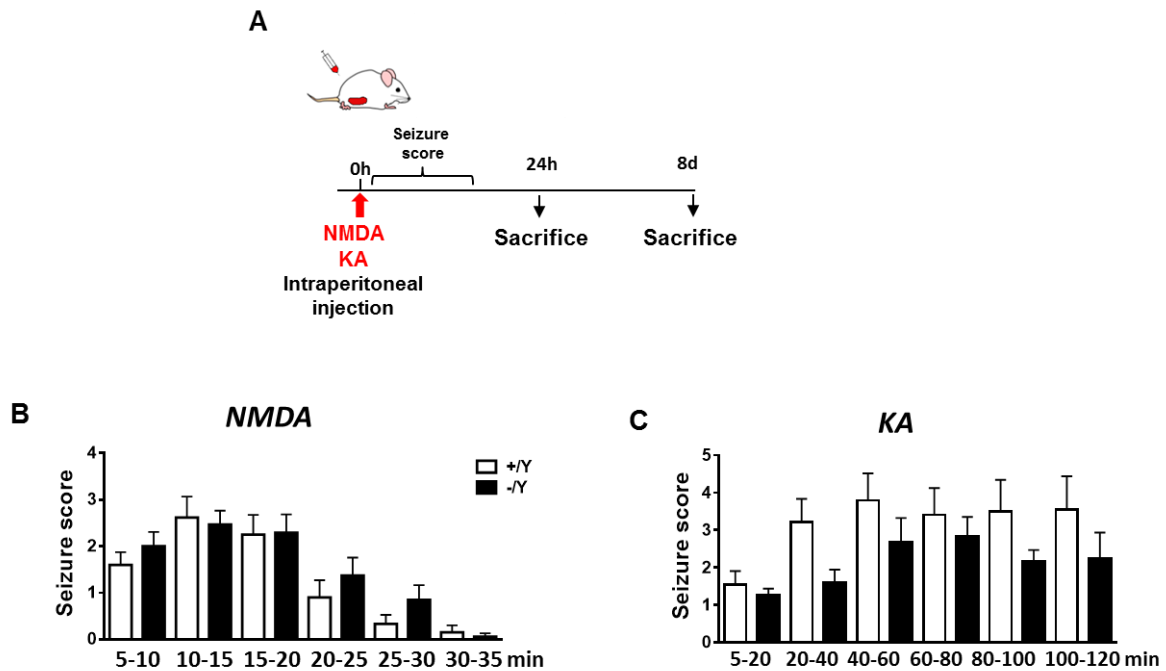


Figure 19
NMDA- or KA-induced seizures in *Cdk15* KO mice.

A: Schematic view of *in vivo* treatments and analysis schedule. **B,C:** Graph represents seizure score NMDA-induced (60 mg/kg) in B or kainic acid-induced (KA; 35 mg/kg) in C, for wild-type (+/Y, n=13, n=6 respectively) and *Cdk15* ^{-/Y} (n=17, n=6 respectively) mice at indicated time points after injections. Values are represented as means ± SE. (Fisher’s LSD after ANOVA).

It has been reported that 24 h after NMDA injection neuronal loss is evident in the CA1 layer of the hippocampus of rodents (Villapol et al., 2013), differently KA injection mainly affects principal neurons in the CA3 layer (Otani et al., 2006, Tripathi et al., 2009), effect particularly evident after 7-8 days post injection. Therefore, we evaluated neuronal damage 24 h after NMDA injection or 8 days after KA injection using Hoechst staining. In the CA1 layer of the hippocampus, NMDA-treated *Cdk15* ^{-/Y} mice showed a lower cell density (Figure 20A-C) and a higher number of pyknotic (Figure 20A-C). In the CA3 layer of the hippocampus, KA-treated *Cdk15* ^{-/Y} mice showed a lower cell density (Figure 20A,B,D) in comparison with treated wild-type mice. Very few pyknotic cells were present 8 days after KA injection and therefore not assessable as index of cell death.

These suggests that *Cdk15* $-/Y$ mice are more vulnerable to neurotoxicity/neurodegeneration induced by excitotoxic stimuli.

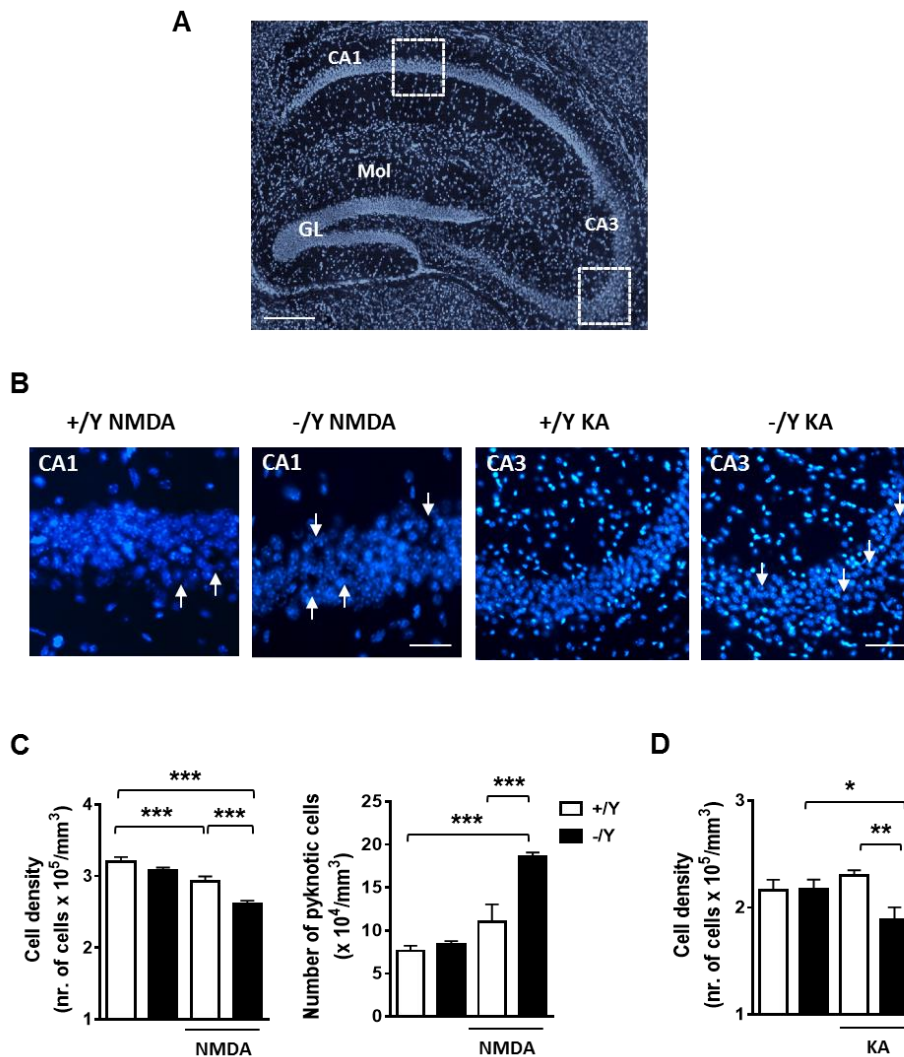


Figure 20

Increased susceptibility to excitotoxic stimuli of *Cdk15* KO mice.

A: Representative fluorescence image of a hippocampal section processed for Hoechst staining. Abbreviations: GL, granule cell layer; Mol, molecular layer. Scale bar = 150 μM . The dotted box in the panel indicates the analyzed region (CA1). **B:** Magnifications panels showing examples of the pyramidal neuron layer in CA1 of a *Cdk15* $+/Y$ and a *Cdk15* $-/Y$ mouse treated with NMDA (60 mg/kg), or KA (35 mg/kg). Arrows indicate the neuronal damage sites with low cell density. Scale bar = 100 μM . **C:** Quantification of Hoechst-positive cells (left) and number of pyknotic nuclei (right) in CA1 of hippocampal sections from untreated ($+/Y$ $n=5$, $-/Y$ $n=5$) and NMDA-treated ($+/Y$ $n=8$, $-/Y$ $n=9$, left; $+/Y$ $n=6$, $-/Y$ $n=7$, right) mice. **D:** Quantification of Hoechst-positive cells in CA3 of hippocampal sections from untreated ($+/Y$ $n=4$, $-/Y$ $n=4$) and KA-treated ($+/Y$ $n=4$, $-/Y$ $n=4$) mice. Values are represented as means \pm SE. * $p<0.05$; ** $p<0.01$; *** $p<0.001$ (Fisher's LSD after ANOVA).

To test whether TGF- β 1 is sufficient to protect *Cdkl5* KO neurons against NMDA-induced cell death, we administered TGF- β 1 to *Cdkl5* $-/\gamma$ mice via intracerebroventricular infusion 1 h after NMDA treatment (Figure 21A). Treatment with TGF- β 1 prevented neurodegeneration of CA1 pyramidal neurons in *Cdkl5* $-/\gamma$ mice assessed using Hoechst staining and immunohistochemistry for activated caspase-3 (Figure 21B-D).

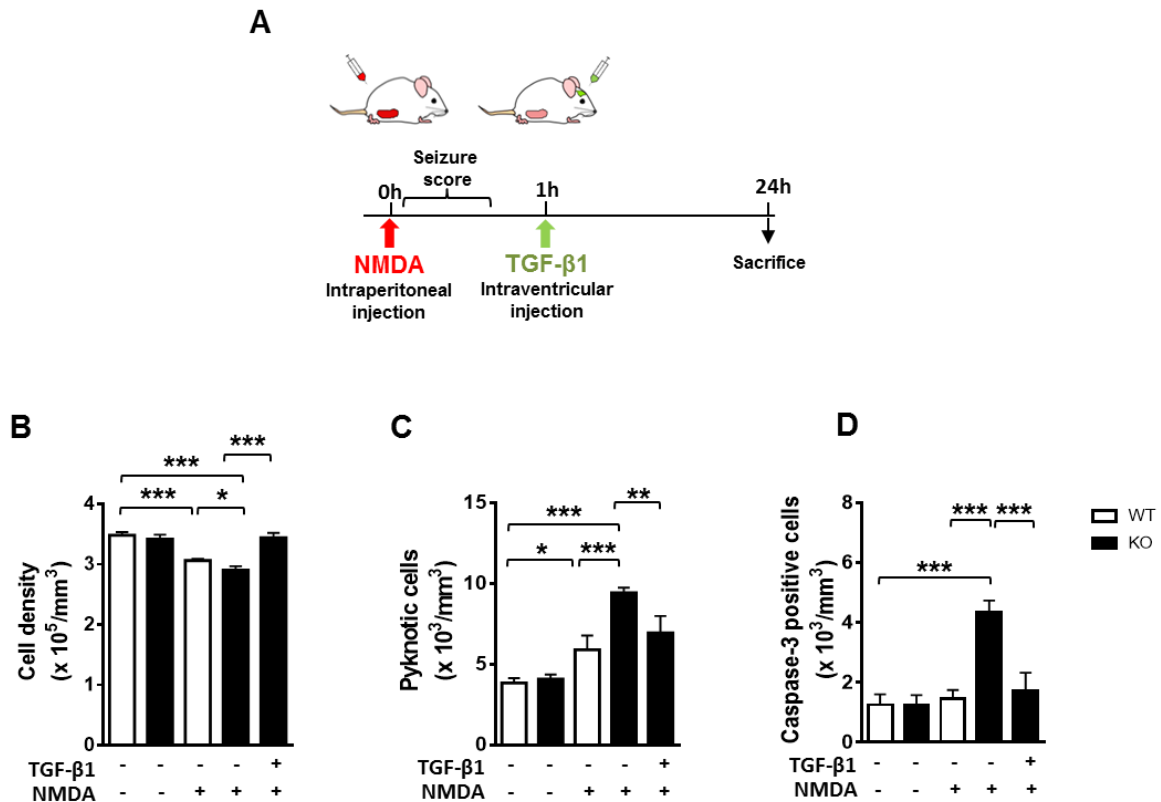


Figure 21

Effect of treatment with TGF- β 1 on NMDA-induced hippocampal neuron cell death in *Cdkl5* KO mice.

A: Schematic view of *in vivo* treatments and analysis schedule. **B-D:** Quantification of Hoechst-positive cells (B), number of pyknotic nuclei (C), and number of cleaved caspase-3 positive cells (D) in CA1 of hippocampal sections from untreated (+/ γ n=5, -/ γ n=5), NMDA-treated ((B) +/ γ n=8, -/ γ n=9; (C) +/ γ n=6, -/ γ n=7; (D) +/ γ n=5, -/ γ n=6), and NMDA + TGF- β 1 treated (-/ γ n=5) mice. Values are represented as means \pm SE. * p <0.05; ** p <0.01; *** p <0.001 (Fisher's LSD after ANOVA).

To determine whether SMAD3 is involved in TGF- β 1-induced neuroprotection against NMDA-induced cell death, we quantified SMAD3 expression in the CA1 layer of the hippocampus

of *Cdkl5* $-/Y$ mice 1 hour after TGF- β 1 treatment (Figure 21A). NMDA-treated *Cdkl5* $-/Y$ mice showed lower SMAD3 levels in comparison with NMDA-treated *Cdkl5* $+/Y$ mice, with a difference of the same amplitude as that found between vehicle-treated *Cdkl5* $+/Y$ and *Cdkl5* $-/Y$ mice (Figure 22A,B). Treatment with TGF- β 1 strongly increased SMAD3 levels in CA1 pyramidal neurons of NMDA-treated *Cdkl5* $-/Y$ mice (Figure 22A,B), suggesting that SMAD3 plays a functional role in TGF- β 1-induced neuroprotection.

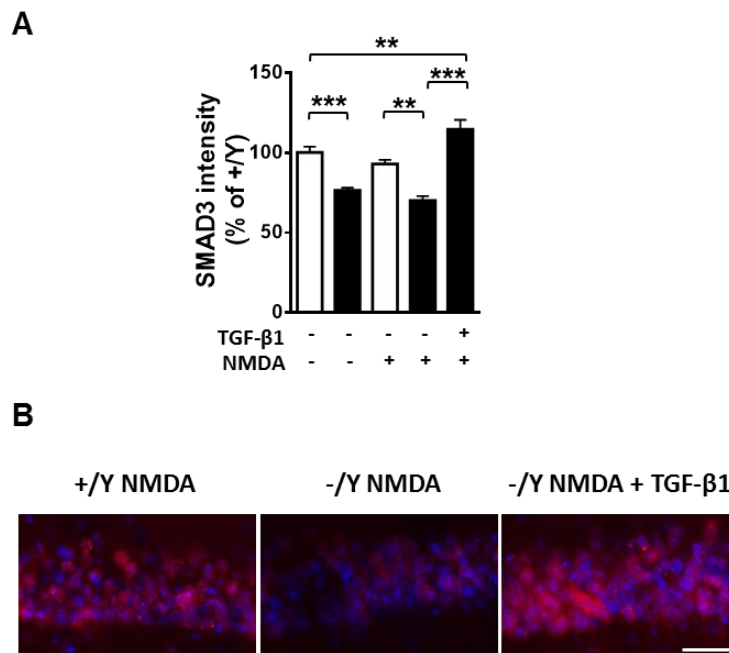


Figure 22

SMAD3 plays a functional role in TGF- β 1-induced neuroprotection.

A: Quantification of SMAD3 signal intensity in the CA1 pyramidal neuron layer from untreated ($+/Y$ $n=10$, $-/Y$ $n=10$), NMDA-treated ($+/Y$ $n=3$, $-/Y$ $n=4$), and NMDA + TGF- β 1 treated ($-/Y$ $n=5$) mice. **B:** Representative fluorescent images of the pyramidal neuron layer in CA1 of a *Cdkl5* $+/Y$ and a *Cdkl5* $-/Y$ mouse treated with NMDA (60 mg/kg), and of a *Cdkl5* $-/Y$ mouse treated with NMDA and TGF- β 1 (50 ng) immunostained for SMAD3 and counterstained with Hoechst. Scale bar = 50 μ M. Values are represented as means \pm SE. ** $p < 0.01$; *** $p < 0.001$ (Fisher's LSD after ANOVA).

DISCUSSION

Involvement of CDKL5 in several cellular pathways

The phospho antibody microarray results were analyzed with Reactome in order to obtain an overview of the misregulated pathways in the absence of CDKL5. This first analysis, that provided an intuitive visualization of the dataset, highlighted the potential involvement of CDKL5 in several cellular functions. Beside the well-known involvement of CDKL5 in neuronal maturation, the analysis revealed alterations in pathways involved in the regulation of gene expression, DNA damage/repair, cell-cycle, and apoptosis. A CDKL5 nuclear activity, in RNA splicing, had already been reported (Ricciardi et al., 2009); future studies are needed to validate the role of CDKL5 in these cellular processes.

As previously reported (Wang et al., 2012, Amendola et al., 2014), our analysis revealed that CDKL5 has an important involvement in signal transduction pathways. Recently, through kinome profiling study, Wang and colleagues demonstrated that several signaling transduction pathways involved in neuronal and synaptic plasticity are disrupted in the forebrain of *Cdkl5* knockout male mice (Wang et al., 2012), with changes in the phosphorylation profiles of AMPK, AKT, PKC, and MAPK substrates. Similarly, Amendola et al. found a decrease in the phosphorylation of AKT Ser473 and rpS6 Ser240/244 in several brain structures (cortex and hippocampus) of hemizygous male and heterozygous and homozygous female *Cdkl5* knockout mice (Amendola et al., 2014). A further characterization of AKT-dependent pathways showed a disruption of AKT-GSK3beta signaling in *Cdkl5* knockout mice (Fuchs et al., 2014b, Fuchs et al., 2015).

Interestingly, the Reactome analysis highlighted the involvement of CDKL5 in signaling associated with the immune system. Immune activation within the central nervous system (CNS) is a classical feature of ischemia, neurodegenerative diseases, immune-mediated disorders, infections and trauma, exerting a dual role for both neurotoxic and neuroprotective response (Amor et al., 2010). It is worth noting that, in CDD patients, a defective inflammation regulatory signaling system has been reported as the primary source of the subclinical immune dysregulation associated with the disease (Leoncini et al., 2015, Cortelazzo et al., 2017). Indeed cytokine changes that are proportional to clinical severity have been observed and increased IL-22 and T-reg cytokine levels were evidenced in patients with CDD (Leoncini et al., 2015, Cortelazzo et al., 2017).

Thus, it would be interesting to further investigate the potential involvement of CDKL5 in the immune system response as a pathomechanism underlying CDD.

Reduced SMAD3 levels due to *Cdkl5* loss of function impair neuron survival and maturation

In the current study, we provide novel evidence that SMAD3 is a direct phosphorylation target of CDKL5. Despite the extensive sequence similarity between SMAD2 and SMAD3, we found that CDKL5 specifically phosphorylates SMAD3 at the MH1 domain. While the MH2 domain is highly conserved among all SMADs, the different structure of the MH1 domain of SMAD3, which does not contain the 30-amino-acid insert that is present in SMAD2 (Dennler et al., 1999), could explain the specificity of the CDKL5-dependent phosphorylation of SMAD3. Though recent observation has raised the possibility that the RPXSA motif might represent a consensus sequence for phosphorylation by CDKL5 (Katayama et al., 2015, Baltussen et al., 2018, Munoz et al., 2018), other studies have identified CDKL5 phosphorylation targets that do not contain this consensus motif (Mari et al., 2005, Kameshita et al., 2008, Ricciardi et al., 2012, Trazzi et al., 2016), suggesting the presence of a different consensus sequence for CDKL5 phosphorylation or of a protein folding that creates a noncontiguous CDKL5 phosphorylation motif (Duarte et al., 2014). SMAD3 seems to belong to this latter group because the MH1 domain does not present a RPXSA motif. Nevertheless, 6 Serine and 7 Threonine are present in the MH1 domain as possible target of CDKL5 phosphorylation. Further studies will be needed to identify the CDKL5 phosphorylation site on SMAD3.

We additionally found that CDKL5-dependent phosphorylation of SMAD3 does not directly affect SMAD3 activity, but that CDKL5 deficiency causes a reduction in SMAD3 protein levels and, consequently, in activity in *Cdkl5* KO neurons. Phosphorylation at different sites of SMAD3 contributes to its stability (Guo et al., 2008, Gao et al., 2016). Most SMAD proteins can be polyubiquitinated and degraded in either a ligand-dependent or a ligand-independent manner (Izzi and Attisano, 2006). Although it still remains to be established how CDKL5-dependent phosphorylation affects SMAD3 protein stability, we found that treatment with TGF- β 1, similarly to CDKL5 re-expression, normalized SMAD3 levels, indicating a reversible SMAD3 stability/activity in *Cdkl5* KO neurons. We found that CDKL5 does not phosphorylate SMAD3 at the C-terminal residues Ser425 in the MH2 domain or at the Ser213 site in the linker region, phosphorylation sites

that drive TGF- β type I receptor-induced SMAD3 nuclear localization and stability (Bruce and Sapkota, 2012). On the other hand, there is no evidence that TGF- β has a direct action on the SMAD3 MH1 domain (Bruce and Sapkota, 2012). The finding that TGF- β 1 can rescue SMAD3 levels and transcriptional activity in the absence of CDKL5 suggests that TGF- β 1 modulates SMAD3 stability through a CDKL5-independent pathway.

Importantly, we provide novel evidence that loss of *Cdkl5* increases cell death of differentiating hippocampal neurons. The restoration of SMAD3 activity through TGF- β 1 treatment fully rescued survival of *Cdkl5* KO neurons, suggesting that SMAD3 signaling dysregulation is involved in the reduced survival of *Cdkl5* KO neurons. Consistent with our findings, primary neurons lacking TGF- β 1 showed a reduced survival rate compared with wild-type controls (Brionne et al., 2003). Moreover, studies on SMAD3-deficient mice have revealed that SMAD3 plays a role in trophic support for nigral dopaminergic neurons (Tapia-Gonzalez et al., 2011) in addition to the maintenance of survival of newborn granule cells in the hippocampal dentate gyrus (Tapia-Gonzalez et al., 2013).

In addition to its role in neuronal survival we found that restoration of SMAD3 signaling recovered the primary axon outgrowth and reduced connectivity caused by *Cdkl5* loss of function. Contrariwise, treatment with TGF- β 1 did not improve the dendritic hypotrophy that characterizes *Cdkl5* KO neurons. This is in agreement with previous evidence that indicates that TGF- β 1 signaling is required for axon specification in the developing brain (Yi et al., 2010), and for synaptic growth and function (Chin et al., 2002, Sweeney and Davis, 2002), while it does not affect the process of branching and the number of dendrite-like processes in hippocampal neurons (Ishihara et al., 1994).

Increased vulnerability of *Cdkl5* KO hippocampal neurons to neurotoxic stress is rescued by treatment with TGF- β 1

Our data provide the first evidence that CDKL5 has a key role in neuronal survival and indicate that CDKL5 deficiency increases the vulnerability of neural cells to apoptosis induced by different types of neurotoxic stress. It is becoming increasingly clear that various types of cell death cascades can share pathways in death execution (Yakovlev and Faden, 2004). Our finding that the increased neuronal vulnerability to oxidative stress, VPA, and excitotoxic injury shown by *Cdkl5* KO hippocampal neurons is fully recovered by TGF- β 1 treatment, suggests that SMAD3

signaling deregulation might be the common mechanism responsible for the enhanced vulnerability of *Cdkl5* KO neurons. The neuroprotective role of TGF- β /SMAD3 signaling in the injured CNS is increasingly being recognized (Dobolyi et al., 2012). TGF- β 1 deficiency in adult TGF- β 1^{-/+} mice does not result in overt neurodegeneration but does increase neuronal cell loss after excitotoxic injury (Brionne et al., 2003). Moreover, SMAD3 deficiency increases cortical and hippocampal neuronal loss following traumatic brain injury (Villapol et al., 2013). Therefore, the reduced SMAD3 activation in NMDA-treated *Cdkl5* KO mice might underlie the increased neurodegeneration observed in the absence of CDKL5. Moreover, our observations that the increased NMDA-induced cell death of hippocampal neurons of *Cdkl5* KO mice was fully rescued by TGF- β 1 treatment correlates well with previous studies that show that activation of TGF- β /SMAD3 dependent signaling protects neurons against NMDA-induced cell death (Prehn et al., 1994, Docagne et al., 2002).

A recent study in a *Cdkl5* KO mouse model (*Cdkl5* exon 2 deletion; (Okuda et al., 2017)) showed increased seizure susceptibility in response to NMDA that was correlated with an upregulation of the NMDA receptor subunits GluN2B at the CA1 hippocampal glutamatergic synapses (Okuda et al., 2017). We did not observe an increase in NMDA-induced tonic-clonic seizure episodes in the *Cdkl5* KO mouse model used in this study (deletion of *Cdkl5* exon 4; (Amendola et al., 2014)). Therefore, the increased hippocampal neuron vulnerability that we observed in *Cdkl5* KO mice in response to NMDA treatment is unlikely to be due to a higher NMDA-induced neuronal hyper-excitability, and is, rather, ascribable to a generalized increased susceptibility to neurotoxic stress due to the impairment of SMAD3 signaling.

Several neurodegenerative diseases, including Alzheimer's disease, Parkinson's disease, and motor neuron diseases have been associated with disturbed cellular or subcellular SMAD localization and disruption of SMAD-controlled transcriptional machinery (Dobolyi et al., 2012). Our findings suggest that, through the deregulation of SMAD3 signaling, CDKL5 loss of function predisposes neurons to multiple forms of cell death. The endangering action of CDKL5 mutations is likely to sensitize neurons in the brain to neurotoxic conditions known to promote neuronal death. Seizures are prominent in CDD patients and are usually severe and untreatable. Conceivably, individuals with CDKL5 deficiency may be more susceptible to oxidative stress as a direct consequence of seizures (Frantseva et al., 2000). Therefore, preventive and therapeutic strategies that target both excitotoxic and apoptotic pathways might be recommended to forestall

neurodegenerative processes in CDD.

CONCLUSION

In conclusion our study provides new insight into CDKL5 deficiency disorder, revealing a new CDKL5 substrate and its crucial role in the neuronal response to neurotoxic stimuli. The increasing definition of the signaling networks in which CDKL5 participates contributes to a better understanding of the pathomechanisms underlying the clinical phenotype of CDD patients.

In addition to the newly discovered CDKL5 target, the phosphoproteomics study revealed misregulated proteins involved in well-known pathways as well as in new interesting physiological processes. Future studies will focus on the characterization of these new potential interactors so as to provide more in-depth knowledge of CDKL5 functions.

Comprehension of the neurodevelopmental alterations that characterize CDKL5 disorder will expedite the discovery of new therapies for CDD.

Citations

- Amendola E, Zhan Y, Mattucci C, Castroflorio E, Calcagno E, Fuchs C, Lonetti G, Silingardi D, Vyssotski AL, Farley D, Ciani E, Pizzorusso T, Giustetto M, Gross CT (2014) Mapping pathological phenotypes in a mouse model of CDKL5 disorder. *PLoS One* 9:e91613.
- Amor S, Puentes F, Baker D, van der Valk P (2010) Inflammation in neurodegenerative diseases. *Immunology* 129:154-169.
- Artuso R, Mencarelli MA, Polli R, Sartori S, Ariani F, Pollazzon M, Marozza A, Cilio MR, Specchio N, Vigeveno F, Vecchi M, Boniver C, Dalla Bernardina B, Parmeggiani A, Buoni S, Hayek G, Mari F, Renieri A, Murgia A (2010) Early-onset seizure variant of Rett syndrome: definition of the clinical diagnostic criteria. *Brain & development* 32:17-24.
- Bahi-Buisson N, Kaminska A, Boddaert N, Rio M, Afenjar A, Gerard M, Giuliano F, Motte J, Heron D, Morel MA, Plouin P, Richelme C, des Portes V, Dulac O, Philippe C, Chiron C, Nabbout R, Bienvenu T (2008a) The three stages of epilepsy in patients with CDKL5 mutations. *Epilepsia* 49:1027-1037.
- Bahi-Buisson N, Nectoux J, Rosas-Vargas H, Milh M, Boddaert N, Girard B, Cances C, Ville D, Afenjar A, Rio M, Heron D, N'Guyen Morel MA, Arzimanoglou A, Philippe C, Jonveaux P, Chelly J, Bienvenu T (2008b) Key clinical features to identify girls with CDKL5 mutations. *Brain : a journal of neurology* 131:2647-2661.
- Baltussen LL, Negraes PD, Silvestre M, Claxton S, Moeskops M, Christodoulou E, Flynn HR, Snijders AP, Muotri AR, Ultanir SK (2018) Chemical genetic identification of CDKL5 substrates reveals its role in neuronal microtubule dynamics. *EMBO J*.
- Barbiero I, Peroni D, Tramarin M, Chandola C, Rusconi L, Landsberger N, Kilstrup-Nielsen C (2017a) The neurosteroid pregnenolone reverts microtubule derangement induced by the loss of a functional CDKL5-IQGAP1 complex. *Hum Mol Genet* 26:3520-3530.
- Barbiero I, Valente D, Chandola C, Magi F, Bergo A, Monteonofrio L, Tramarin M, Fazzari M, Soddu S, Landsberger N, Rinaldo C, Kilstrup-Nielsen C (2017b) CDKL5 localizes at the centrosome and midbody and is required for faithful cell division. *Scientific reports* 7:6228.
- Beenstock J, Mooshayef N, Engelberg D (2016) How Do Protein Kinases Take a Selfie (Autophosphorylate)? *Trends in biochemical sciences* 41:938-953.
- Bertani I, Rusconi L, Bolognese F, Forlani G, Conca B, De Monte L, Badaracco G, Landsberger N, Kilstrup-Nielsen C (2006) Functional consequences of mutations in CDKL5, an X-linked gene involved in infantile spasms and mental retardation. *J Biol Chem* 281:32048-32056.
- Brionne TC, Tesseur I, Masliah E, Wyss-Coray T (2003) Loss of TGF-beta 1 leads to increased neuronal cell death and microgliosis in mouse brain. *Neuron* 40:1133-1145.
- Brown KA, Pietenpol JA, Moses HL (2007) A tale of two proteins: differential roles and regulation of Smad2 and Smad3 in TGF-beta signaling. *J Cell Biochem* 101:9-33.
- Bruce DL, Sapkota GP (2012) Phosphatases in SMAD regulation. *FEBS Lett* 586:1897-1905.
- Calvo M, Sanz-Blasco S, Caballero E, Villalobos C, Nunez L (2015) Susceptibility to excitotoxicity in aged hippocampal cultures and neuroprotection by non-steroidal anti-inflammatory drugs: role of mitochondrial calcium. *J Neurochem* 132:403-417.
- Canning P, Park K, Goncalves J, Li C, Howard CJ, Sharpe TD, Holt LJ, Pelletier L, Bullock AN, Leroux MR (2018) CDKL Family Kinases Have Evolved Distinct Structural Features and Ciliary Function. *Cell reports* 22:885-894.
- Caraci F, Gulisano W, Guida CA, Impellizzeri AA, Drago F, Puzzo D, Palmeri A (2015) A key role for TGF-beta1 in hippocampal synaptic plasticity and memory. *Scientific reports* 5:11252.
- Carouge D, Host L, Aunis D, Zwiller J, Anglard P (2010) CDKL5 is a brain MeCP2 target gene regulated by DNA methylation. *Neurobiol Dis* 38:414-424.

- Chen Q, Zhu YC, Yu J, Miao S, Zheng J, Xu L, Zhou Y, Li D, Zhang C, Tao J, Xiong ZQ (2010) CDKL5, a protein associated with rett syndrome, regulates neuronal morphogenesis via Rac1 signaling. *J Neurosci* 30:12777-12786.
- Chen X, Zhang Q, Cheng Q, Ding F (2009) Protective effect of salidroside against H₂O₂-induced cell apoptosis in primary culture of rat hippocampal neurons. *Mol Cell Biochem* 332:85-93.
- Cheng HC, Qi RZ, Paudel H, Zhu HJ (2011) Regulation and function of protein kinases and phosphatases. *Enzyme research* 2011:794089.
- Chico LK, Van Eldik LJ, Watterson DM (2009) Targeting protein kinases in central nervous system disorders. *Nature reviews Drug discovery* 8:892-909.
- Chin J, Angers A, Cleary LJ, Eskin A, Byrne JH (2002) Transforming growth factor beta1 alters synapsin distribution and modulates synaptic depression in Aplysia. *J Neurosci* 22:RC220.
- Choura M, Rebai A (2011) Receptor tyrosine kinases: from biology to pathology. *Journal of receptor and signal transduction research* 31:387-394.
- Cortelazzo A, de Felice C, Leoncini S, Signorini C, Guerranti R, Leoncini R, Armini A, Bini L, Ciccoli L, Hayek J (2017) Inflammatory protein response in CDKL5-Rett syndrome: evidence of a subclinical smouldering inflammation. *Inflamm Res* 66:269-280.
- Daly AC, Vizan P, Hill CS (2010) Smad3 protein levels are modulated by Ras activity and during the cell cycle to dictate transforming growth factor-beta responses. *J Biol Chem* 285:6489-6497.
- Deininger MW, Vieira S, Mendiola R, Schultheis B, Goldman JM, Melo JV (2000) BCR-ABL tyrosine kinase activity regulates the expression of multiple genes implicated in the pathogenesis of chronic myeloid leukemia. *Cancer research* 60:2049-2055.
- Della Sala G, Putignano E, Chelini G, Melani R, Calcagno E, Michele Ratto G, Amendola E, Gross CT, Giustetto M, Pizzorusso T (2016) Dendritic Spine Instability in a Mouse Model of CDKL5 Disorder Is Rescued by Insulin-like Growth Factor 1. *Biol Psychiatry* 80:302-311.
- Denkler S, Huet S, Gauthier JM (1999) A short amino-acid sequence in MH1 domain is responsible for functional differences between Smad2 and Smad3. *Oncogene* 18:1643-1648.
- Denkler S, Itoh S, Vivien D, ten Dijke P, Huet S, Gauthier JM (1998) Direct binding of Smad3 and Smad4 to critical TGF beta-inducible elements in the promoter of human plasminogen activator inhibitor-type 1 gene. *EMBO J* 17:3091-3100.
- Dobolyi A, Vincze C, Pal G, Lovas G (2012) The neuroprotective functions of transforming growth factor beta proteins. *Int J Mol Sci* 13:8219-8258.
- Docagne F, Nicole O, Gabriel C, Fernandez-Monreal M, Lesne S, Ali C, Plawinski L, Carmeliet P, MacKenzie ET, Buisson A, Vivien D (2002) Smad3-dependent induction of plasminogen activator inhibitor-1 in astrocytes mediates neuroprotective activity of transforming growth factor-beta 1 against NMDA-induced necrosis. *Mol Cell Neurosci* 21:634-644.
- Duarte ML, Pena DA, Nunes Ferraz FA, Berti DA, Paschoal Sobreira TJ, Costa-Junior HM, Abdel Baqui MM, Disatnik MH, Xavier-Neto J, Lopes de Oliveira PS, Schechtman D (2014) Protein folding creates structure-based, noncontiguous consensus phosphorylation motifs recognized by kinases. *Science signaling* 7:ra105.
- Endicott JA, Noble ME, Johnson LN (2012) The structural basis for control of eukaryotic protein kinases. *Annual review of biochemistry* 81:587-613.
- Eyers PA (2018) A new consensus for evaluating CDKL5/STK9-dependent signalling mechanisms. *EMBO J*.
- Fabregat A, Sidiropoulos K, Viteri G, Forner O, Marin-Garcia P, Arnau V, D'Eustachio P, Stein L, Hermjakob H (2017) Reactome pathway analysis: a high-performance in-memory approach. *BMC bioinformatics* 18:142.
- Fehr S, Leonard H, Ho G, Williams S, de Klerk N, Forbes D, Christodoulou J, Downs J (2015) There is variability in the attainment of developmental milestones in the CDKL5 disorder. *J Neurodev Disord* 7:2.
- Fehr S, Wilson M, Downs J, Williams S, Murgia A, Sartori S, Vecchi M, Ho G, Polli R, Psoni S, Bao X, de Klerk N, Leonard H, Christodoulou J (2013) The CDKL5 disorder is an independent clinical entity associated with early-onset encephalopathy. *Eur J Hum Genet* 21:266-273.

- Fehr S, Wong K, Chin R, Williams S, de Klerk N, Forbes D, Krishnaraj R, Christodoulou J, Downs J, Leonard H (2016) Seizure variables and their relationship to genotype and functional abilities in the CDKL5 disorder. *Neurology* 87:2206-2213.
- Feng XH, Derynck R (2005) Specificity and versatility in tgf-beta signaling through Smads. *Annu Rev Cell Dev Biol* 21:659-693.
- Flanders KC, Ren RF, Lippa CF (1998) Transforming growth factor-betas in neurodegenerative disease. *Prog Neurobiol* 54:71-85.
- Frantseva MV, Perez Velazquez JL, Tsoraklidis G, Mendonca AJ, Adamchik Y, Mills LR, Carlen PL, Burnham MW (2000) Oxidative stress is involved in seizure-induced neurodegeneration in the kindling model of epilepsy. *Neuroscience* 97:431-435.
- Fuchs C, Gennaccaro L, Trazzi S, Bastianini S, Bettini S, Martire VL, Ren E, Medici G, Zoccoli G, Rimondini R, Ciani E (2018) Heterozygous CDKL5 Knockout Female Mice Are a Valuable Animal Model for CDKL5 Disorder. *Neural Plast* 2018:9726950.
- Fuchs C, Rimondini R, Viggiano R, Trazzi S, De Franceschi M, Bartesaghi R, Ciani E (2015) Inhibition of GSK3beta rescues hippocampal development and learning in a mouse model of CDKL5 disorder. *Neurobiol Dis* 82:298-310.
- Fuchs C, Trazzi S, Roberta T, Viggiano R, De Franceschi M, E. A, Gross CT, Calzà L, Bartesaghi R, Ciani E (2014a) Loss of Cdkl5 impairs survival and dendritic growth of newborn neurons by altering AKT/GSK-3beta signaling. *Neurobiology of disease* doi: 10.1016/j.nbd.2014.06.006.
- Fuchs C, Trazzi S, Torricella R, Viggiano R, De Franceschi M, Amendola E, Gross C, Calza L, Bartesaghi R, Ciani E (2014b) Loss of CDKL5 impairs survival and dendritic growth of newborn neurons by altering AKT/GSK-3beta signaling. *Neurobiol Dis* 70:53-68.
- Gao H, Yan P, Zhang S, Huang H, Huang F, Sun T, Deng Q, Huang Q, Chen S, Ye K, Xu J, Liu L (2016) Long-Term Dietary Alpha-Linolenic Acid Supplement Alleviates Cognitive Impairment Correlate with Activating Hippocampal CREB Signaling in Natural Aging Rats. *Mol Neurobiol* 53:4772-4786.
- Guerrini R, Parrini E (2012) Epilepsy in Rett syndrome, and CDKL5- and FOXP1-gene-related encephalopathies. *Epilepsia* 53:2067-2078.
- Guo X, Ramirez A, Waddell DS, Li Z, Liu X, Wang XF (2008) Axin and GSK3- control Smad3 protein stability and modulate TGF- signaling. *Genes Dev* 22:106-120.
- Hamilton AT (1998) Protein Kinases. *Encyclopedia of Immunology (Second Edition)* Pages 2028-2033.
- Hanks SK, Hunter T (1995) Protein kinases 6. The eukaryotic protein kinase superfamily: kinase (catalytic) domain structure and classification. *FASEB journal : official publication of the Federation of American Societies for Experimental Biology* 9:576-596.
- Hector RD, Dando O, Landsberger N, Kilstrup-Nielsen C, Kind PC, Bailey ME, Cobb SR (2016) Characterisation of CDKL5 Transcript Isoforms in Human and Mouse. *PLoS One* 11:e0157758.
- Hector RD, Kalscheuer VM, Hennig F, Leonard H, Downs J, Clarke A, Benke TA, Armstrong J, Pineda M, Bailey MES, Cobb SR (2017) CDKL5 variants: Improving our understanding of a rare neurologic disorder. *Neurol Genet* 3:e200.
- Hill CS (2009) Nucleocytoplasmic shuttling of Smad proteins. *Cell Res* 19:36-46.
- Huse M, Kuriyan J (2002) The conformational plasticity of protein kinases. *Cell* 109:275-282.
- Hwang JJ, Lee SJ, Kim TY, Cho JH, Koh JY (2008) Zinc and 4-hydroxy-2-nonenal mediate lysosomal membrane permeabilization induced by H2O2 in cultured hippocampal neurons. *J Neurosci* 28:3114-3122.
- Inman GJ (2005) Linking Smads and transcriptional activation. *Biochem J* 386:e1-e3.
- Inoue Y, Kitagawa M, Onozaki K, Hayashi H (2004) Contribution of the constitutive and inducible degradation of Smad3 by the ubiquitin-proteasome pathway to transforming growth factor-beta signaling. *J Interferon Cytokine Res* 24:43-54.
- Intusoma U, Hayeeduereh F, Plong-On O, Sripo T, Vasiknanonte P, Janjindamai S, Lusawat A, Thammongkol S, Visudtibhan A, Limprasert P (2011) Mutation screening of the CDKL5 gene in cryptogenic infantile intractable epilepsy and review of clinical sensitivity. *Eur J Paediatr Neurol* 15:432-438.

- Inui M, Manfrin A, Mamidi A, Martello G, Morsut L, Soligo S, Enzo E, Moro S, Polo S, Dupont S, Cordenosi M, Piccolo S (2011) USP15 is a deubiquitylating enzyme for receptor-activated SMADs. *Nat Cell Biol* 13:1368-1375.
- Ishihara A, Saito H, Abe K (1994) Transforming growth factor-beta 1 and -beta 2 promote neurite sprouting and elongation of cultured rat hippocampal neurons. *Brain research* 639:21-25.
- Izzi L, Attisano L (2006) Ubiquitin-dependent regulation of TGFbeta signaling in cancer. *Neoplasia* 8:677-688.
- Jhang CL, Huang TN, Hsueh YP, Liao W (2017) Mice lacking cyclin-dependent kinase-like 5 manifest autistic and ADHD-like behaviors. *Hum Mol Genet* 26:3922-3934.
- Johnson LN (2011) Substrates of mitotic kinases. *Science signaling* 4:pe31.
- Kalscheuer VM, Tao J, Donnelly A, Hollway G, Schwinger E, Kubart S, Menzel C, Hoeltzenbein M, Tommerup N, Eyre H, Harbord M, Haan E, Sutherland GR, Ropers HH, Geicz J (2003) Disruption of the serine/threonine kinase 9 gene causes severe X-linked infantile spasms and mental retardation. *American journal of human genetics* 72:1401-1411.
- Kameshita I, Sekiguchi M, Hamasaki D, Sugiyama Y, Hatano N, Suetake I, Tajima S, Sueyoshi N (2008) Cyclin-dependent kinase-like 5 binds and phosphorylates DNA methyltransferase 1. *Biochem Biophys Res Commun* 377:1162-1167.
- Katayama S, Sueyoshi N, Kameshita I (2015) Critical Determinants of Substrate Recognition by Cyclin-Dependent Kinase-like 5 (CDKL5). *Biochemistry* 54:2975-2987.
- Kilstrup-Nielsen C, Rusconi L, La Montanara P, Ciceri D, Bergo A, Bedogni F, Landsberger N (2012) What we know and would like to know about CDKL5 and its involvement in epileptic encephalopathy. *Neural Plast* 2012:728267.
- Kim SG, Kim HA, Jong HS, Park JH, Kim NK, Hong SH, Kim TY, Bang YJ (2005) The endogenous ratio of Smad2 and Smad3 influences the cytotstatic function of Smad3. *Molecular biology of the cell* 16:4672-4683.
- Krebs EG (1985) The phosphorylation of proteins: a major mechanism for biological regulation. Fourteenth Sir Frederick Gowland Hopkins memorial lecture. *Biochemical Society transactions* 13:813-820.
- Kurisasi A, Kose S, Yoneda Y, Heldin CH, Moustakas A (2001) Transforming growth factor-beta induces nuclear import of Smad3 in an importin-beta1 and Ran-dependent manner. *Molecular biology of the cell* 12:1079-1091.
- Leoncini S, De Felice C, Signorini C, Zollo G, Cortelazzo A, Durand T, Galano JM, Guerranti R, Rossi M, Ciccoli L, Hayek J (2015) Cytokine Dysregulation in MECP2- and CDKL5-Related Rett Syndrome: Relationships with Aberrant Redox Homeostasis, Inflammation, and omega-3 PUFAs. *Oxid Med Cell Longev* 2015:421624.
- Lepanto P, Badano JL, Zolessi FR (2016) Neuron's little helper: The role of primary cilia in neurogenesis. *Neurogenesis* 3:e1253363.
- Levinson JN, El-Husseini A (2005) Building excitatory and inhibitory synapses: balancing neuroligin partnerships. *Neuron* 48:171-174.
- Levy L, Howell M, Das D, Harkin S, Episkopou V, Hill CS (2007) Arkadia activates Smad3/Smad4-dependent transcription by triggering signal-induced SnoN degradation. *Mol Cell Biol* 27:6068-6083.
- Liang JS, Huang H, Wang JS, Lu JF (2019) Phenotypic manifestations between male and female children with CDKL5 mutations. *Brain & development*.
- Lin C, Franco B, Rosner MR (2005) CDKL5/Stk9 kinase inactivation is associated with neuronal developmental disorders. *Hum Mol Genet* 14:3775-3786.
- Livide G, Patriarchi T, Amenduni M, Amabile S, Yasui D, Calcagno E, Lo Rizzo C, De Falco G, Ulivieri C, Ariani F, Mari F, Mencarelli MA, Hell JW, Renieri A, Meloni I (2015) GluD1 is a common altered player in neuronal differentiation from both MECP2-mutated and CDKL5-mutated iPSCs. *Eur J Hum Genet* 23:195-201.
- Lowry OH, Rosebrough NJ, Farr AL, Randall RJ (1951) Protein measurement with the Folin phenol reagent. *J Biol Chem* 193:265-275.
- Luo J (2012) The role of GSK3beta in the development of the central nervous system. *Front Biol* 7:212 – 220.

- Macias MJ, Martin-Malpartida P, Massague J (2015) Structural determinants of Smad function in TGF-beta signaling. *Trends in biochemical sciences* 40:296-308.
- Manning G, Whyte DB, Martinez R, Hunter T, Sudarsanam S (2002) The protein kinase complement of the human genome. *Science* 298:1912-1934.
- Mari F, Azimonti S, Bertani I, Bolognese F, Colombo E, Caselli R, Scala E, Longo I, Grosso S, Pescucci C, Ariani F, Hayek G, Balestri P, Bergo A, Badaracco G, Zappella M, Broccoli V, Renieri A, Kilstrup-Nielsen C, Landsberger N (2005) CDKL5 belongs to the same molecular pathway of MeCP2 and it is responsible for the early-onset seizure variant of Rett syndrome. *Hum Mol Genet* 14:1935-1946.
- Montini E, Andolfi G, Caruso A, Buchner G, Walpole SM, Mariani M, Consalez G, Trump D, Ballabio A, Franco B (1998) Identification and characterization of a novel serine-threonine kinase gene from the Xp22 region. *Genomics* 51:427-433.
- Morales M, Fikova E (1989) Distribution of MAP2 in dendritic spines and its colocalization with actin. An immunogold electron-microscope study. *Cell Tissue Res* 256:447-456.
- Moustakas A, Heldin CH (2009) The regulation of TGFbeta signal transduction. *Development* 136:3699-3714.
- Munoz IM, Morgan ME, Peltier J, Weiland F, Gregorczyk M, Brown FC, Macartney T, Toth R, Trost M, Rouse J (2018) Phosphoproteomic screening identifies physiological substrates of the CDKL5 kinase. *EMBO J*.
- Nawaz MS, Giarda E, Bedogni F, La Montanara P, Ricciardi S, Ciceri D, Alberio T, Landsberger N, Rusconi L, Kilstrup-Nielsen C (2016) CDKL5 and Shootin1 Interact and Concur in Regulating Neuronal Polarization. *PLoS One* 11:e0148634.
- Oi A, Katayama S, Hatano N, Sugiyama Y, Kameshita I, Sueyoshi N (2017) Subcellular distribution of cyclin-dependent kinase-like 5 (CDKL5) is regulated through phosphorylation by dual specificity tyrosine-phosphorylation-regulated kinase 1A (DYRK1A). *Biochem Biophys Res Commun* 482:239-245.
- Okuda K, Kobayashi S, Fukaya M, Watanabe A, Murakami T, Hagiwara M, Sato T, Ueno H, Ogonuki N, Komano-Inoue S, Manabe H, Yamaguchi M, Ogura A, Asahara H, Sakagami H, Mizuguchi M, Manabe T, Tanaka T (2017) CDKL5 controls postsynaptic localization of GluN2B-containing NMDA receptors in the hippocampus and regulates seizure susceptibility. *Neurobiol Dis* 106:158-170.
- Okuda K, Takao K, Watanabe A, Miyakawa T, Mizuguchi M, Tanaka T (2018) Comprehensive behavioral analysis of the Cdkl5 knockout mice revealed significant enhancement in anxiety- and fear-related behaviors and impairment in both acquisition and long-term retention of spatial reference memory. *PLoS One* 13:e0196587.
- Olson HE, Demarest ST, Pestana-Knight EM, Swanson LC, Iqbal S, Lal D, Leonard H, Cross JH, Devinsky O, Benke TA (2019) Cyclin-Dependent Kinase-Like 5 Deficiency Disorder: Clinical Review. *Pediatric neurology* 97:18-25.
- Otani N, Nawashiro H, Fukui S, Ooigawa H, Ohsumi A, Toyooka T, Shima K, Gomi H, Brenner M (2006) Enhanced hippocampal neurodegeneration after traumatic or kainate excitotoxicity in GFAP-null mice. *Journal of clinical neuroscience : official journal of the Neurosurgical Society of Australasia* 13:934-938.
- Pini G, Bigoni S, Engerstrom IW, Calabrese O, Felloni B, Scusa MF, Di Marco P, Borelli P, Bonuccelli U, Julu PO, Nielsen JB, Morin B, Hansen S, Gobbi G, Visconti P, Pintaudi M, Edvige V, Romanelli A, Bianchi F, Casarano M, Battini R, Cioni G, Ariani F, Renieri A, Benincasa A, Delamont RS, Zappella M, group E (2012) Variant of Rett syndrome and CDKL5 gene: clinical and autonomic description of 10 cases. *Neuropediatrics* 43:37-43.
- Pizzo R, Gurgone A, Castroflorio E, Amendola E, Gross C, Sassoe-Pognetto M, Giustetto M (2016) Lack of Cdkl5 Disrupts the Organization of Excitatory and Inhibitory Synapses and Parvalbumin Interneurons in the Primary Visual Cortex. *Front Cell Neurosci* 10:261.
- Poncelet AC, Schnaper HW, Tan R, Liu Y, Runyan CE (2007) Cell phenotype-specific down-regulation of Smad3 involves decreased gene activation as well as protein degradation. *J Biol Chem* 282:15534-15540.

- Prehn JH, Bindokas VP, Marcuccilli CJ, Krajewski S, Reed JC, Miller RJ (1994) Regulation of neuronal Bcl2 protein expression and calcium homeostasis by transforming growth factor type beta confers wide-ranging protection on rat hippocampal neurons. *Proc Natl Acad Sci U S A* 91:12599-12603.
- Purpura DP (1974) Dendritic spine "dysgenesis" and mental retardation. *Science* 186:1126-1128.
- Rauch J, Volinsky N, Romano D, Kolch W (2011) The secret life of kinases: functions beyond catalysis. *Cell communication and signaling : CCS* 9:23.
- Ren E, Roncacé V, Trazzi S, Fuchs C, Medici G, Gennaccaro L, Loi M, Galvani G, Ye K, Rimondini R, Aicardi G, Ciani E (2019) Functional and Structural Impairments in the Perirhinal Cortex of a Mouse Model of CDKL5 Deficiency Disorder Are Rescued by a TrkB Agonist. *Frontiers in Cellular Neuroscience* 13.
- Ricciardi S, Kilstrup-Nielsen C, Bienvenu T, Jacqueline A, Landsberger N, Broccoli V (2009) CDKL5 influences RNA splicing activity by its association to the nuclear speckle molecular machinery. *Hum Mol Genet* 18:4590-4602.
- Ricciardi S, Ungaro F, Hambrook M, Rademacher N, Stefanelli G, Brambilla D, Sessa A, Magagnotti C, Bachi A, Giarda E, Verpelli C, Kilstrup-Nielsen C, Sala C, Kalscheuer VM, Broccoli V (2012) CDKL5 ensures excitatory synapse stability by reinforcing NGL-1-PSD95 interaction in the postsynaptic compartment and is impaired in patient iPSC-derived neurons. *Nat Cell Biol* 14:911-923.
- Rusconi L, Kilstrup-Nielsen C, Landsberger N (2011) Extrasynaptic N-methyl-D-aspartate (NMDA) receptor stimulation induces cytoplasmic translocation of the CDKL5 kinase and its proteasomal degradation. *J Biol Chem* 286:36550-36558.
- Rusconi L, Salvatoni L, Giudici L, Bertani I, Kilstrup-Nielsen C, Broccoli V, Landsberger N (2008) CDKL5 expression is modulated during neuronal development and its subcellular distribution is tightly regulated by the C-terminal tail. *J Biol Chem* 283:30101-30111.
- Sekiguchi M, Katayama S, Hatano N, Shigeri Y, Sueyoshi N, Kameshita I (2013) Identification of amphiphysin 1 as an endogenous substrate for CDKL5, a protein kinase associated with X-linked neurodevelopmental disorder. *Arch Biochem Biophys* 535:257-267.
- Shchemelinin I, Sefc L, Necas E (2006) Protein kinases, their function and implication in cancer and other diseases. *Folia biologica* 52:81-100.
- Shi Y, Massague J (2003) Mechanisms of TGF-beta signaling from cell membrane to the nucleus. *Cell* 113:685-700.
- Sivilia S, Mangano C, Beggiato S, Giuliani A, Torricella R, Baldassarro VA, Fernandez M, Lorenzini L, Giardino L, Borelli AC, Ferraro L, Calza L (2016) CDKL5 knockout leads to altered inhibitory transmission in the cerebellum of adult mice. *Genes Brain Behav* 15:491-502.
- Sweeney ST, Davis GW (2002) Unrestricted synaptic growth in spinster-a late endosomal protein implicated in TGF-beta-mediated synaptic growth regulation. *Neuron* 36:403-416.
- Symonds JD, Zuberi SM, Stewart K, McLellan A, O'Regan M, MacLeod S, Jollands A, Joss S, Kirkpatrick M, Brunklaus A, Pilz DT, Shetty J, Dorris L, Abu-Arafeh I, Andrew J, Brink P, Callaghan M, Cruden J, Diver LA, Findlay C, Gardiner S, Grattan R, Lang B, MacDonnell J, McKnight J, Morrison CA, Nairn L, Slean MM, Stephen E, Webb A, Vincent A, Wilson M (2019) Incidence and phenotypes of childhood-onset genetic epilepsies: a prospective population-based national cohort. *Brain : a journal of neurology* 142:2303-2318.
- Szafranski P, Golla S, Jin W, Fang P, Hixson P, Matalon R, Kinney D, Bock HG, Craigen W, Smith JL, Bi W, Patel A, Wai Cheung S, Bacino CA, Stankiewicz P (2015) Neurodevelopmental and neurobehavioral characteristics in males and females with CDKL5 duplications. *Eur J Hum Genet* 23:915-921.
- Tang S, Terzic B, Wang IJ, Sarmiento N, Sizov K, Cui Y, Takano H, Marsh ED, Zhou Z, Coulter DA (2019) Altered NMDAR signaling underlies autistic-like features in mouse models of CDKL5 deficiency disorder. *Nature communications* 10:2655.
- Tang S, Wang IJ, Yue C, Takano H, Terzic B, Pance K, Lee JY, Cui Y, Coulter DA, Zhou Z (2017) Loss of CDKL5 in Glutamatergic Neurons Disrupts Hippocampal Microcircuitry and Leads to Memory Impairment in Mice. *J Neurosci* 37:7420-7437.
- Tao J, Van Esch H, Hagedorn-Greiwe M, Hoffmann K, Moser B, Raynaud M, Sperner J, Fryns JP, Schwinger E, Gecz J, Ropers HH, Kalscheuer VM (2004) Mutations in the X-linked cyclin-dependent kinase-like 5

- (CDKL5/STK9) gene are associated with severe neurodevelopmental retardation. *American journal of human genetics* 75:1149-1154.
- Tapia-Gonzalez S, Giraldez-Perez RM, Cuartero MI, Casarejos MJ, Mena MA, Wang XF, Sanchez-Capelo A (2011) Dopamine and alpha-synuclein dysfunction in Smad3 null mice. *Mol Neurodegener* 6:72.
- Tapia-Gonzalez S, Munoz MD, Cuartero MI, Sanchez-Capelo A (2013) Smad3 is required for the survival of proliferative intermediate progenitor cells in the dentate gyrus of adult mice. *Cell communication and signaling : CCS* 11:93.
- Tarasewicz E, Jeruss JS (2012) Phospho-specific Smad3 signaling: impact on breast oncogenesis. *Cell Cycle* 11:2443-2451.
- Tramarin M, Rusconi L, Pizzamiglio L, Barbiero I, Peroni D, Scaramuzza L, Williams T, Cavalla D, Antonucci F, Kilstrup-Nielsen C (2018) The antidepressant tianeptine reverts synaptic AMPA receptor defects caused by deficiency of CDKL5. *Hum Mol Genet* 27:2052-2063.
- Trazzi S, De Franceschi M, Fuchs C, Bastianini S, Viggiano R, Lupori L, Mazziotti R, Medici G, Lo Martire V, Ren E, Rimondini R, Zoccoli G, Bartesaghi R, Pizzorusso T, Ciani E (2018) CDKL5 protein substitution therapy rescues neurological phenotypes of a mouse model of CDKL5 disorder. *Hum Mol Genet* 27:1572-1592.
- Trazzi S, Fuchs C, Viggiano R, De Franceschi M, Valli E, Jedynek P, Hansen FK, Perini G, Rimondini R, Kurz T, Bartesaghi R, Ciani E (2016) HDAC4: a key factor underlying brain developmental alterations in CDKL5 disorder. *Hum Mol Genet* 25:3887-3907.
- Tripathi PP, Sgado P, Scali M, Viaggi C, Casarosa S, Simon HH, Vaglini F, Corsini GU, Bozzi Y (2009) Increased susceptibility to kainic acid-induced seizures in Engrailed-2 knockout mice. *Neuroscience* 159:842-849.
- Ueberham U, Arendt T (2013) The Role of Smad Proteins for Development, Differentiation and Dedifferentiation of Neurons. In: *Trends in Cell Signaling Pathways in Neuronal Fate Decision*, pp 75-111: IntechOpen.
- Unsicker K, Kriegstein K (2000) Co-activation of TGF- β and cytokine signaling pathways are required for neurotrophic functions. *Cytokine Growth Factor Rev* 11:97-102.
- Valente EM, Rosti RO, Gibbs E, Gleeson JG (2014) Primary cilia in neurodevelopmental disorders. *Nature reviews Neurology* 10:27-36.
- Valli E, Trazzi S, Fuchs C, Erriquez D, Bartesaghi R, Perini G, Ciani E (2012) CDKL5, a novel MYCN-repressed gene, blocks cell cycle and promotes differentiation of neuronal cells. *Biochim Biophys Acta* 1819:1173-1185.
- Villapol S, Wang Y, Adams M, Symes AJ (2013) Smad3 deficiency increases cortical and hippocampal neuronal loss following traumatic brain injury. *Exp Neurol* 250:353-365.
- Waddell DS, Liberati NT, Guo X, Frederick JP, Wang XF (2004) Casein kinase Iepsilon plays a functional role in the transforming growth factor-beta signaling pathway. *J Biol Chem* 279:29236-29246.
- Wang IT, Allen M, Goffin D, Zhu X, Fairless AH, Brodtkin ES, Siegel SJ, Marsh ED, Blendy JA, Zhou Z (2012) Loss of CDKL5 disrupts kinome profile and event-related potentials leading to autistic-like phenotypes in mice. *Proc Natl Acad Sci U S A* 109:21516-21521.
- Wang Y, Wang W, Li D, Li M, Wang P, Wen J, Liang M, Su B, Yin Y (2014) IGF-1 alleviates NMDA-induced excitotoxicity in cultured hippocampal neurons against autophagy via the NR2B/PI3K-AKT-mTOR pathway. *J Cell Physiol* 229:1618-1629.
- Weaving LS, Christodoulou J, Williamson SL, Friend KL, McKenzie OL, Archer H, Evans J, Clarke A, Pelka GJ, Tam PP, Watson C, Lahooti H, Ellaway CJ, Bennetts B, Leonard H, Gecz J (2004) Mutations of CDKL5 cause a severe neurodevelopmental disorder with infantile spasms and mental retardation. *American journal of human genetics* 75:1079-1093.
- Williamson SL, Giudici L, Kilstrup-Nielsen C, Gold W, Pelka GJ, Tam PP, Grimm A, Prodi D, Landsberger N, Christodoulou J (2012) A novel transcript of cyclin-dependent kinase-like 5 (CDKL5) has an alternative C-terminus and is the predominant transcript in brain. *Human genetics* 131:187-200.
- Wrighton KH, Lin X, Feng XH (2009) Phospho-control of TGF-beta superfamily signaling. *Cell Res* 19:8-20.

- Wu G, Lu ZH, Wang J, Wang Y, Xie X, Meyenhofer MF, Ledeen RW (2005) Enhanced susceptibility to kainate-induced seizures, neuronal apoptosis, and death in mice lacking ganglioside GM1: protection with LIGA 20, a membrane-permeant analog of GM1. *J Neurosci* 25:11014-11022.
- Xu DJ, Zhao YZ, Wang J, He JW, Weng YG, Luo JY (2012) Smads, p38 and ERK1/2 are involved in BMP9-induced osteogenic differentiation of C3H10T1/2 mesenchymal stem cells. *BMB Rep* 45:247-252.
- Yakovlev AG, Faden AI (2004) Mechanisms of neural cell death: implications for development of neuroprotective treatment strategies. *NeuroRx* 1:5-16.
- Yennawar M, White RS, Jensen FE (2019) AMPA receptor dysregulation and therapeutic interventions in a mouse model of CDKL5 Deficiency Disorder. *J Neurosci*.
- Yi JJ, Barnes AP, Hand R, Polleux F, Ehlers MD (2010) TGF-beta signaling specifies axons during brain development. *Cell* 142:144-157.
- Zhou A, Han S, Zhou ZJ (2017) Molecular and genetic insights into an infantile epileptic encephalopathy - CDKL5 disorder. *Front Biol (Beijing)* 12:1-6.
- Zhu YC, Li D, Wang L, Lu B, Zheng J, Zhao SL, Zeng R, Xiong ZQ (2013) Palmitoylation-dependent CDKL5-PSD-95 interaction regulates synaptic targeting of CDKL5 and dendritic spine development. *Proc Natl Acad Sci U S A* 110:9118-9123.
- Zhu YC, Xiong ZQ (2019) Molecular and Synaptic Bases of CDKL5 Disorder. *Dev Neurobiol* 79:8-19.